UNIVERSITAT POLITÈCNICA DE CATALUNYA

PONTIFICIA UNIVERSIDAD CATOLICA DEL PERU

CENTRE TECNOLÒGIC DE TELECOMUNICACIONS DE CATALUNYA

Ultra-Wideband (UWB) rectenna design for Electromagnetic Energy Harvesting

by
César Meneses Ghiglino

A thesis submitted in partial fulfillment for the
degree of Engineer.

In the
Escola Técnica Superior d'Enginyeria de Telecomunicació de Barcelona
Departament de Teoria del Senyal i Comunicacions

October 2010

UNIVERSITAT POLITÉCNICA DE CATALUNYA
PONTIFICIA UNIVERSIDAD CATÓLICA DEL PERÚ
CENTRE TECNOLÓGIC DE TELECOMUNICACIONS DE CATALUNYA

Abstract

Escola Técnica Superior d'Enginyeria de Telecomunicació de Barcelona
Departament de Teoria del Senyal i Comunicacions

degree of Engineer

by César Meneses Ghiglino

This work focuses on designing, fabricating, measuring and testing each component of a Rectenna. A rectenna consists of an antenna and a rectifier circuit that is optimized for incoming signals of low power density. This rectenna is used to harvest electric energy from the RF signals that have been radiated at:

- GSM-850
- GSM-900 (downlink: *935-960MHz*)
- GSM-1800 (downlink: *1805-1880MHz*)
- ISM band centered in 2.45 GHz.

This work contains antenna design techniques using Ansoft HFSS software and methods to simulate rectennas using Harmonic Balance and electromagnetic full-wave Momentum with the Agilent Advanced Design Software (ADS2008).
For the antenna fabrication it was used a LPKF Milling machine. And for measurements a Vector Network Analyzer (VNA), spectral analyzer, analog signal generator, multimeter, and anechoic chamber were used.

Agradecimientos

En las siguientes líneas, quiero agradecer a aquellas personas, a las que considero más importantes en esta etapa, sin el apoyo emocional, material, etc. por su parte, este trabajo hubiera sido más duro.

Primero agradecer a mis padres y mis hermanos, por su apoyo y total confianza, por ser una motivación y ejemplo para mí, por animarme a hacer cosas de las cuales se puedan sentir orgullosos, a Yvett que siempre ha sido la primera persona en animarme y apoyarme en todo, tanto en Perú, como cuando empezó esta etapa de mi vida en España. A mis tíos, Eric y Diana, con su apoyo hicieron que yo me sintiera en familia siempre, a mis primas, Indira y Zoraida, por ser el toque infantil, necesario, que no había experimentado hasta ahora y que alegró muchas tardes. A todos mis compañeros de la UPC, principalmente a aquellos que como yo, vinieron desde lejos y comprenden el sacrificio de una tesis, más aun cuando la familia y las personas más cercanas a tu vida están lejos.

A todas las personas del CTTC: a Apostolos y Ana, por ser los principales artífices de esta tesis, por su paciencia, comprensividad, y por propiciar un excelente ambiente de trabajo, a Selva, por su infinita colaboración, paciencia y ayuda en los momentos importantes del proyecto.

A todos los amigos que he conocido en el transcurso de estos dos años en Barcelona, ¡son parte de esta excelente etapa!

¡Muchas Gracias!

Contents

Chapter 1

Introduction

Wireless multimedia systems are receiving increasing research and application interests. But improvements are still required to provide higher data-rate links, for instance, the transmission of video signals. Therefore, ultra-wideband (UWB) communication systems are currently under investigation and the design of a compact wideband antenna is very essential. To overcome the inherently narrow bandwidth of microstrip antennas, various techniques have been developed to cover the entire UWB bandwidth, such as L-/F-shaped probe to feed the patch, triangular patch, U-/V-slot monopoles, among others.

And, why don't we use the same antenna to collect the energy that is being radiated at several frequencies? Clearly it is much more effective to harvest the energy of several services at the same time than collecting only one service energy; this is why the idea of an UWB antenna for harvesting energy is entirely feasible.

The meaning of Energy Harvesting (also called energy scavenging or power harvesting), is the process by which energy from different sources is captured and stored. Generally, this definition applies when we talk about autonomous devices that require a low amount of energy to function.

Currently, energy harvesters do not provide sufficient amount of power to produce mechanical movements or temperature changes (cooks, refrigerators, etc) because there

aren't technologies that capture energy with great efficiency. But these technologies do provide the amount of energy needed for low-power devices that can operate autonomously.

Another advantage of this type of technology is that, unlike the production of large-scale power, we can consider that the energy source is free if you take into account the electromagnetic energy of transmitting mobile stations and radio and TV broadcasting antennas.

The use of batteries has two disadvantages: the lifetime of the batteries is very limited even for low-power batteries, requiring impractical periodical battery replacement, the use of commercial batteries usually overkills the power requirements for uW sensor nodes, adding size and weight while creating the problem of environmental pollution due to the deposition of these batteries, as well as increases significantly the cost overhead of disposable nodes.

This work focuses on incident low-power density; designing, measuring and testing a Rectenna to harvest electric energy from the RF signals that have been radiated by public communications systems (GSM-900 and GSM-1800) and the 2.4 GHz ISM band; also the work is motivated by two types of applications: powering low-power sensor networks and RF energy recycling

1.1 Overview

In this thesis, the work involves the design, simulation, fabrication and measurement of each of the components of a rectenna (rectifying antenna circuit) has been divided into the following chapters.

- Chapter 1 is this overview.
- Chapter 2 reviews some of the history of microwave power transmission from its beginnings with the empirical work of Hertz, to Tesla's experiments and describing the evolution of power transmission in free space. Subsequently, it describes how the approaches of some projects, together with studies funded by various companies, encourage the evolution of technologies in the field of microwave power transmission. After the history, an overview of some low power sources for energy harvesting is shown, then we emphasize in the RF-EM energy harvesting and a feasibility study for our application is shown.
- Chapter 3 first describes the main parameters of an antenna for its design. A brief background about UWB antennas and microstrip antennas is introduced. The introduction of the design software (Ansoft HFSS 11) and a brief description of the

simulation method used for the antennas will be shown as well. Then a description of the design procedure and simulations of our base-antenna, which bandwidth range from 850 MHz to 6 GHz is explained. Thereafter, the miniaturization techniques that we applied to the base-antenna and the subsequent building procedures of the “size-improved" antenna will be shown. Finally, some pictures and measures will be explained.

- Chapter 4 describes everything about the rectifier circuit. It begins by describing the operation of a half-wave rectifier and an introduction to the Schottky diode is made, then a brief review of the efficiency of power conversion from RF to DC is shown. For rectifier circuit simulations, the software used was the Agilent ADS2008; this chapter also explains each of the tools used to perform these simulations. For a good overall efficiency, several rectifier circuits were tested, in this chapter, the simulations of each of them and their schemes are detailed. In order to avoid the soldering of a high number of components that may affect the overall efficiency, a transformation from LC components to Microstrip Lines, and their simulations, will be explained. Finally the results of the measurements are shown.
- Chapter 5 shows some possible future applications of rectennas as well as some new substrates materials for antennas that are currently being studied and tested. Finally the conclusions are shown.

Chapter 2

State of the Art

2.1 History of Power Transmission by Radio Waves.

When we talk about power transmission by radio waves, we mean a complex process that can be divided into three stages: 1) to transform the DC power in RF power, 2) RF transmit this RF power through a wireless medium from one point to another; and 3) turn back the received RF power to DC power. Then, we can conclude that the overall system efficiency is directly dependent on the efficiency of each of these stages. The modern history of power transmission studies, in many respects, has focused on improving and developing the elements of the transmitting and receiving ends of this system, focusing on high efficiency, low costs, reliability and low mass.

2.1.1 The Early History

Power transmission dates back to the early work of Hertz [1], He wasn't only the first who showed the propagation of electromagnetic waves in free space, he was also the first to experiment with parabolic reflectors at both the transmitter and receiver ends.

At the end of the 19th century, Nikola Tesla, a genius in the area of generation and power transmission became interested in their studies applied to power transmission from one place to another without wires. His first attempt was carried out in 1899 in Colorado, USA,

with the support of the Colorado Springs Electricity Company. He built a giant coil over which rose a mast of 70 meters with a copper sphere at the end. However, there is no record of how many energy was radiated to the space and whether there was any collected energy at any other place. From today's perspective, we can say that Tesla's attempts of efficient power transmission were ahead of the developed technology of this time. 30 years later, in 1934, H. V. Noble, this time in a laboratory, using two 100 MHz dipoles separated by 8 meters, collected several hundred of watts. With this experiment, he laid the basis for power transfer demonstrations.

The main cause of the lack of interest to develop this area was that several experts had determined that to achieve high efficiencies, concentrations of electromagnetic energy in a narrow band were needed. During the first 35 years of the 20th century, there were no devices that have these capabilities, but in the late 30's, the development of the velocity-modulated beam tube (Klystron tube) and the microwave cavity magnetron, allowed the generation of microwave power dedicated to this new technology.

2.1.2 The Modern History of Free-Space Power Transmission.

The modern history of power transmission, as far as microwaves are concerned, not only includes the development of technologies for microwave power transmission (MPT), the approach also includes various applications, whose achievements contributed to the development of new ideas and new technologies. This history of free-space power transmission will be divided in the early period beginning in 1958 and the period beginning in 1977 with the assessment study, by the DOE / NASA, of the concept of the solar-power satellite.

2.1.2.1 The Early Beginning

In the late 50's, several developments, made the idea of transmitting large amounts of power with high efficiency a reasonable concept, among these developments was the growing need to be able to communicate over long distances with line of sight. This could be solved with some kind of platform located at high altitude. Subsequently, this was solved with a satellite, but back then, a microwave powered vehicle was a logical approach.

Raytheon Company proposed a platform supported by a large helicopter, but did not get the necessary support of the Defense Department; however, they encouraged the development of technologies necessary to make it feasible. Among the technologies that were needed to develop were the high-power microwave tubes required for the transmitter and the technology to directly convert microwave-dc power to drive the motors of helicopter rotors. Between the years 1960-63 were developed some solutions to these problems (the Amplitron and thermionic rectifier respectively) and they did some demonstrations to

receive funds, but some flaws (as the high directivity of the receiving antennas attached to the helicopter and the short-life of thermionic diode) made that the project couldn't be successfully finalized. Due to the low collection efficiency of energy and the directivity of the horns, the concept of rectenna was conceived. This solution consisted in to attach the rectifiers in half-wave dipoles and put a reflector panel behind them. With the application of this rectenna concept the helicopter project (Fig 2.1), the first of July 1964, the first flight of a heavier than air vehicle supported solely by power received from a microwave beam was made.

2.1.2.2 Sponsorship by Marshall Space Flight Center (MSFC)

In 1970, due to the emphasis on developing a free-space power transmission system for a set of physically separate satellites, the MSFC, contracted Raytheon for a system study to be carried out in 1970. In this experiment conducted in 1970, the overall system efficiency obtained was 26%; over the next four years, with the aim of improving the overall system efficiency some other developments were made like a better antenna design, the develop of better ways to launch the microwave beam, the develop for better tools to measure the overall efficiency and better analytical tools for a better understanding of the operation of the rectenna.

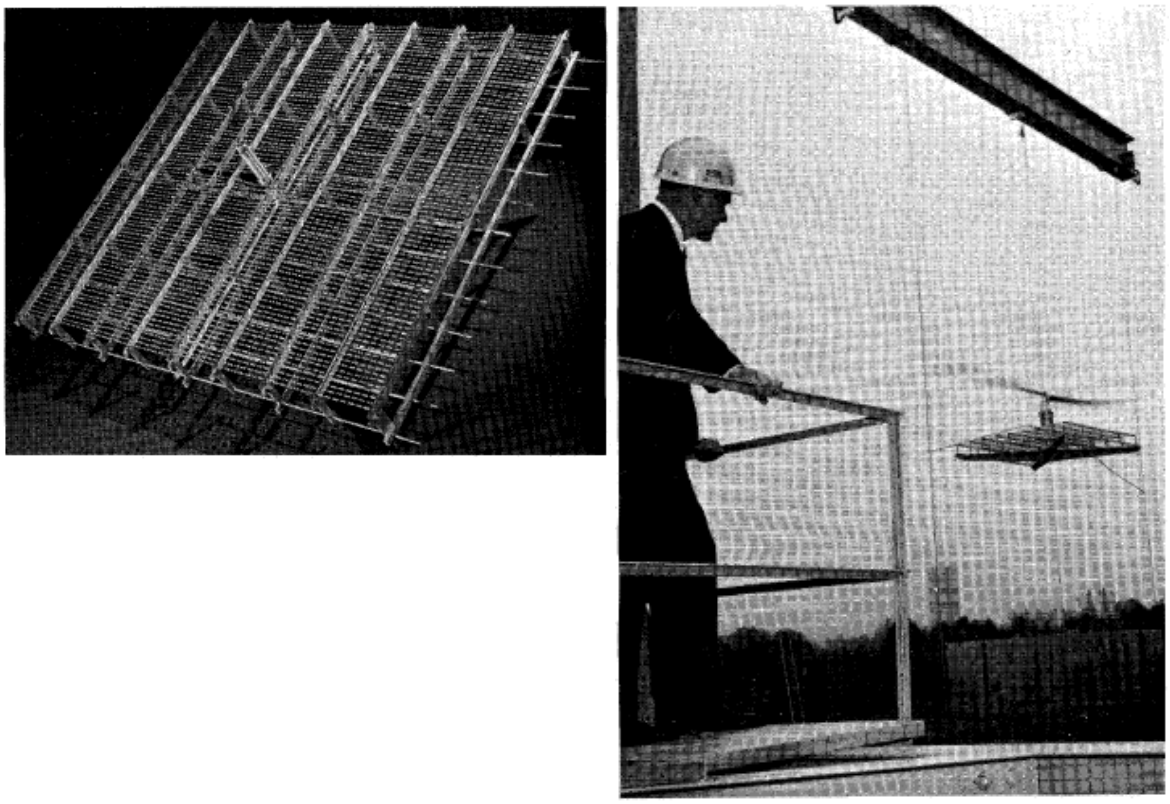

Fig 2.1.1 (left) shows the rectenna made to fly the first helicopter powered by microwaves and (right) the complete system in a test flight of 10 hours, held in October 1964

In 1971, the introduction of the gallium arsenide Schottky-barrier diode with an improved efficiency and greater power handling capacity that the diode that was previously used. This sponsorship program culminated with the construction of a laboratory power transmission system with all the technology that had been developed during the last years. In this experiment, the efficiency obtained was 48% +- 2%.

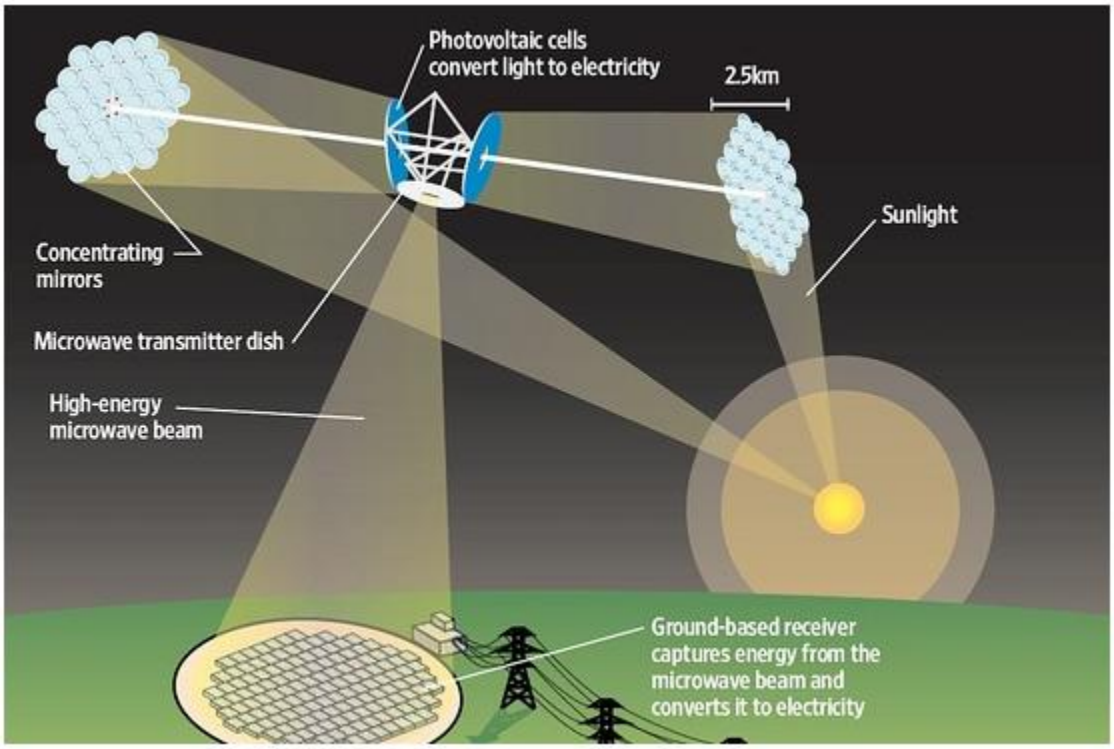

Fig. 2.1.2 Show the complete diagram of the SPS concept [2].

2.1.2.3 Progress Associated with Initial Interest in the Solar-Power Satellite (SPS) Concept

In 1968, Dr. Peter Glaser introduced the concept of SPS (Fig. 2.2). In this concept, the sun's energy is captured in orbit, converted into microwave power and then beamed to the Earth where subsequently it would be converted into electric power. This idea caught the attention of many companies interested in developing this project that seemed to be a possible solution for the growing demand for energy. A team of four companies (Arthur D. Little, Raytheon, Grumman Aerospace and Textron) was formed to develop a technical and economic feasibility study of the project. After six months of study, in 1971, the results of the technical investigation with favorable results encouraged them to send a letter to the director of NASA suggesting support for the SPS concept.

In 1973, the NASA's Office of Implementation, showed support for any additional development and also an special interest in the demonstration of the part of the system that

was responsible for power transmission. In 1975, the Goldstone demonstration was carried out, using a rectenna of 88 square meters, the power was transferred over a distance of 1 mile and a DC output of 30 kW was obtained; for the NASA and aerospace communities this demonstration was very important because it gave credibility to the power transmission and its use in the SPS concept. Concurrently, Raytheon developed a study sought to determine the critical technology areas of the SPS concept; this study concluded that these areas were: the DC to microwave conversion and the phased array antenna in the satellite. The development and improvement of these areas is considered the basis for many other technologies used in future applications.

A study supported by LERC in 1976-77, resulted in significant improvements in electrical and mechanical rectenna technology. The most important improvement was the mechanical change of format of rectenna, moving from a three-plane system, where bussing is done behind the reflector plane, making it more expensive, heavy and complex, to a system of two planes where there is only the reflector plane and a fore plane where all the microwave functions, rectification and DC bussing are held.

2.1.2.4 Later Period: Microwave Activity under DOE/NASA Concept Development and Evaluation Program for the SPS.

NASA, with the purpose of managing the energy that would be collected on Earth from the SPS system, involved ERDA (Energy Research and Development Agency) in the project. In 1977 ERDA began a three-year program called DOE/NASA Concept Development and Evaluation Program that resulted in a 670-page report summarizing the studies and findings. From these results, the most important for the development of microwave power transmission (MPT) was the suggestion of using the microwave oven magnetron. The program DOE/NASA SPS ended in 1980 with the conclusion that there was no reason for not continuing with the development and implementation of the project, but a program did not materialize. In retrospect, we can say that the greatest contribution of the SPS concept upon microwave power transmission (MPT) was the development of technologies that later replaced the classic super power tubes, for active phased array consisting of a large number of identical modules easy to manufacture using low-power microwave generators derived from the magnetron.

2.2 Low Power Energy Harvesting

Energy harvesting has been around in the form of windmills, watermills and passive solar power systems. In recent decades, technologies such as wind turbines, hydro-electric generators and solar panels have turned harvesting into a small but growing contributor to

the world's energy needs. This technology offers two significant advantages over battery-powered solutions: inexhaustible sources and little or no adverse environmental effects.

The most promising low power harvesting technologies extract energy from vibration, temperature differentials and light. Scavenging energy from RF emissions is interesting, but the energy availability is at least an order of magnitude less than the first three. Table 2.1 shows the estimated harvested power for different kinds of energy sources; we can observe that the estimated RF/EM harvested power along with the human vibration/motion harvested power, are the lowest values. Generally energy harvesting suffers from low, variable and unpredictable levels of available power.

The large reduction in power consumption achieved in electronics, along with the numbers of mobiles and other autonomous devices are continuously increasing the attractiveness of low power harvesting techniques. Consequently the amount of research in the field, and the number of publications has risen greatly.

Energy harvesting devices are particularly attractive as replacements for batteries in low-power wireless electronic devices. The cost of procuring, storing and getting someone to change a battery can easily cost as much as an energy harvester. A recent study [3] found that energy-harvesting systems are cost-comparable with systems using long-life batteries, over a ten-year lifetime.

2.3 EM/RF energy harvesting

When we refer to EM/RF harvesting, we do not refer to energy sources that have been specifically designed for powering wireless devices, we talk about the energy that we can collect from public services. In cities and very populated areas there is a large number of EM/RF sources like broadcasting radio and TV stations, mobile telephony base stations, and wireless networks. It is possible to collect part of this energy and convert it into useful energy. For our application, the main interest is in telecommunication services operating in the microwave region of the frequency spectrum, especially Global System for Mobile Communications (GSM) and Wireless Local Area Network (WLAN). As the most commonly used frequencies are well known, low-power devices have an antenna and a rectifier circuit (Rectenna), optimized to maximize energy harvesting at these frequencies[4]. For these services and their frequency bands, we can design printed antennas with dimension in the order of a few cm^2.

In laboratory environments, efficiencies above 90% have been observed, but when harvesting energy in the GSM or WLAN band on real scenarios, one has to deal with very low power density levels [5].

Table 2.1: Energy Harvesting Estimates [6] [7]

Energy Source Harvested Power	Harvested Power
Vibration/Motion	
Human	4 μW/cm^2
Industry	100 μW/ m^2
Temperature Difference	
Industry	1 – 10 mW/ cm^2
Light	
Indoor	10 μW/ cm^2
Outdoor	10 mW/ cm^2
RF/EM	
GSM	0.1 μW/ cm^2
Wi-Fi	0.001 mW/ cm^2
Solar	
Outdoor	10 mW/ cm^2
Indoor	< 0.1 mW/ cm^2
Acoustic	
75 – 10 dB of noise	0.003 – 0.96 μW/ cm^2
Human Body Sources	
Body heat	0.2 – 0.32 W (neck)
Walking	5 – 8.3 W

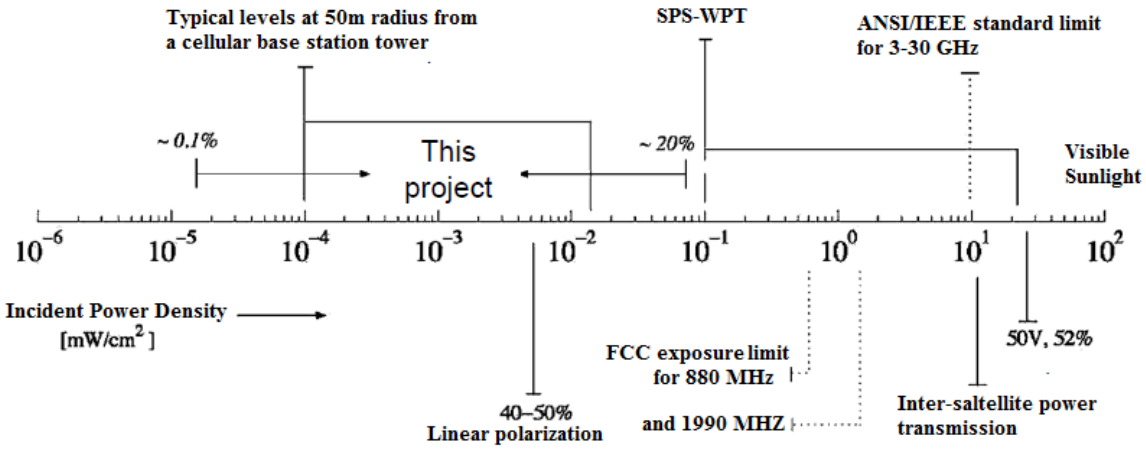

Fig. 2.2.1 Diagram of various microwave power sources and their typical power density levels. Also shown is the range of expected power densities used in the solar power satellite (SPS) and wireless power transmission (WPT) applications. The range of power densities for this work is indicated.

In Fig. 2.3.1 we see that the measured values of any kind of environment, at ground level, have a greater variation of power density, this is due to ground level, not always line of sight is obtained. For distances ranging from 25m to 100m from a GSM base station, power density levels ranging from 0.1mW/m2 to 1.0mW/m2 may be expected for single frequencies.

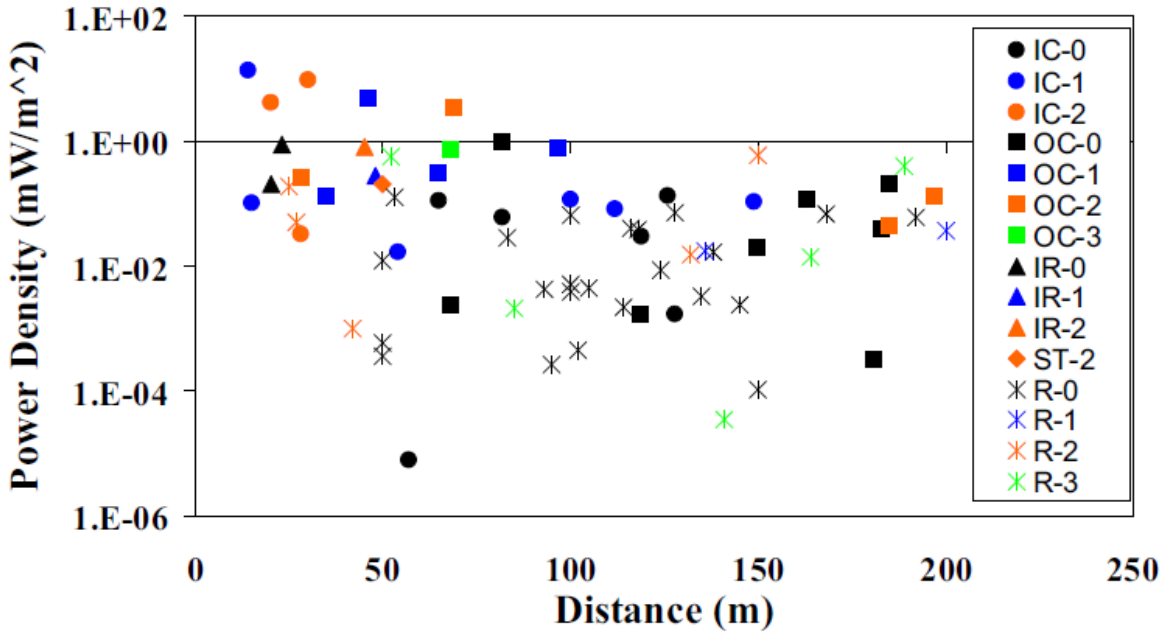

Fig. 2.3.1 Measured GSM-900 peak power density levels as a function of distance to the nearest base station. Data is taken from. Code "XY-a" indicates area and measurement site characteristics. XY: IC=Inner City, OC=Outer Country, IR=Industrial area, ST=Small Town, R=Rural or country-side are. "a": 0=outdoors on the ground, 1=outdoors on roof, terrace or balcony, 2=indoors, close to windows, 1.5m or less, 3=indoors, not close to windows.[8]

Figure 2.3.2 shows measurements over the entire 935-960 MHz band of the summed power density as a function of distance, we can conclude that between 25m and 100m, for indoor and outdoor environments, a high density power with values between 3.0 and mW/m2 0.3mW/m2 is expected. The measures over the entire frequency band are closely related to the traffic density at the moment of measurement, these measurements can vary by a factor form one to ten when compared with the measurements of a single Frequency (Fig. 2.3.1). Although the frequency of GSM-1800 band has doubled the GSM-900 band and therefore the free space loss has been quadrupled, ICNIRP (International Commission on Non-Ionizing Radiation Protection) exposures have only doubled. As for GSM-900, the actual exposures are well below the ICNIRP limits, we expect that power density levels for GSM-1800 are similar. This can be justified by measurements carried out in UK [9] and in Australia [10] for a mix of GSM-900/1800 base stations. From Figure 2.3.3, we can conclude that the power density measurements for GSM-900 and GSM-1800 are, up to 100 m, in the same order of magnitude.

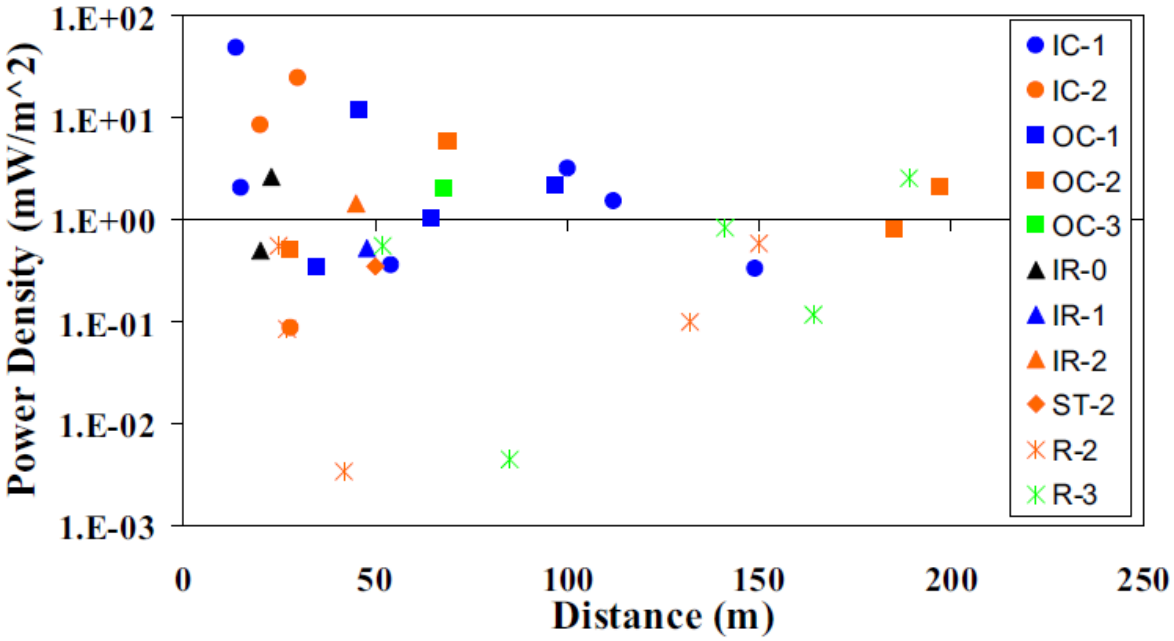

Fig. 2.3.2 Measured GSM-900 summed power density levels as a function of distance to the nearest base station, without data taken on ground level [8].

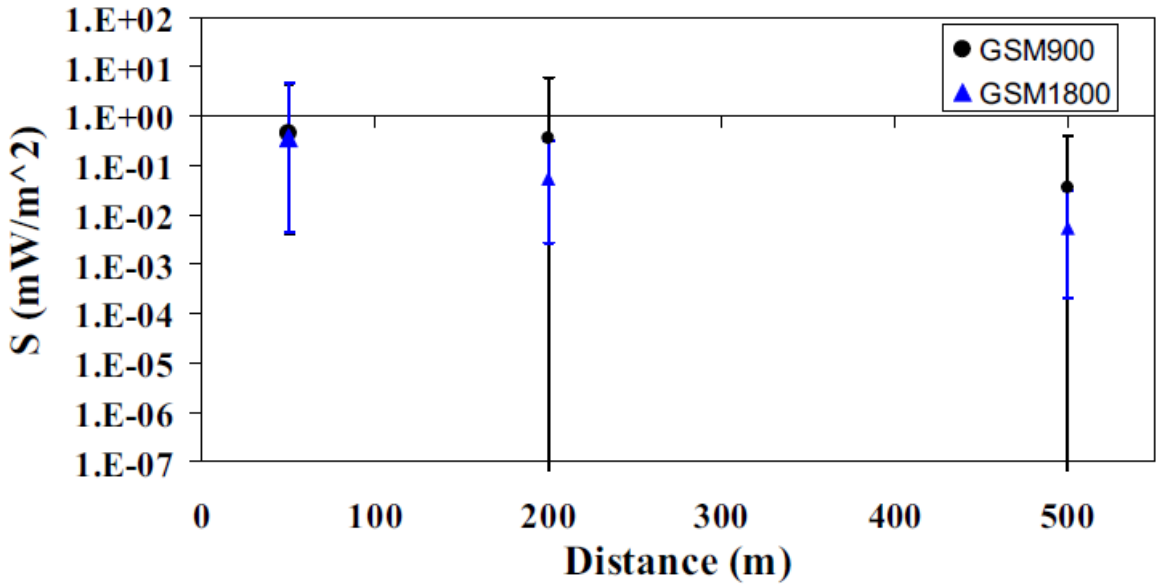

Fig. 2.3.3 Measured summed power density levels as a function of distance to the nearest GSM-900 and GSM-1800 base station [8].

If we refer to the 2.4 GHz band, whose efficiency in the environment is very high, Wi-Fi wireless local area networks (WLAN) applications are also useful with this concept. A WLAN router, transmit much less power than a GSM base station [8]. But because a router is confined to indoor environments and also that the distance would be much lower, reflections and low path loss may help to achieve suitable levels of power density. Fig.

2.3.4 shows the power density as a function of distance from the router. Although, during measurements of traffic levels were very low, we see that the power density levels are at least one order below the measurements obtained from GSM base stations.

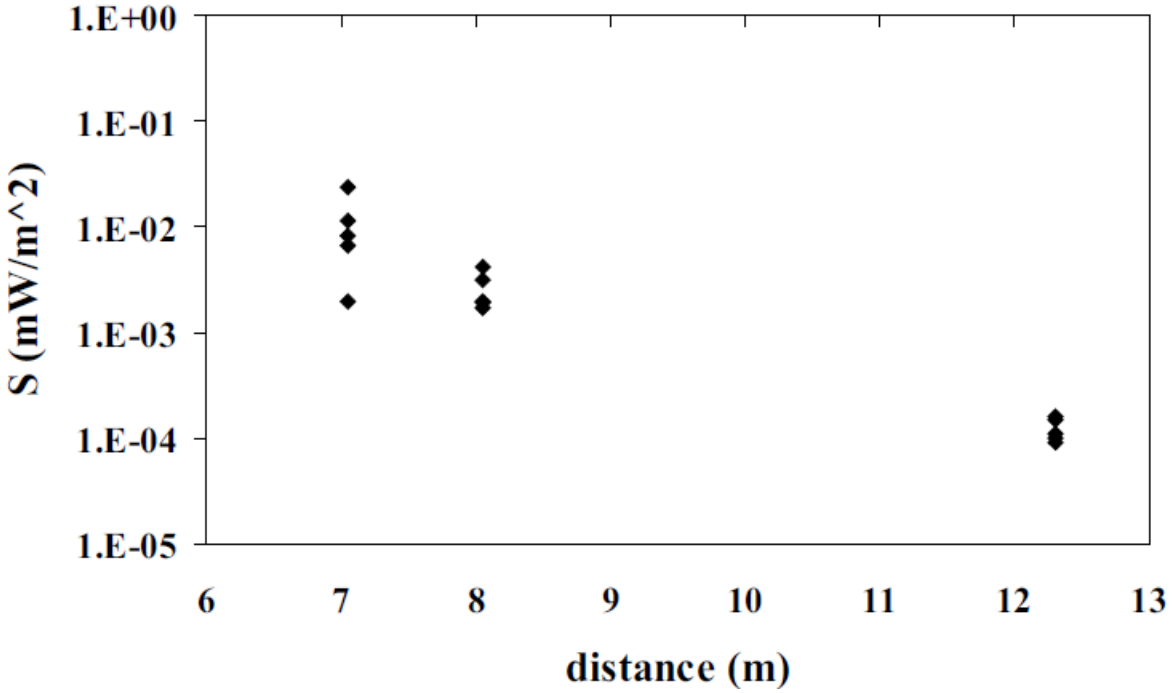

Fig. 2.3.4 Measured WLAN peak power density levels as a function of distance to the WLAN router [8].

2.4 Recent Technologies of Rectenna.

As explained above, a rectenna is a system that basically consists of a receiving antenna and a rectifier circuit which converts RF or microwave power into useful DC power. Fig. 2.1.2 shows the Schematic of a rectenna and associated power management circuit. The incident waves within a certain spectral range are received by the antenna, coupled to the rectifying device (diode in this case), and the low-pass filter (LPF) ensures that no RF is input to the power management circuit. A controller provides input to the power management circuit, which enables storage of the received energy over time, and delivery of DC power at the level and time when it is needed. This work will focus over the receiving antenna, the matching circuit and the rectifier circuit.

In recent years, a new approach to the use of rectennas has been reached and compared to other periods of microwave power transmission (MPT), where only high-power applications were developed (such as helicopter powering [1], solar-powered satellite-to-ground transmission [11], mechanical actuators for space-based telescopes [12], driving

motor [13], etc.), currently the develop of low-power applications is evolving. Rectennas implementing Ultra wideband (UWB) and narrow-band (essentially single frequency) antennas with smaller dimensions and new rectifier circuits configurations with new detectors that allow better performance are been used[14]. Self-powered sensors, short distances RFID tags, biomedical implants and energy harvesting devices, are some of the new low-power applications.

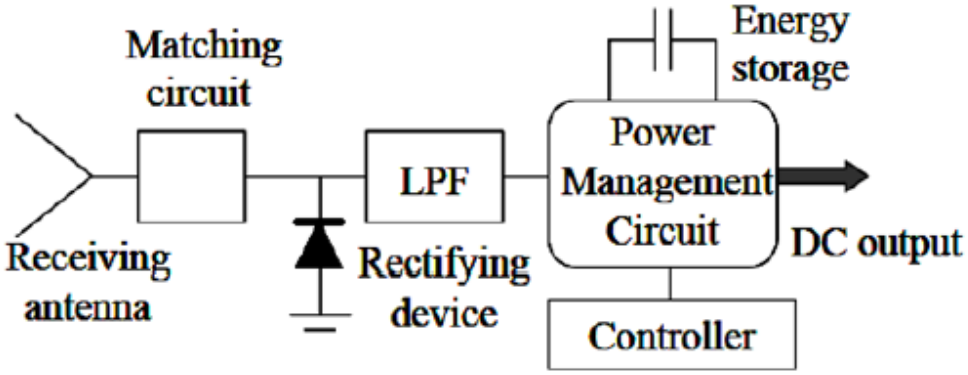

Fig. 2.4.1 Basic rectenna schematic with the power management system

Chapter 3

Antenna Design

In this chapter is described the design process, simulations and fabrication of an Ulta-WideBand antenna that operates from 900 MHz up to 6GHz. First we start with a brief explanation of the main design parameters of an antenna then we briefly explain the advantages of using UWB and microstrip antennas in these applications. Also a brief introduction of the software used for the design and simulations stages, as well as the method used for the simulator will be presented.

A parametric study of semicircular printed monopoles is included. Then we will explain how making some changes to the shape of the ground plane and the radiating patch of the antenna can improve the performance. After all the parametric simulations a final antenna version was chosen and subsequently built. Some pictures of the milling machine and the procedures after the milling are shown.

To improve the size of the antenna, a final version with some miniaturization techniques was built and the parametric simulations are included in a final study.

3.1 Antenna characteristics

To design an antenna, previously it is necessary to establish certain performance parameters that will be our goals in the design process and that are specific to our application.

3.1.1 Bandwidth

Bandwidth can be expressed as the range of frequencies over which the antenna characteristics are acceptable. In the case of broadband antennas, the bandwidth is often denoted as the ratio between the highest and lowest operating frequency. For example, 6:1 means that the higher frequency is six times greater than the lowest frequency.

3.1.2 Radiation Pattern

Is the mathematical representation or graphical representation of the radiation from an antenna as a function of spatial coordinates. Some of the properties of radiation are power flux density, radiation intensity, field strength, phase and polarization directivity, being the most important the spatial two and three dimensional radiation energy. A stroke of the power received at a constant radius is called power pattern. On the other hand, a plot of the spatial variation of an electric field (or magnetic) at a constant radius is called field amplitude pattern.

In practice, a three dimensional representation is obtained through various cuts of two-dimensional patterns. However for most practical applications, only some measures in terms of THETA for certain values of PHI and some measures in term of PHI for some values of THETA give us more useful information.

3.1.3 Radiation Power Density

Electromagnetic waves are used to carry information from one point to another through a wireless medium or through a guide structure, then it is natural to assume that the power and energy are associated with electromagnetic fields. The amount used to describe the power associated with an electromagnetic wave is the instantaneous Poynting vector

$$\mathcal{W} = \mathcal{E}\ x\ \mathcal{H}$$

$$\mathcal{W} = instantaneous\ Poynting\ vector\ \left(\frac{W}{m^2}\right)$$

$$\mathcal{E} = instantaneous\ Poynting\ vector\ \left(\frac{V}{m}\right)$$

$$\mathcal{H} = instantaneous\ magnetic\ field\ intensity\ \left(\frac{A}{m}\right)$$

Since the Poynting vector is a power density, the total power crossing a closed surface can be obtained by integrating the normal component of Poynting vector on this surface.

$$\wp = \oiint_S \mathcal{W}.ds = \oiint_S \mathcal{W}.\check{n}\, da$$

$$\wp = instantaneous\ total\ power\ (W)$$

$$\check{n} = unit\ vector\ normal\ to\ the\ surface$$

$$da = infinitesimal\ area\ of\ the\ colsed\ surface\ (m^2)$$

3.1.4 Radiation Intensity

The radiation density in a specific direction is defined as the power radiated by an antenna per unit solid angle, is a far-field parameter and is the product of multiplying the intensity of radiation by the square of the distance.

$$U = r^2.W_{rad}$$

$$U = radiation\ intensity\ (\frac{W}{unit\ solid\ angle})$$

$$W_{rad} = radiation\ density\ \left(\frac{W}{m^2}\right)$$

The radiation density in a certain direction is defined as the power radiated by an antenna per unit solid angle, is a far-field parameter and is the product of multiplying the intensity of radiation by the square of the distance.

$$P_{rad} = \oiint_\Omega U d\Omega = \int_0^{2\pi} \int_0^{2\pi} U.\sin\theta\, d\theta\, d\phi$$

$$d\Omega = element\ of\ solid\ angle = \sin\theta\, d\theta\, d\phi$$

In an isotropic antenna U is independent of the angles THETA and PHI.

$$P_{rad} = \oiint_\Omega U_0 d\Omega = U_0 \oiint_\Omega d\Omega = 4\pi U_0$$

$$U_0 = \frac{P_{rad}}{4\pi}$$

3.1.5 Directivity

In an isotropic antenna U the directivity is independent of the angles THETA and PHI. Directivity of an antenna is the ratio between the intensity of radiation in one direction from the antenna with the radiation intensity averaged over all directions. The average radiation level is equal to the total radiated power divided by 4PII. If the direction is not specified it is assumed the maximum intensity of radiation. In other words, the directivity of an antenna is not isotropic in a particular direction is equal to the ratio between the intensity of radiation with the radiation of an isotropic antenna.

$$D = \frac{U}{U_0} = \frac{4\pi U}{P_{rad}}$$

If the direction is not specified, it implies the direction of the maximum radiation intensity (maximum directivity) expressed as:

$$D_{max} = D_0 = \frac{U_{max}}{U_0} = \frac{4\pi U_{max}}{P_{rad}}$$

$$D = directivity\ (dimensionless)$$

$$D_0 = maximum\ directivity\ (dimensionless)$$

$$U = \text{radiation intensity (W/unit solid angle)}$$

$$U_{max} = \text{maximum radiation intensity (W/unit solid angle)}$$

$$U_0 = \text{radiation intensity of isotropic source (W/unit solid angle)}$$

$$P_{rad} = \text{total radiated power (W)}$$

3.1.6 Polarization

Polarization of an antenna can be defined as the polarization of the radiated fields measured or "seen" from far fields, some of the typical classifications are the linear polarization and circular (Right / Left Hand).

Because of the reciprocity theorem, antennas transmit and receive in the same way, then a vertically polarized antenna will communicate with another antenna vertically polarized and an horizontally polarized antenna will communicate with another horizontally polarized antenna, if, for example, a horizontally polarized antenna try to communicate with another whose polarization is vertical, there won't be communication at all.

To describe in general terms the loss of polarization we use the Polarization Loss Factor (PLF):

$$PLF = \cos\phi^2$$

The PFL describes the loss ratio in function of a rotation angle between two linearly polarized antennas.

A circular polarization is desired in many applications because there is no loss of polarization as a function of antenna rotation angles.

If, for example, a circularly polarized antenna receives a linearly polarized antenna signal(or vice versa), we must recall that the circular polarization is actually the product of two linearly polarized waves orthogonal to each shifted 90 degrees, then the receiving antenna will receive only the linear part which is half of the total power.

$$PLF(linear\ to\ circular) = 0.5 = -3dBm$$

3.1.7 Axial ratio

The axial ratio is a parameter used to quantify the polarization of an antenna and to denote deviations from a desired polarization and can be defines as the ratio of orthogonality of E fields components. When an antenna has a perfect circular polarization, the axial ratio is 1 (or 0 dB), because you have E-field components of the same magnitude, if it's an antenna with elliptical polarization, the axial ratio is greater than 1 and if it is a purely linear polarized antenna, the axial ratio tends to infinity because one of the components of E field is zero. The value of the axial ratio is degraded at a greater distance of the mainbeam.

3.1.8 Gain

The term gain describes how much power is transmitted in the direction of peak radiation to that of an isotropic source. The gain of an antenna is defined as the ratio of power delivered to the antenna and the power that is actually radiated. Ideally, the radiated power is equal to the received power, but in real specifications of antennas, due to various types of losses (conduction losses and dielectric losses) as well as mismatching losses, the ideal value is never obtained.

3.2 UWB Antennas

Broadband and UWB antennas date back to the earliest days of radio [15]. The wide scale commercial deployment of ultra wideband (UWB) systems has led to increased interest in UWB antenna design. The requirements imposed by UWB systems place stringent demands on UWB antennas. For example, the spectral and impedance matching properties of a UWB antenna influence on an overall UWB system design. A well-designed UWB antenna can contribute to system performance by notching out undesired frequencies.

UWB wireless technology is most thought for some application like:

- Very high-data-rate and short-range wireless communication systems
- Coding for security and low probability of interception
- Rejection of multipath effect
- Modern radar systems
- Energy harvesting
- Self powering devices

Printed antennas, commonly fabricated on FR4 substrate, are very cost effective, which is ideally suited for UWB technology-based low-cost systems.

3.2.1 Microstrip Antennas

Microstrip antennas date back to the 50's when they were patented, but it is in the 70's when they receive considerable attention [16]. With the development of the high data rate wireless communication systems, antenna engineers are faced with increasing demand for smaller antennas which still retain broadband characteristics.

A microstrip antenna is formed basically by a dielectric substrate between two metal layers, one layer is the antenna and the other is the ground, Fig. 3.2.1.1 shows the basic configuration of a microstrip antenna

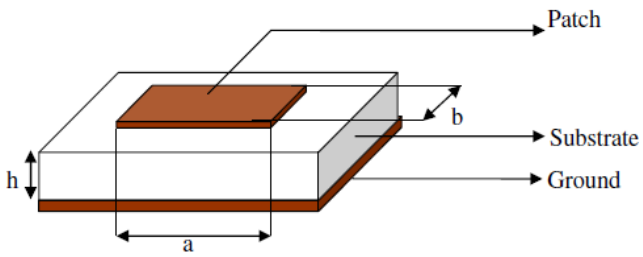

Fig. 3.2.1.1: basic layers of a microstrip antenna

Microstrip antennas, also known as patch antennas, performance is affected by the patch geometry, substrate properties and feed techniques, they often have the radiating elements and the feeding line etched in the dielectric substrate, they have its maximum radiation in the normal direction of the plane of the antenna that is achieved with an appropriate excitation below the antenna.

There are many types of substrate with dielectric constant values usually in the range of 2.2 <ER <12. Thick substrates with low dielectric constants are desired because they have higher bandwidth efficiency at the cost of a larger antenna size. On the other hand thin substrates with a high dielectric constant are desired in applications of microwave circuitry because they minimize unwanted coupling and radiation, and also because they allow to design smaller antennas. Since the microstrip antennas are closely linked to microwave circuits, a compromise between efficiency, bandwidth and size is necessary [16].

In recent years, printed planar monopole antennas have become very popular [16] and some of the main advantages of these antennas are:

- Low profile
- Low cost
- Light weight
- Ease of fabrication and installation
- Large bandwidth
- Radiation properties, wide impedance bandwidth and nearly omnidirectional azimuthal radiation pattern)
- Some of the various applications are covered with fewer or with a single antenna.

3.2.2 Feed mechanisms

Most of the performance and complexity of the design of a microstrip antenna depends on how the antenna patch will be fed. We can classify the techniques of feeding in three large groups.

- *Directly connected*: in this technique, a connection is made directly to the radiator element. For example, a microstrip line or a coaxial cable. This technique is very efficient in thin undertreated and one advantage is that the feeding line and the patch antenna are on the same plane, so it becomes a planar construction. In the case of a coaxial cable, it connects to the patch antenna through a hole in the substrate and the outer shell is grounded by merging it with the ground plane of the antenna.
- *Aperture Coupling*: This technique was introduced to overcome the technical problems of the directly connected feeding technique. It basically consists of two

substrates separated by a ground plane; in the bottom of the lower substrate, there is a microstrip line whose energy is coupled to the patch that is in the top of the upper substrate through a hole in ground plane. This feeding is the most difficult to manufacture and has a narrow bandwidth, but it is easier to model and has moderate spurious radiation [16].

- *Proximity Coupling*: The technique of proximity coupling consists of a power line located between two substrates, at the bottom of the lower substrate is the ground plane, and at the top of the upper substrate is the patch. Of the four feeding techniques, proximity coupling is the one with the higher bandwidth, is relatively simple to model and the spurious radiations are low, however its manufacturing is more difficult.

3.2.3 Software

For the stage of physical design and simulation, the Ansoft HFSS 11 software has been used. In order to generate an electromagnetic field solution, HFSS employs the finite element method. Fig. 3.2.1.1 shows the main window of the HFSS11; in the right side, a preview of the design is shown, the middle part, lists the components that make up our design, such as, solids, sheets, and planes. The left side shows the configurable features of the project such as the frequency sweep settings and simulation results.

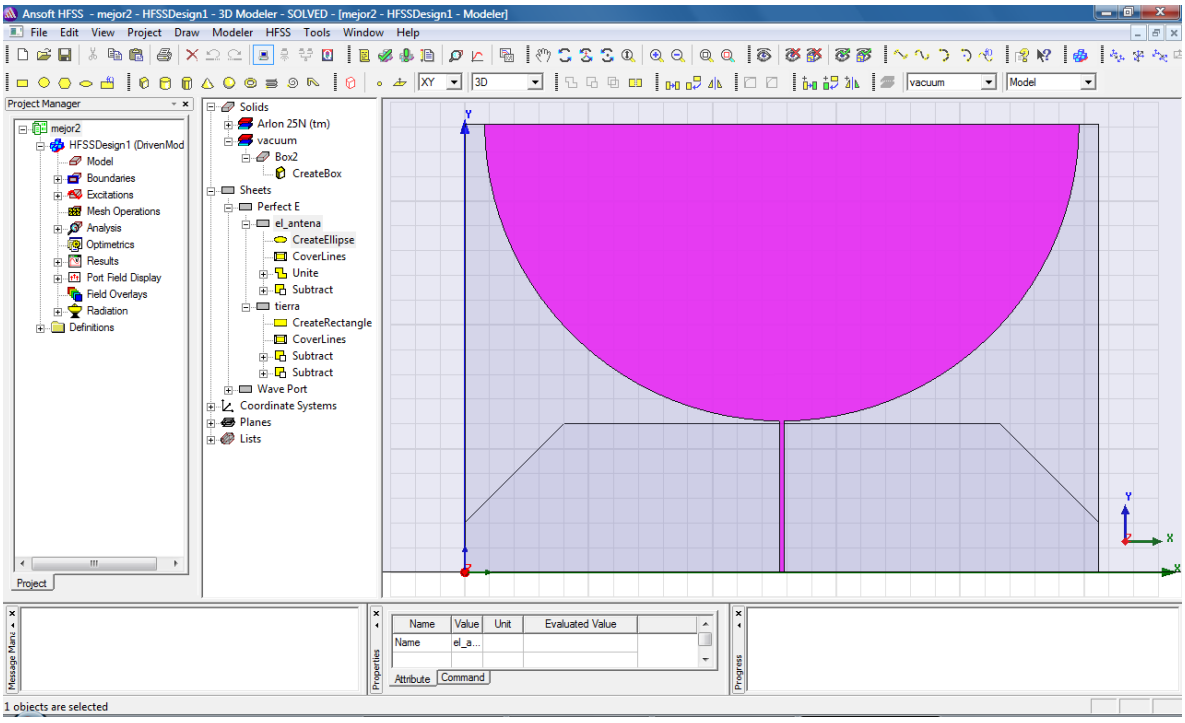

Fig. 3.2.1.1: Main HFSS11 window.

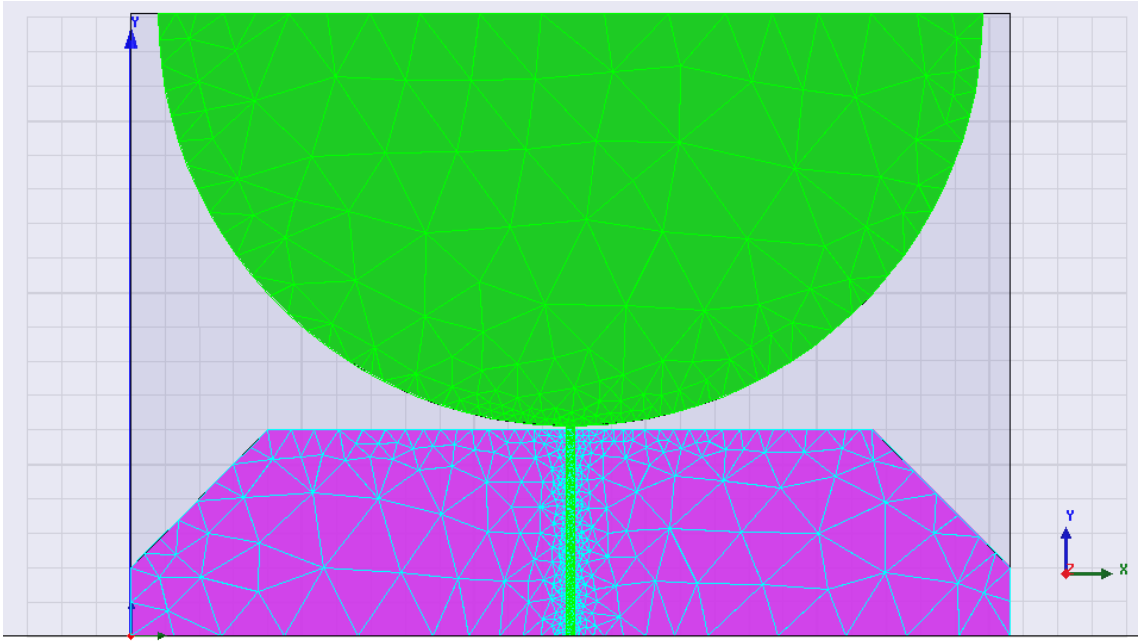

Figure 3.2.1.2: Generated mesh to solve the antenna design employing the finite element method

In general, the finite element method divides the full problem space into thousands of smaller regions and represents the field in each sub-region (element) with a local function. One feature of this method is that in areas of interest, the resolution of elements (Mesh) becomes denser in order to obtain more accurate predictions. Fig. 3.2.1.2 shows an example of how the antenna is divided into smaller sections and then apply the finite element method and Fig. 3.2.1.3 shows the higher density of elements.

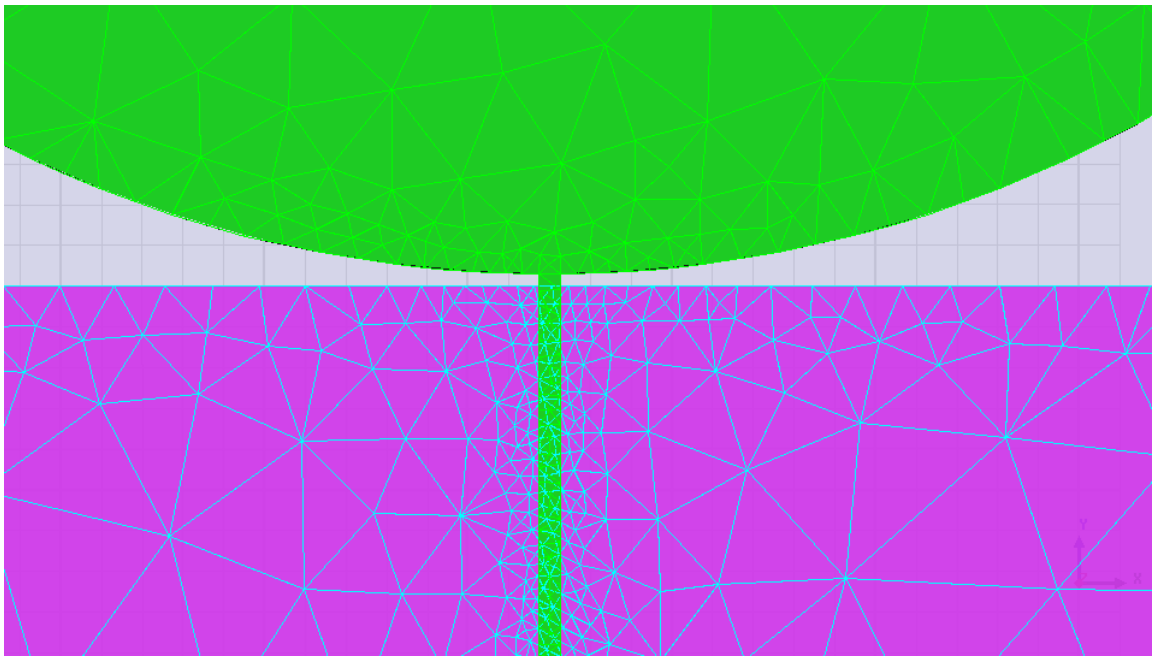

Figure 3.2.1.3: Higher density of elements to obtain a more accurate result

3.3 Antenna Simulations

In this section, we will explain the process for the design and choice of two UWB antennas that were subsequently built. A bandwidth covering form 900 MHz - 6 GHz (so that the main 900/1800 GSM downlink bands and the 2.4 - 2.5 GHz ISM band, were covered) and not very large physical dimensions were the main characteristics desired for our antennas. The results of the simulations and parametric studies will be shown and analyzed. According to these studies, the best antenna was chosen and then, a modification to the ground plane was made; this analysis will be detailed later. After this last modification, the antenna was built and we will call it, from now on, base-antenna.

In order to reduce the size of the base-antenna, but maintaining the bandwidth, miniaturization techniques were applied, a parametric study of this process will be included and explained, to be then built; we will call this antenna, from now on, size-improved antenna.

For the design of our antennas, we have started with a single shape, and, according to the simulation results and references, we have tuned some parameters to reach the best possible performance. The table 3.3.1 shows the parameters of the available substrate.

Table 3.3.1: Dielectric parameters

	Arlon 25N (A25N)
Er	3.38
TanD	0.0025
H	0.508mm
Cond (copper)	5.813×10^7

3.3.1 Base Antenna

For antenna design we have not followed a parametric design procedure. The design has started with a pre-existing half disc antenna and we have adapted it to our needs through simulations. We have varied the parameters shown in Fig. 3.3.2.1. In general terms, the main differences between a full disc antenna and the half disc are that low frequency limit of the band increases slightly, but the phase response remains linear, also, the received peak amplitude is also deceased by about 20% from the disc antenna [18]. This is not a large penalty for obtaining the substantial shortening of the height to half of the original disc antenna. A small size and a broadband antenna are our main goals.

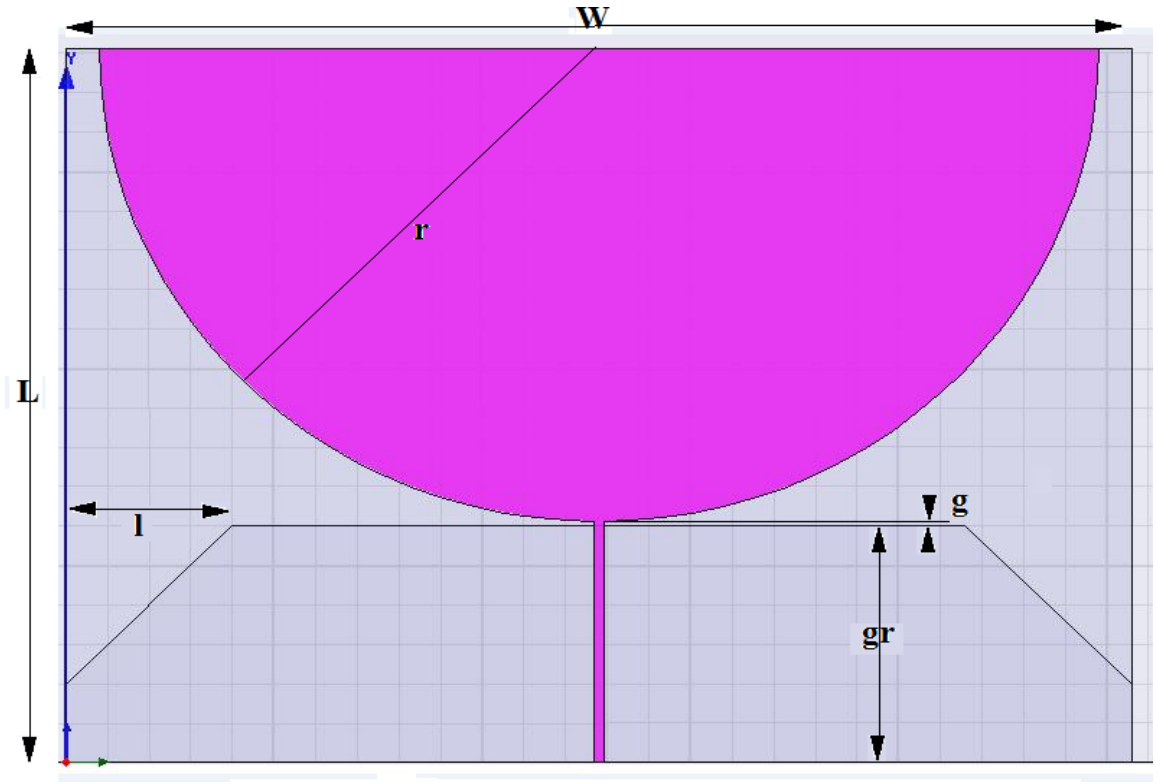

Fig. 3.3.1.1: 2D view of the base-antenna.

As if it were a circular monopole patch, the radius r of the circle is the main parameter to optimize for the lowest return loss and widest bandwidth. We will do a parametric sweep of "r" while the other parameters are kept constant. Fig. 3.3.1.1 shows the behavior of changing this parameter; we can observe that as the radius of the circle increases, the lower frequency decreases.

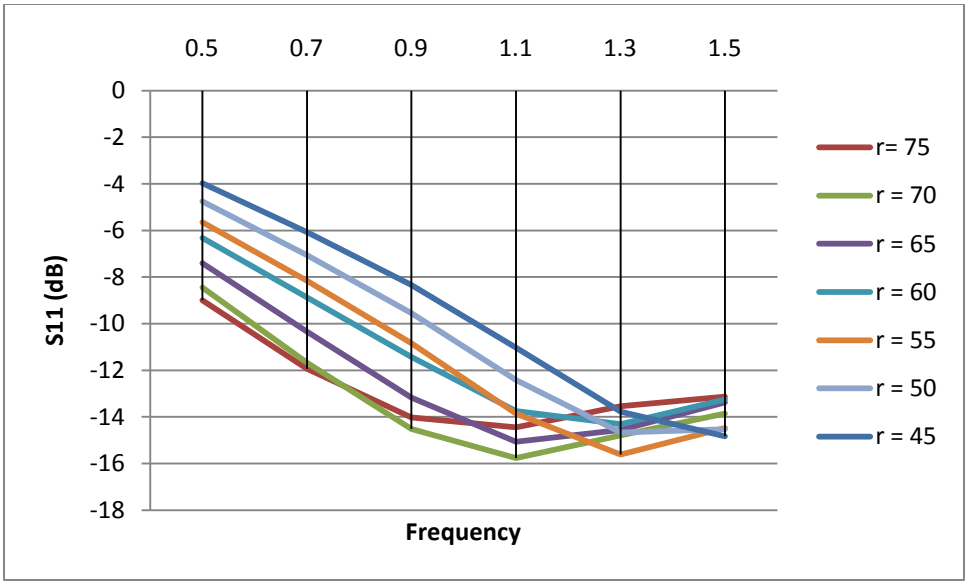

Fig. 3.3.1.2: low-frequency return-losses as a function of the "a" parameter

The following parameter to tune is the gap between the patch and ground plane ("g"). Parameter is stated to:

- Have positive value if the patch is at a higher level than the ground layer.
- Have null value when the ground plane ends where the patch begins.
- Have a negative value if the patch and ground layer overlap.

Since the simulation software does not accept negative values, we have denoted the parameter "h" as "g + gr", and the ground plane height is 30mm.

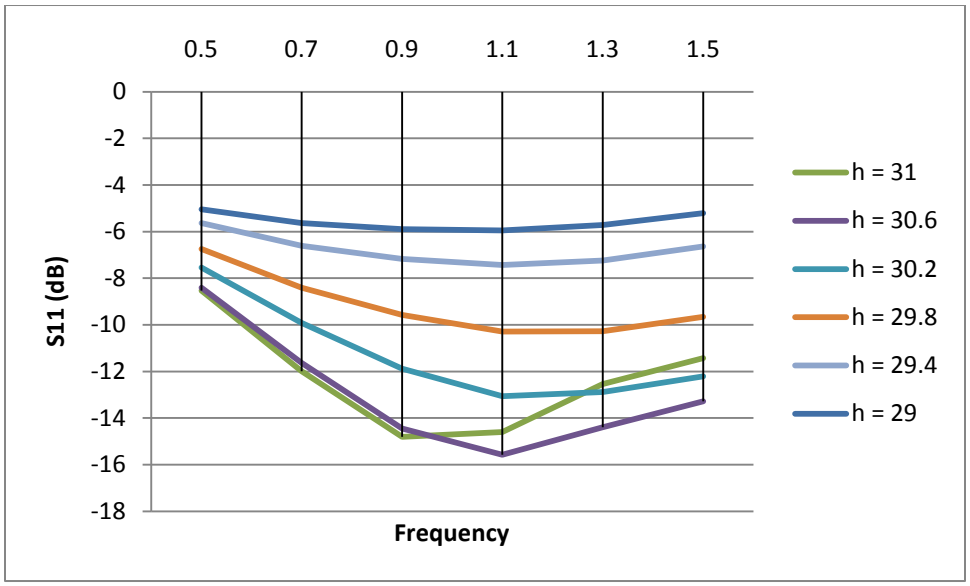

Fig. 3.3.1.3: low-frequency return-losses as a function of the "a" parameter

From Fig. 3.3.1.3 we can conclude that the best performance value is h = 30.6 mm (g = 0.6 mm)

3.3.2 Ground Modification

To improve the bandwidth of the antenna, we have removed the upper corners of the ground plane and we will vary them to reach the best performance. Fig. 3.3.2.1 shows the results of the variation of the "l" parameter. It also shows that "l" has not considerable effect at low frequencies. But at frequencies above 1 GHz is a noticeable difference.

Fig.3.2.2.3 shows the radiation patters for each frequency and Fig. 3.2.2.4 represents the gain pattern of the base-antenna

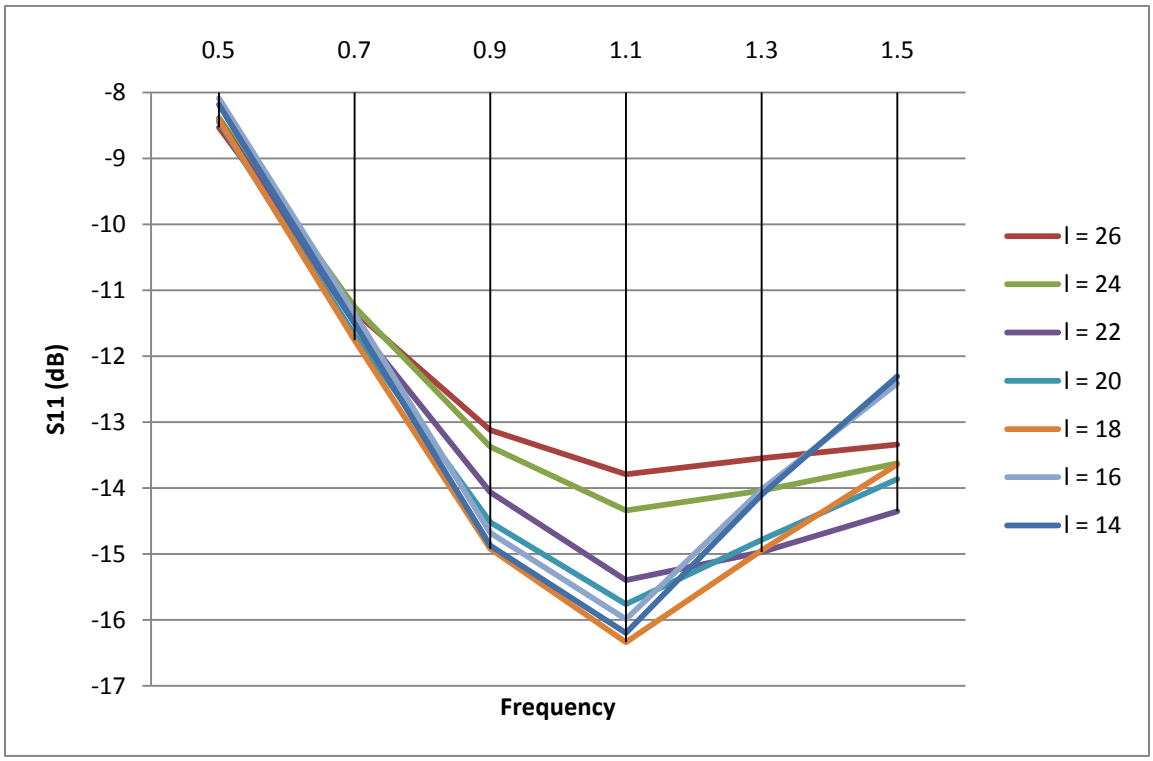

Fig. 3.3.2.1: low-frequency return-losses as a function of the "l" parameter

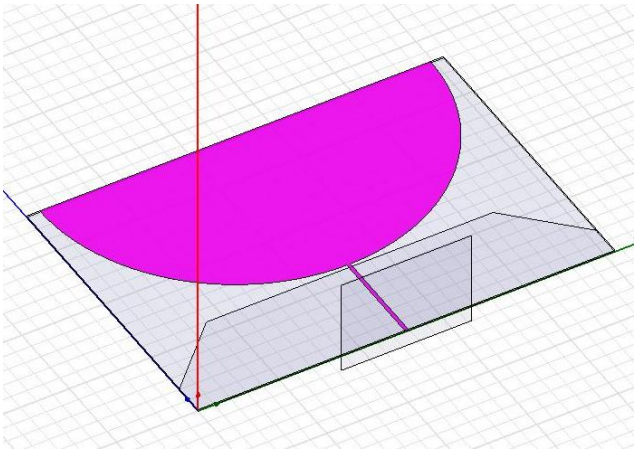

Fig. 3.3.2.2: 3D view of the base-antenna (HFSS11)

Table 3.3.2.1: Final values for the base-antenna, the name of the values are taken from Fig. 3.3.2.2.

Name	Value
L	100,6 mm
W	148 mm
l	20 mm
gr	30 mm
g	0.6 mm
r	70 mm

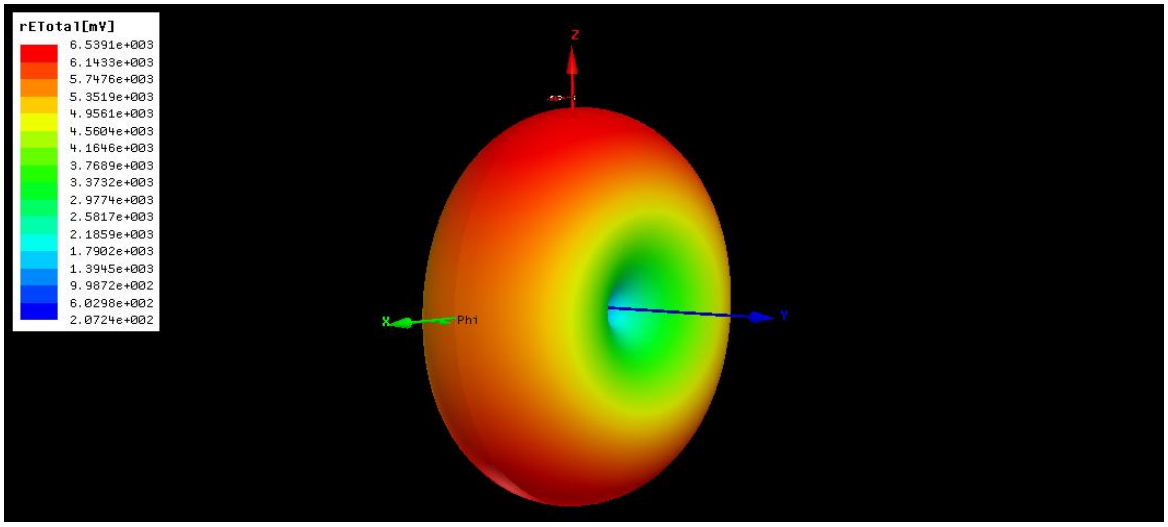

(a)

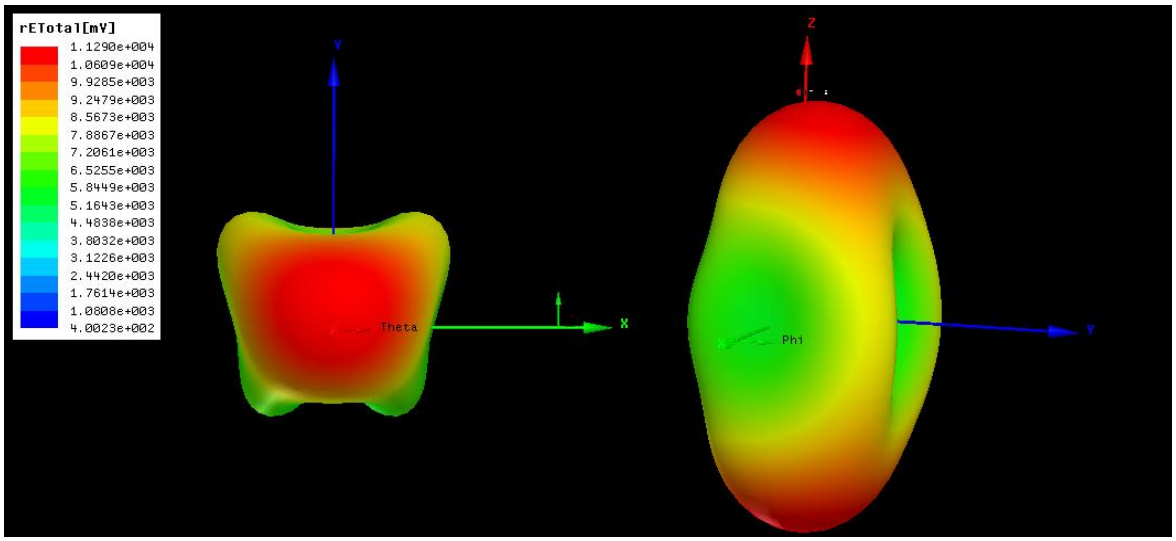

(b)

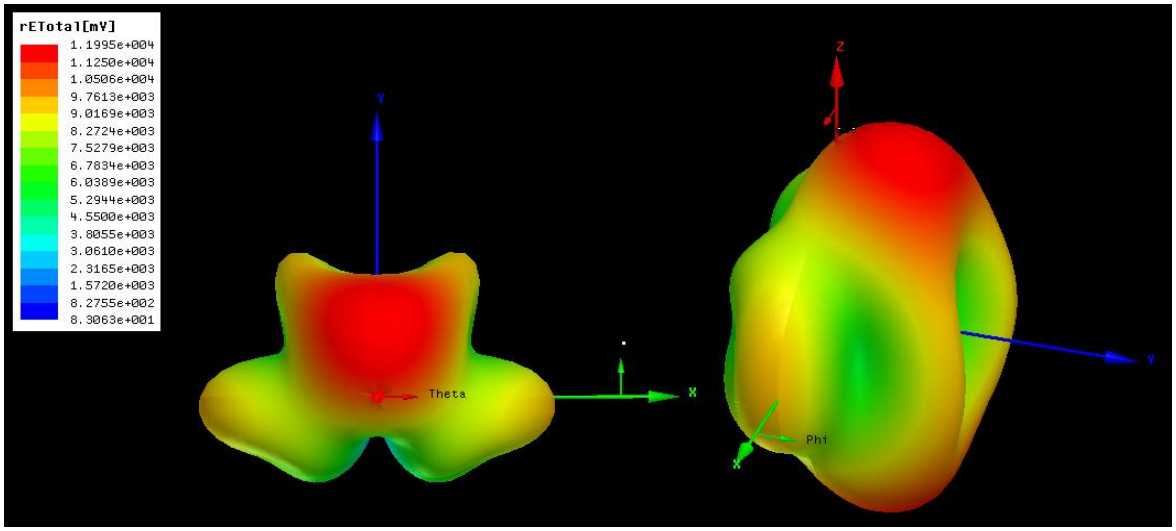

(c)

Fig. 3.3.2.3: Base-antenna radiation patterns at (a) 900 MHz, (b) 1.85 GHz and (c) 2.45 GHz

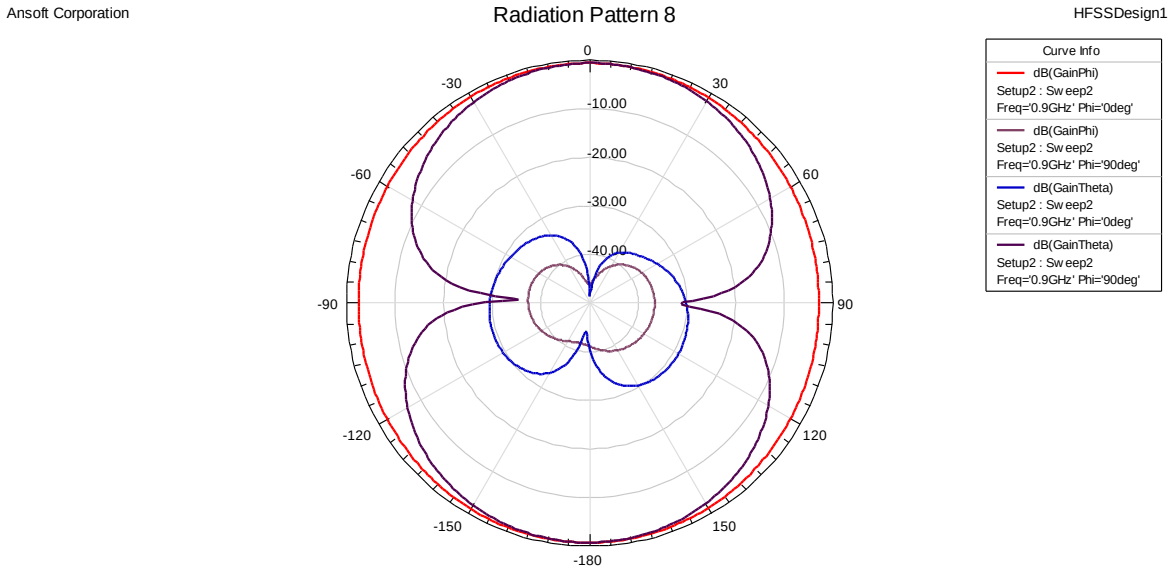

Fig. 3.3.2.4: base-antenna gain pattern at 900 MHz

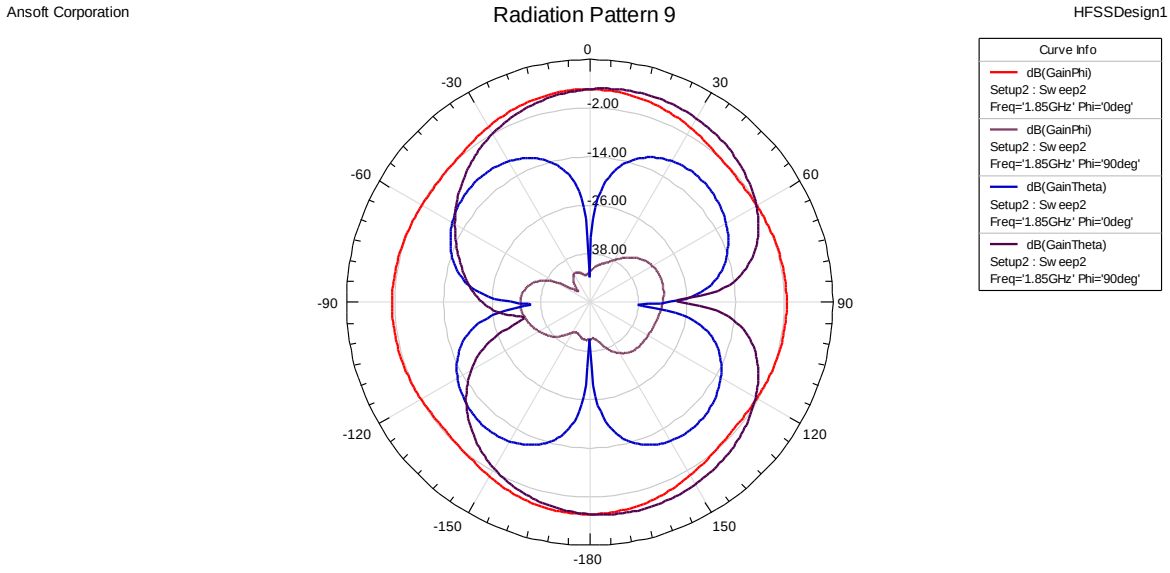

Fig. 3.3.2.5: base-antenna gain pattern at 1.85 GHz

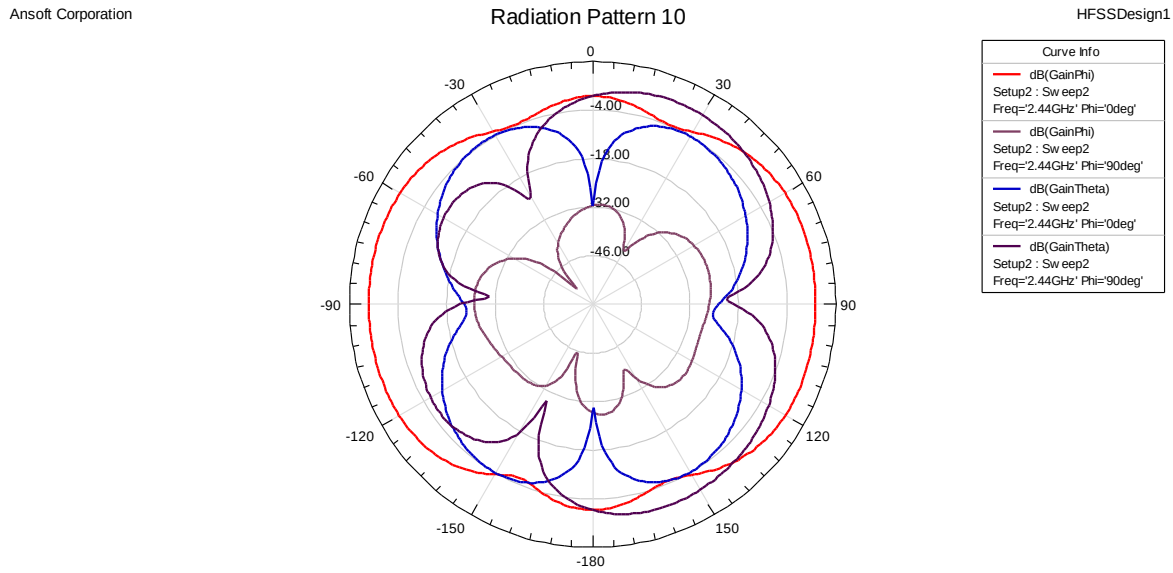

Fig. 3.3.2.6: base-antenna gain pattern at 2.45 GHz

3.3.3 Miniaturization Techniques

This section is intended to reduce the size of the design that we had previously. In [19], a series of procedures that aim to alter the current distribution at the antenna surface by inserting a slot is shown. As we have a different antenna (in the paper is a rectangular antenna), we cannot guide from the slot dimensions that are presented in this paper.

To overcome this, we'll perform simulations by varying some parameters to finally choose appropriate slot values.

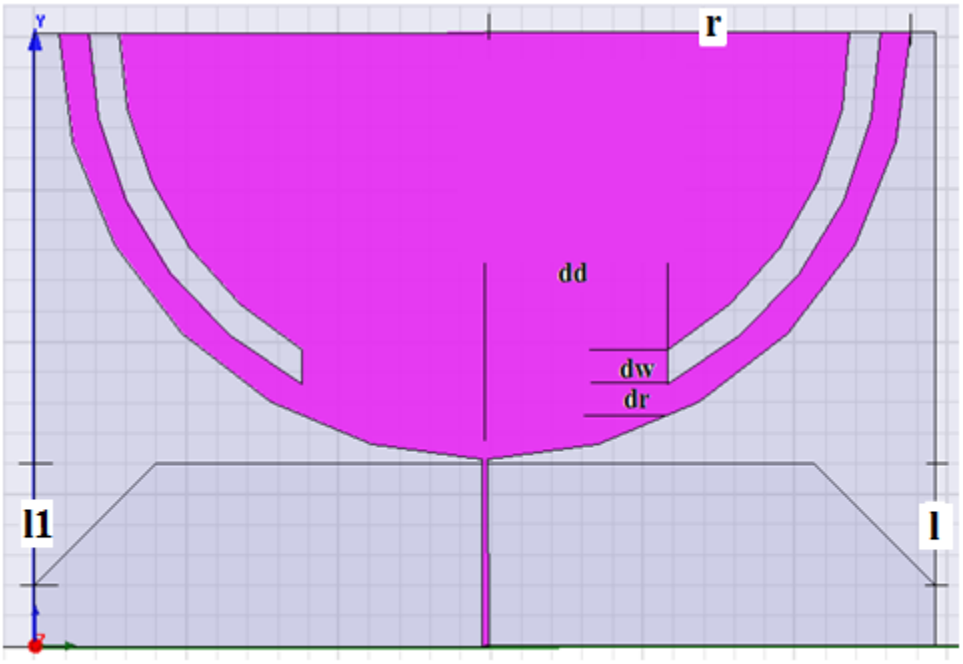

Fig. 3.3.3.1: Slotted antenna and its parameters

Fig. 3.3.3.1 shows the first slotted antenna prototype. The dimensions of the slot are denoted with the "dd", "dr", "dw" variables. We will vary each one of these parameters in a given range to see how they affect the antenna performance.

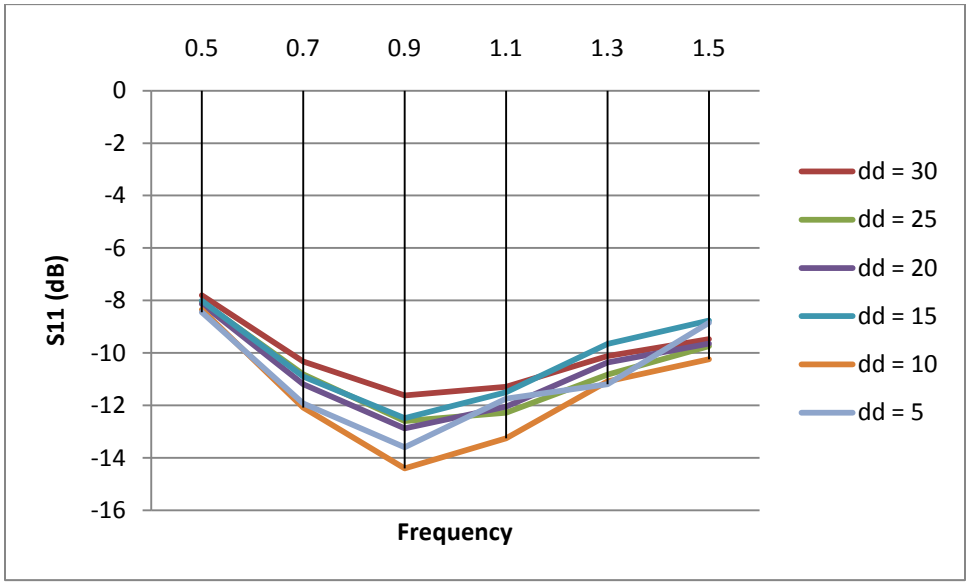

Fig. 3.3.3.2: low-frequency return-losses as a function of the “dd” parameter

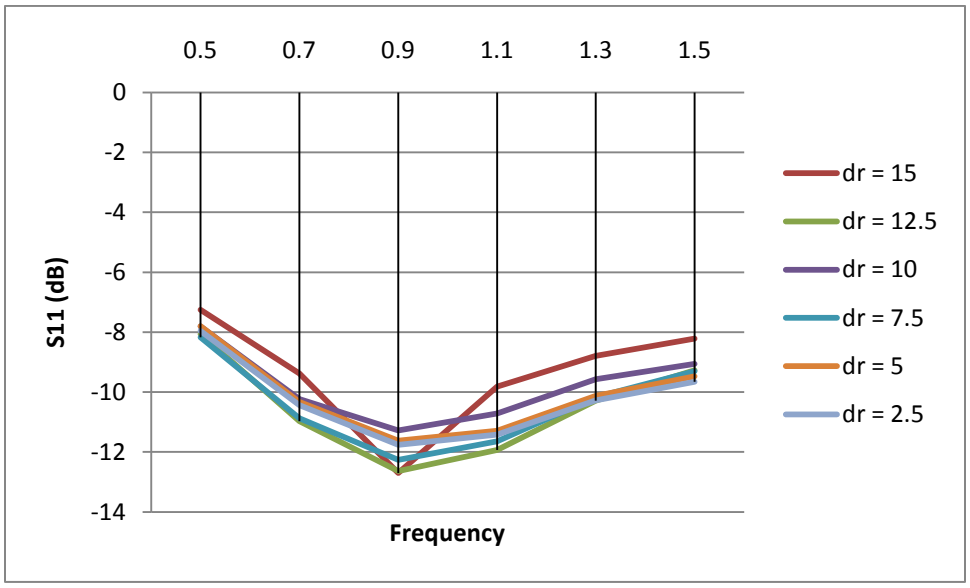

Fig. 3.3.3.3: low-frequency return-losses as a function of the "dr" parameter

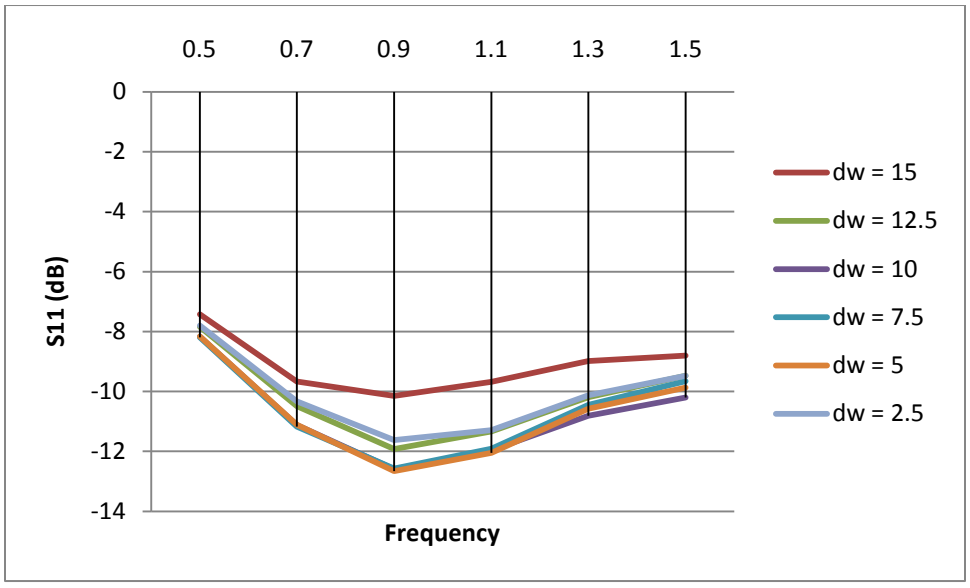

Fig. 3.3.3.4: low-frequency return-losses as a function of the "dw" parameter

After seeing these parametric simulations, we can observe that the slot length has effect on the impedance matching, especially at low frequencies. The width and location of the slot slightly influence the low frequencies. In general, all parameters related to the slot have some influence in the impedance matching.

The next step is to reduce overall the size of the antenna; in this step reduction will be done by reducing the radius "r" of the semi-circle. Because of the total dimensions of the substrate are as a function of the radius, they are automatically accommodated after a radius change. Fig. 3.3.3.5 shows how return loss varies by changing this parameter.

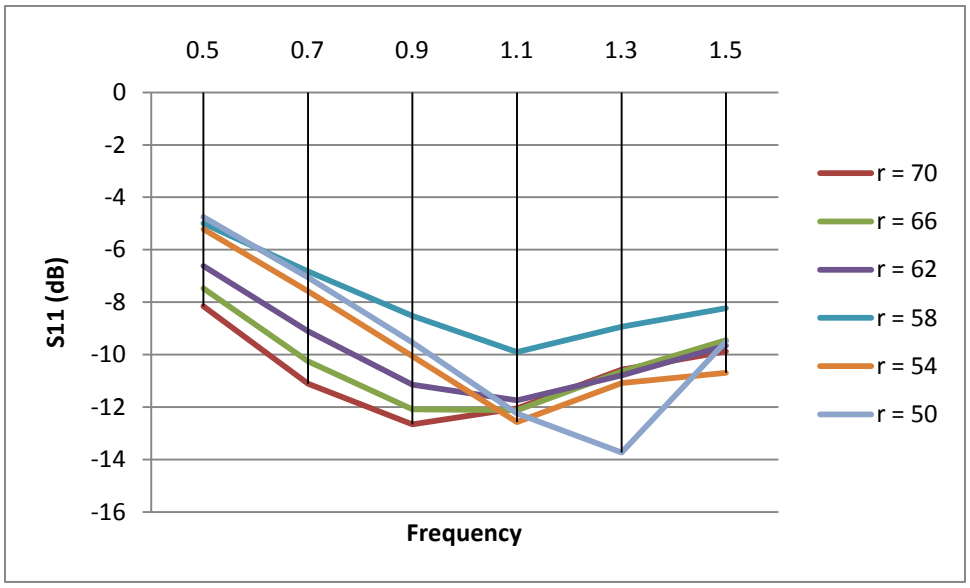

Fig. 3.3.3.5: low-frequency return-losses as a function of the "a" parameter

After seeing the results in Fig. 3.3.3.5, we have decided to reduce the radius "r" from 70mm to 60mm, with this adjustment, dimensions of the substrate, have been reduced from 148mm x 100mm to 120mm x 90.6, 19% and 9.4% respectively. Because of the change of th antenna, the response is not the same, but as we know the behavior of each parameter we have adjusted them and the final values now are: dd:14mm, dr:10mm and dw:7mm.

The next antenna design will intend to reduce even more the previous antenna design by inserting an angle cut as we know that current distribution is supposed to concentrate close to the slot (we will verify this in section 3.3.4), then, we will try to concentrate it in one slot. The next step is to make an angle cut to the patch. Fig. 3.3.3.6 shows the way we will do this, we will use the middle line of our antenna as a reference, and moving to the left, we will find the proper angle.

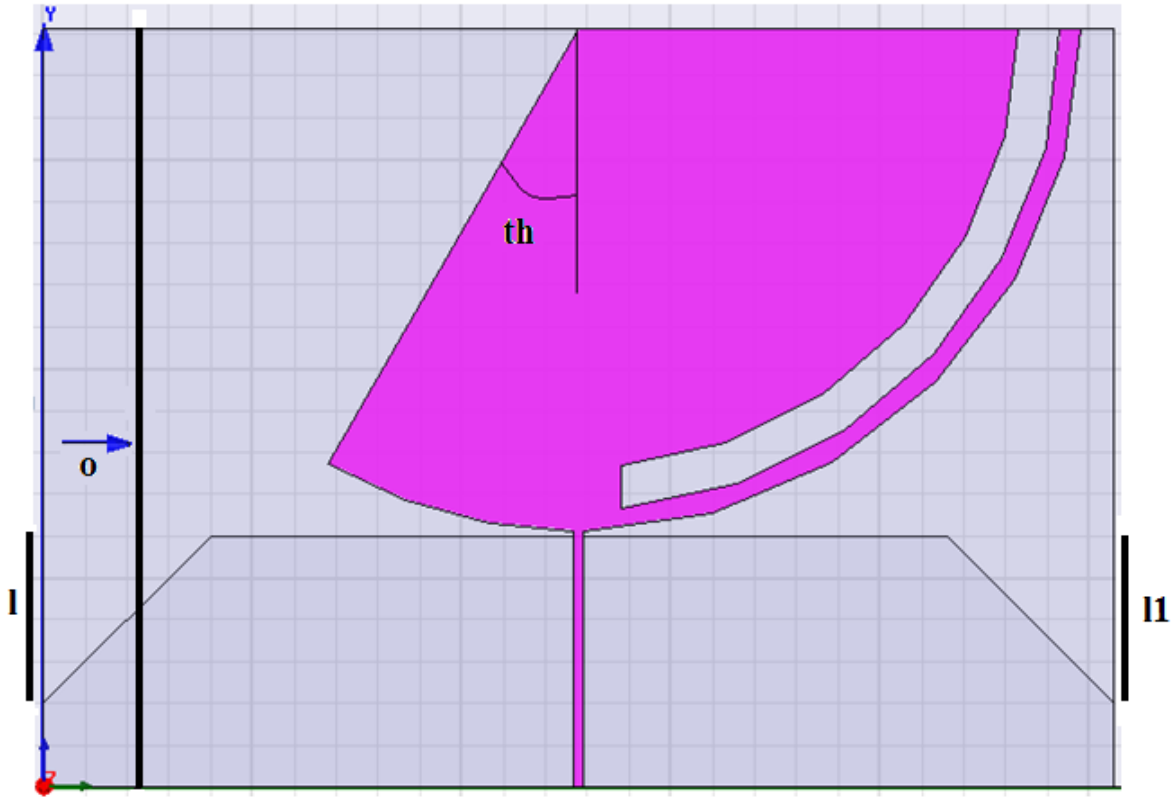

Fig. 3.3.3.6: shows the antenna and the "th" parameter

From Fig. 3.3.3.7, we can conclude that as the angle increases, frequencies above 1GHz change their performance dramatically. Lower values of "th" are desired, because they would provide us more free-area in the left side of the antenna.

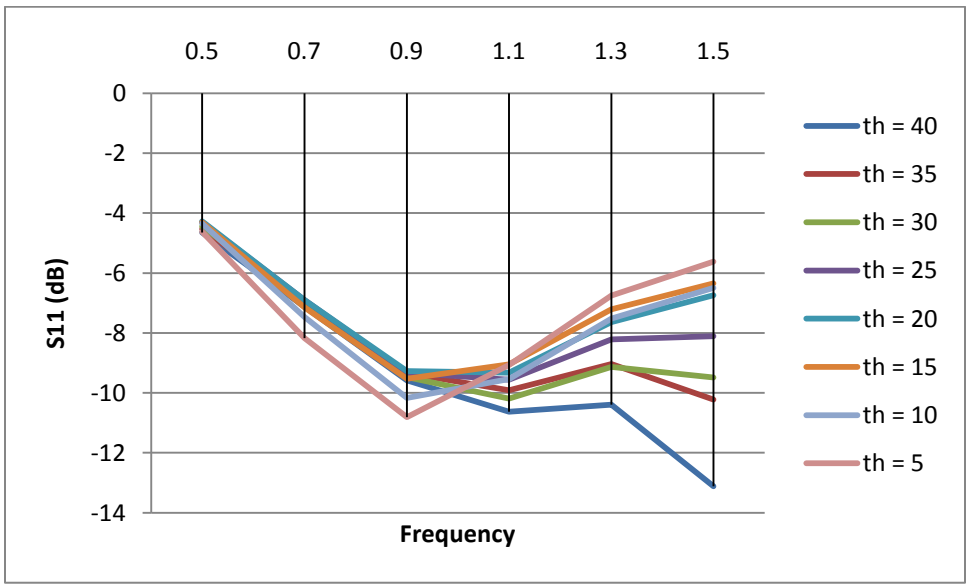

Fig. 3.3.3.7: low-frequency return-losses as a function of the "th" parameter

After choosing a particular angle of cut, the next step is to cut the substrate starting from the left edge. The parameter "o" indicates the number of millimeters that we will cut the substrate. For this simulation, we have determined that the angle "th" will be 30 degrees, as it is a good balance between return loss and space saving. Fig. 3.3.3.8 shows the response of the parameter "o", we can conclude that a nice cut value is 8mm.

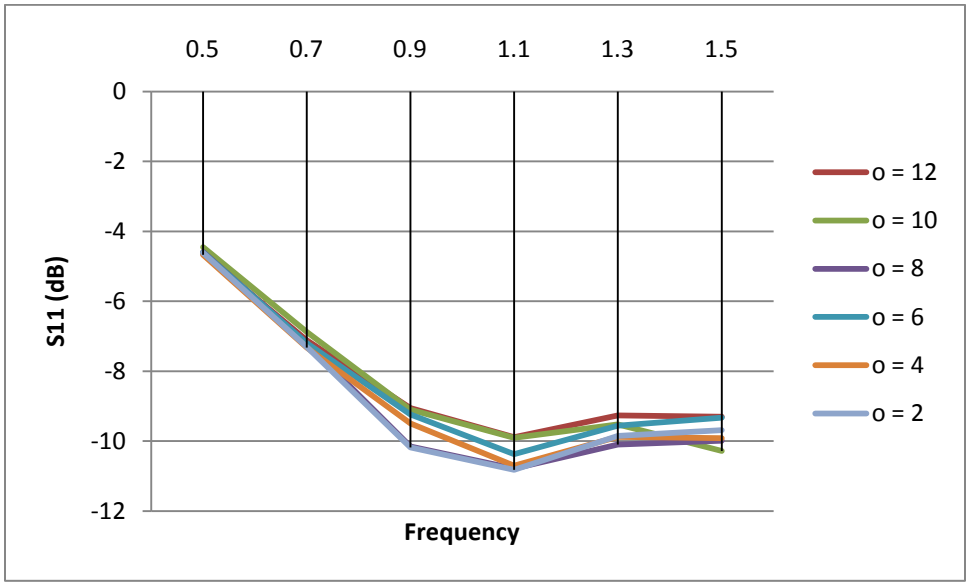

Fig. 3.3.3.8: low-frequency return-losses as a function of the “o” parameter

The next step is to try to improve the ground plane, for this issue we have tried the following (remember that until now, we have two edges, each one of 20mm at both sides of the antenna):

- Keeping the right edge (l = 20mm) and varying the value of the edge of the left (l1).
- Keeping the left edge (l1 = 20mm) and varying the value of the edge of the right (l).

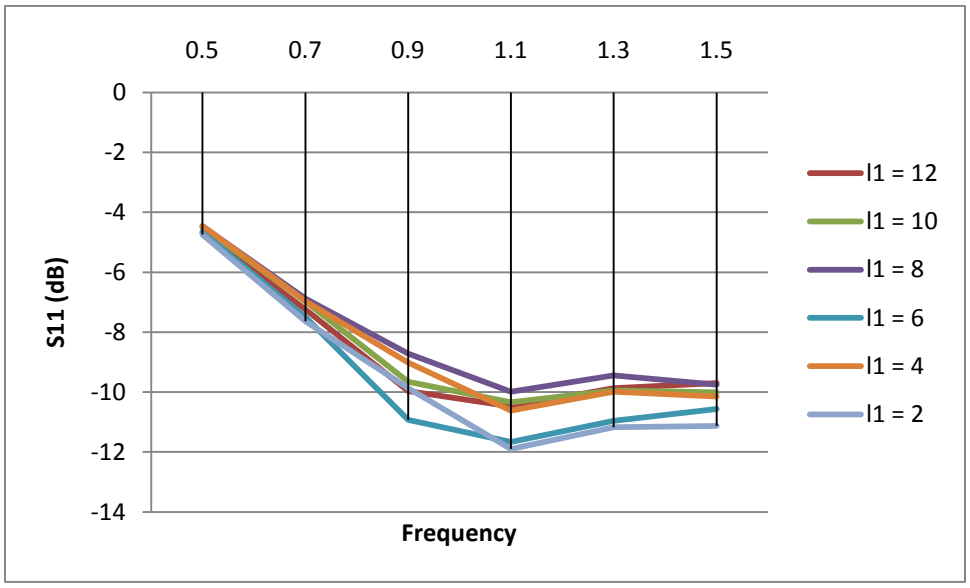

Fig. 3.3.3.9: low-frequency return-losses as a function of the "l1" parameter

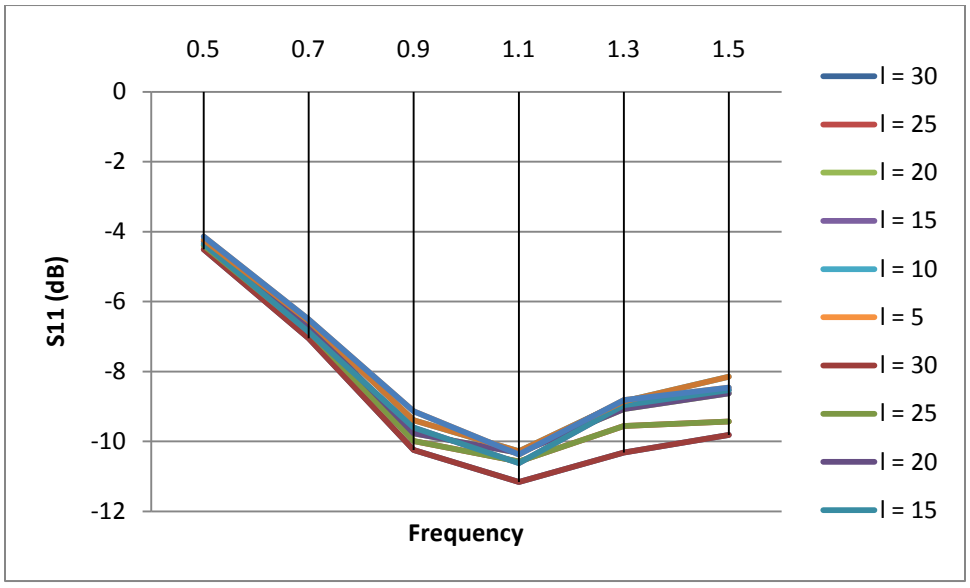

Fig. 3.3.3.10: low-frequency return-losses as a function of the "l" parameter

Because a variation of the left edge has provided better results, and moreover, a low value for the left side has shown a good performance (Fig. 3.3.3.9), we have decided to cancel the left edge and perform another simulation varying the right edge.

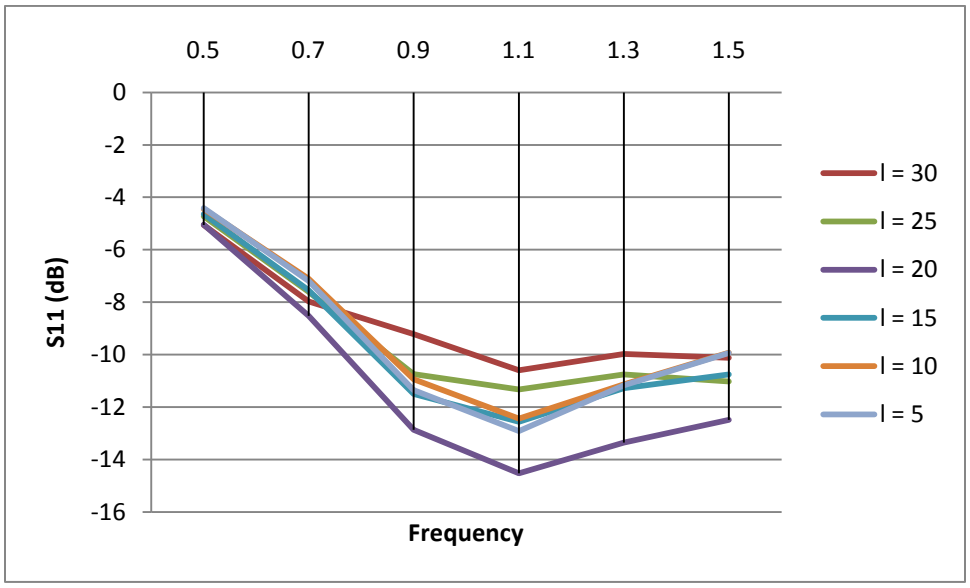

Fig. 3.3.3.11: low-frequency return-losses as a function of the "l" parameter

From Fig. 3.3.3.11 we can conclude that the best performance was obtained by removing the left edge and by maintaining the right edge with 20 mm side long.

3.3.4 Size-Improved Antenna

After having analyzed each of the previous settings and after making many simulations, we have concluded that the antenna to be manufactured would be the one shown in Fig. 3.3.4.1. We had to make a consideration with the angle of cut, as the most optimum was "th = 40", but because with this value the overall size of the antenna was almost the same, a compromise between S11 and dimension is made, so we choose the 30 degree angle.

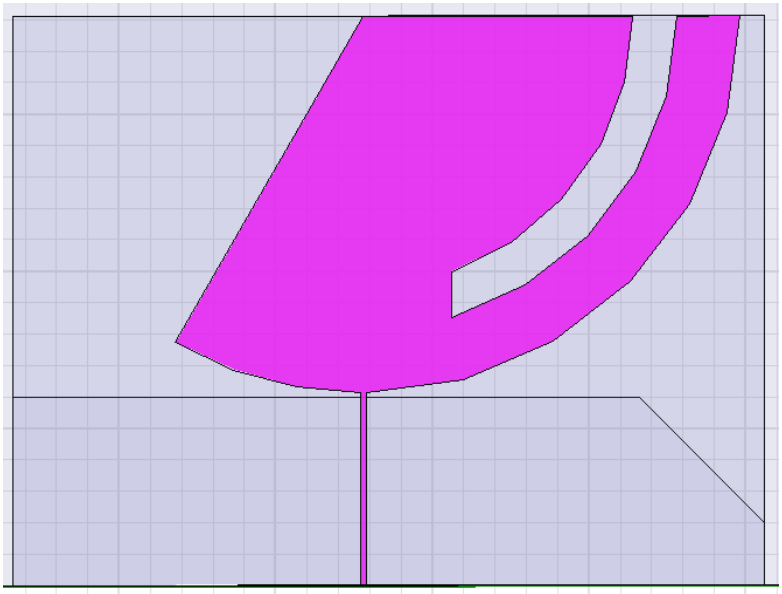

Fig. 3.3.4.1: Size-Improved antenna.

Table 3.3.2.1: Final values for the 2D base-antenna, the name of the values are taken from Fig. 3.3.3.1 and Fig. 3.3.3.6

Name	Value
L	90.6 mm
W	120 mm
l	20 mm
gr	30 mm
g	0.6 mm
r	60 mm
dd	14 mm
dr	10mm
dw	7mm
th	30 degrees
o	8mm

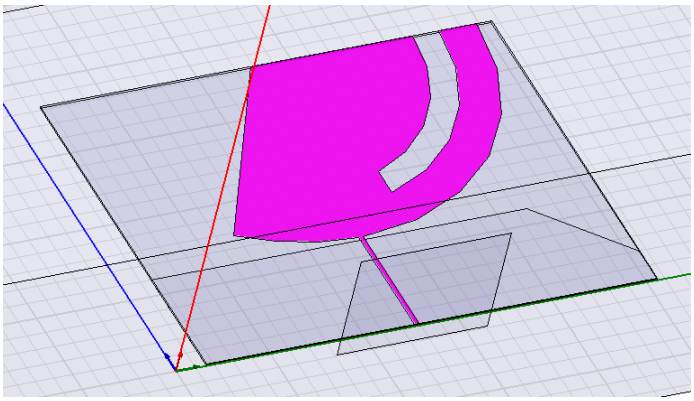

Fig. 3.3.4.2: 3D view of the size-improved antenna (HFSS11)

As explained above, now that we have decided on our new size-improved antenna values, the current distribution between the antennas are not the same. In the following figures we will appreciate that, as for the radiating patch and for the ground plane as well, the current distributions have changed. The differences for each frequency could also be seen clearly.

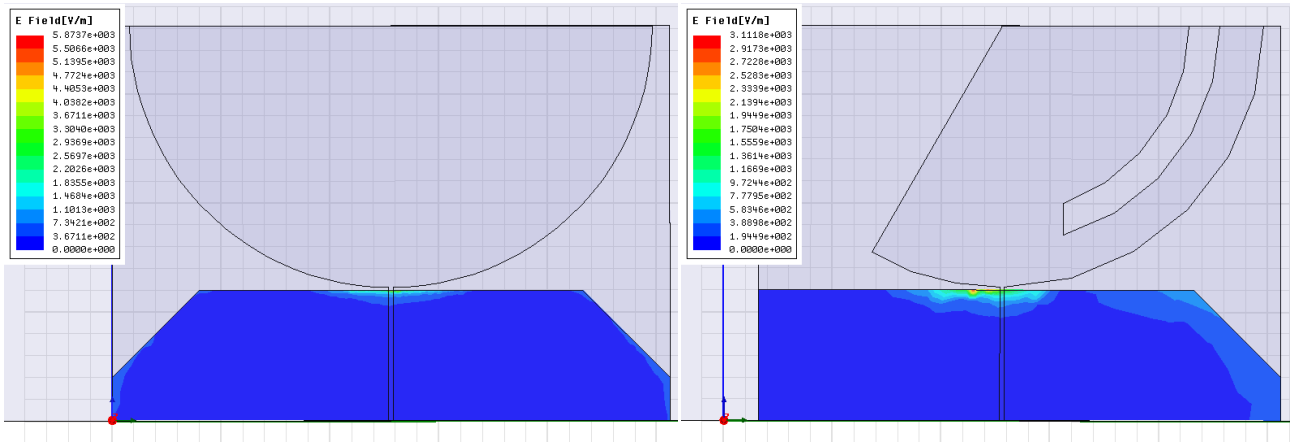

(a)

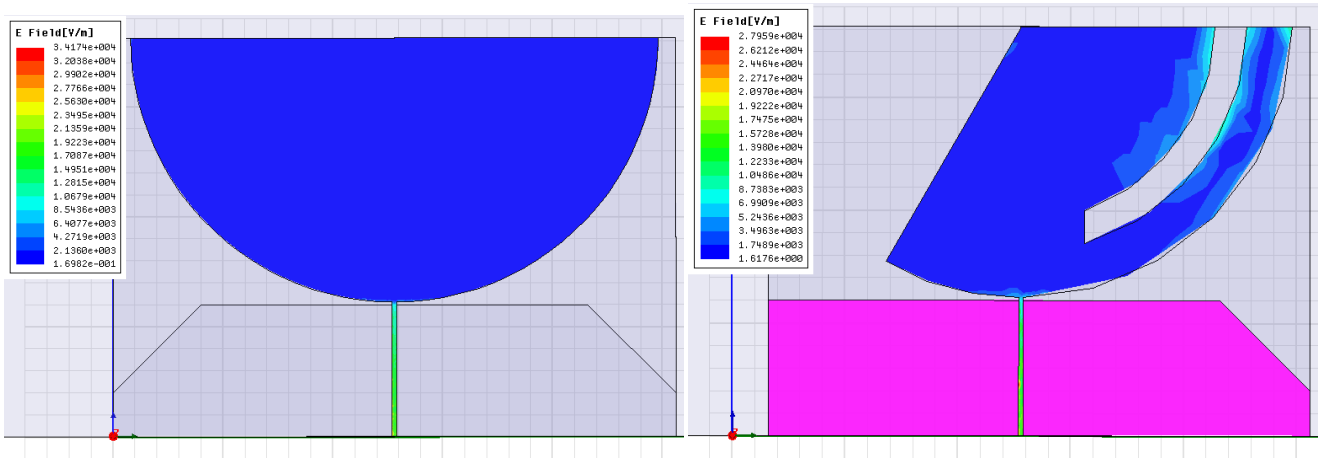

(b)

Fig. 3.3.4.3: Current distributions for (a) ground plane and (b) radiating patch at 900 MHz

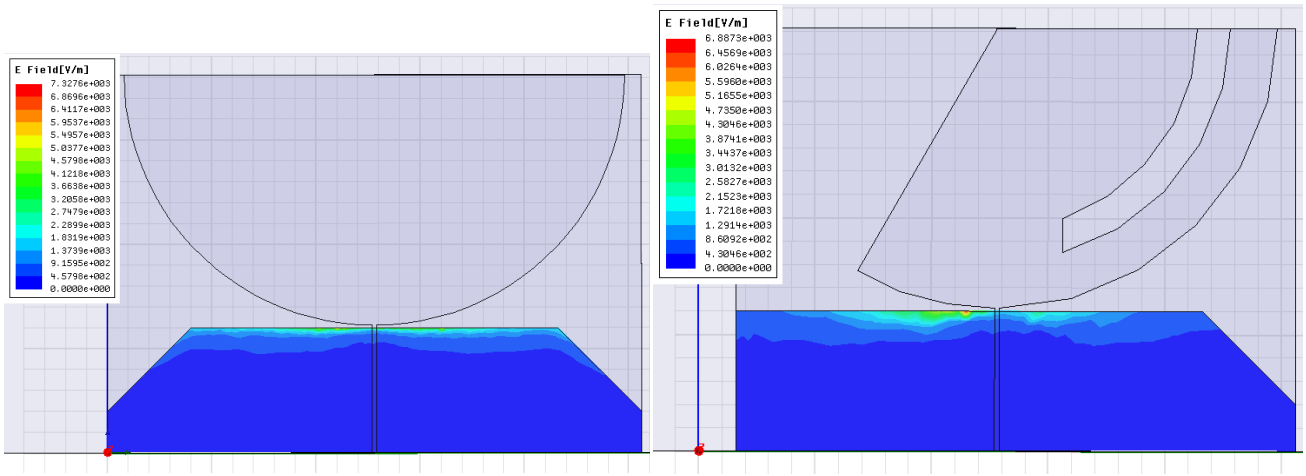

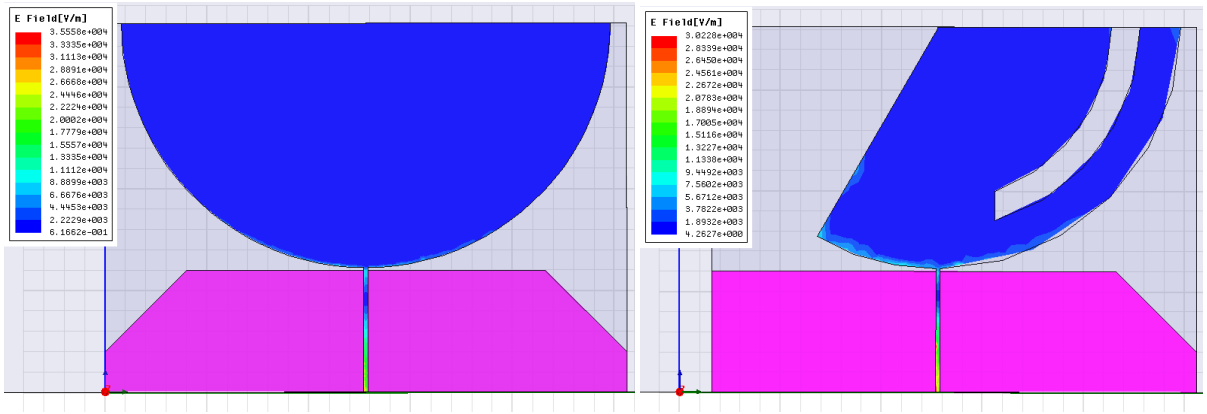

Fig. 3.3.4.4: Current distributions for (a) ground plane and (b) radiating patch at 1.85 GHz

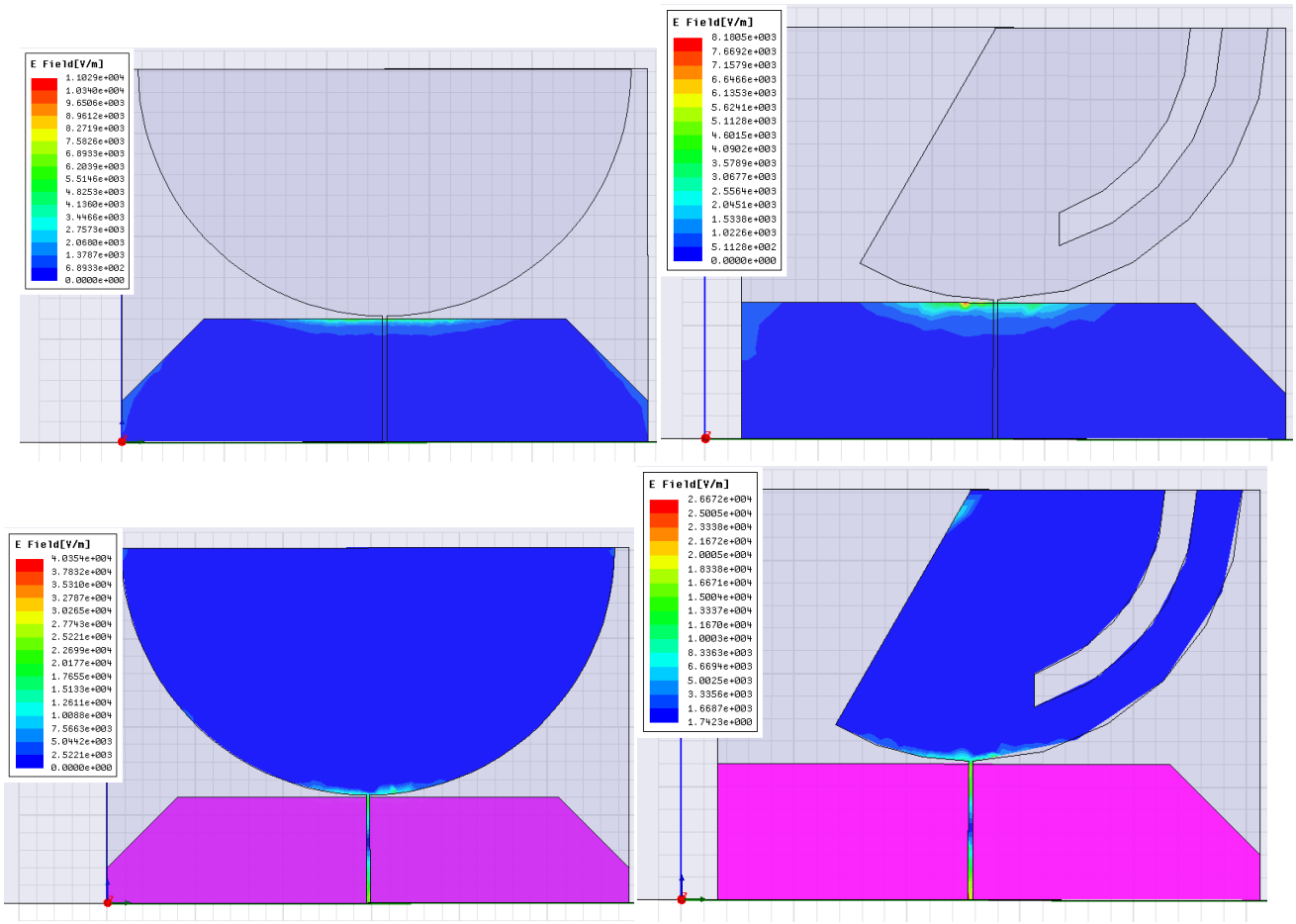

Fig. 3.3.4.5: Current distributions for (a) ground plane and (b) radiating patch at 2.45 GHz

We can see that for low frequencies, most of the current is concentrated around the right side of the antenna, where the slot is located. And we also can observe that the current on the left side of the antenna is very weak. The graphs also suggest that this behavior (current distribution) affects lower frequencies more than higher frequencies. For higher frequencies, we see that the current is distributed in the feed line and the base of the antenna.

Some of the drawbacks of applying these techniques miniaturization are that the result, as in our case, turns out to be asymmetrical. The feed lines, as well as the notch in the ground plane are no longer symmetrical. Direct consequence of this asymmetrical physical change is the radiation pattern.

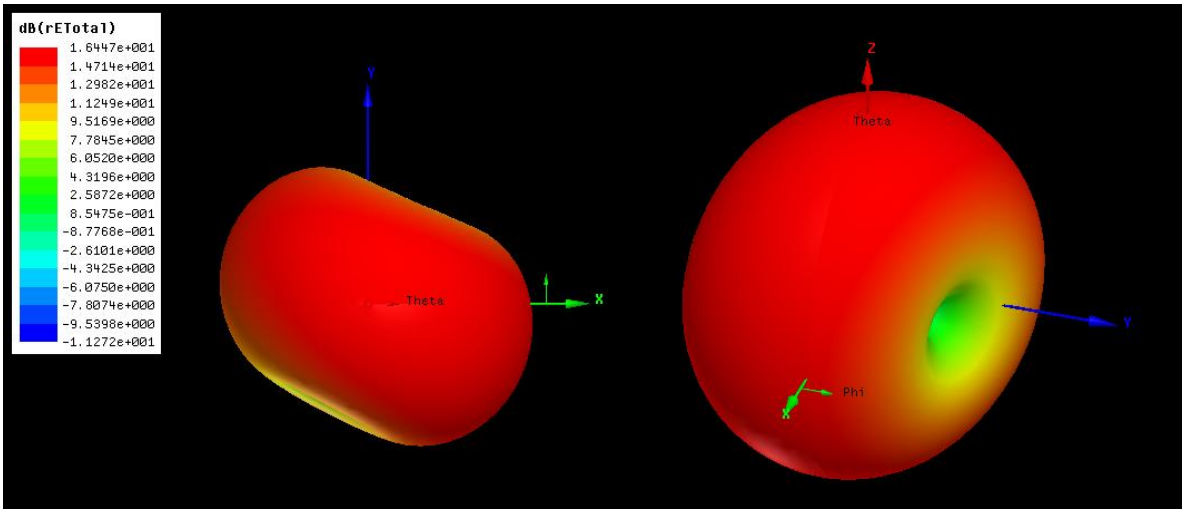

(a)

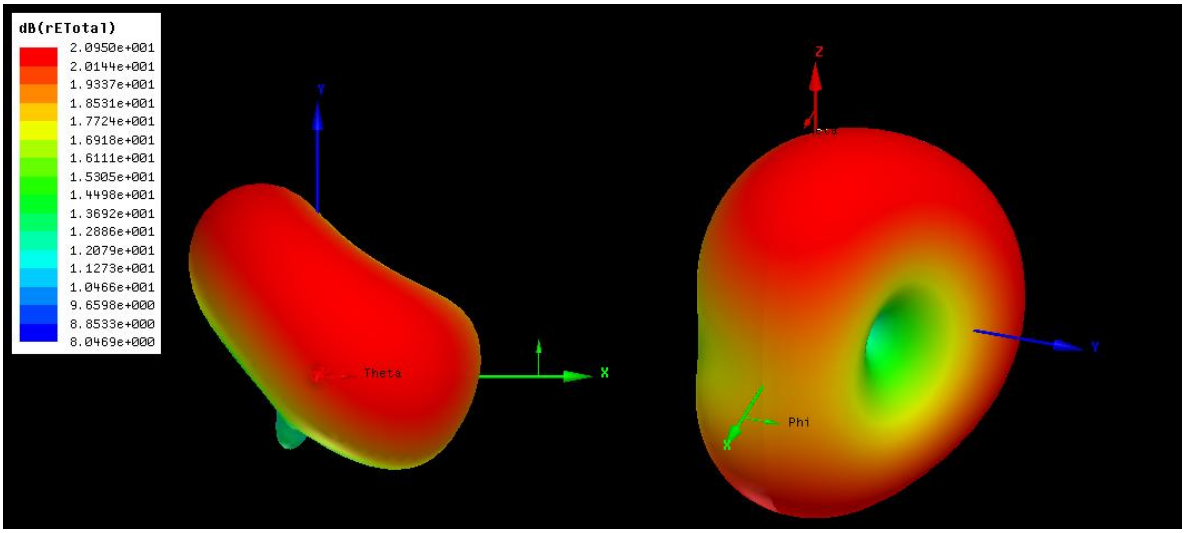

(b)

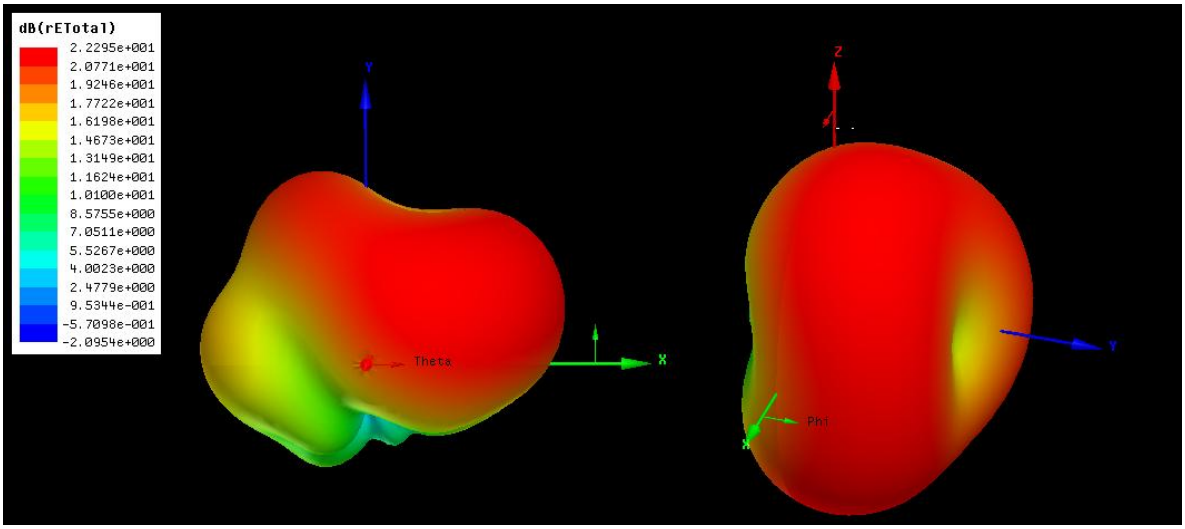

(c)

Fig. 3.3.4.6: Size-improved antenna radiation pattern at(a) 900 MHz, (b) 1.85 Ghz and (c) 2.45 GHz

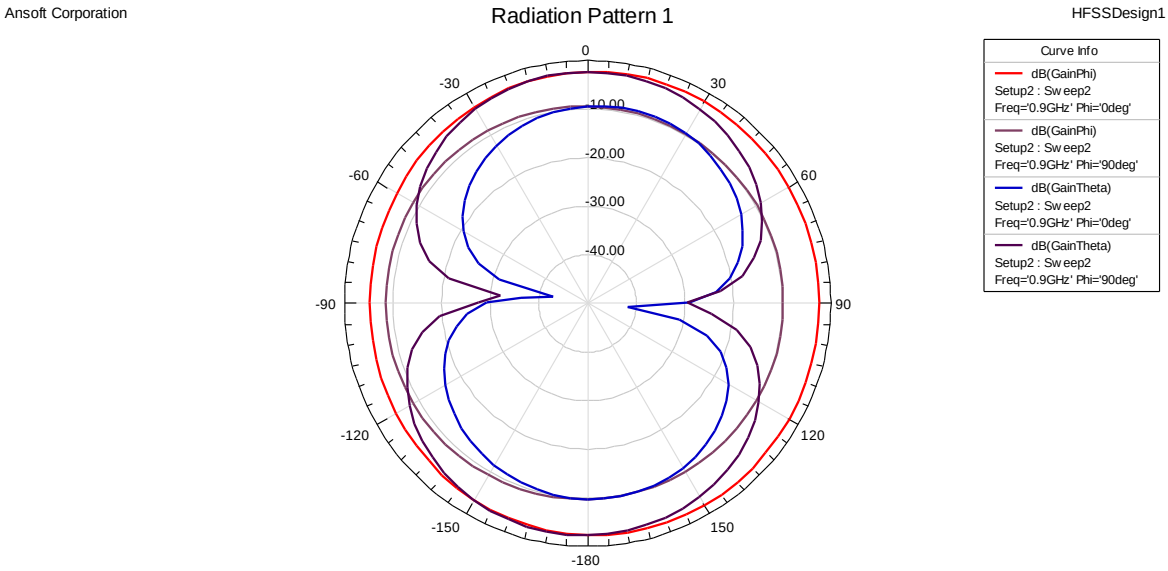

Fig. 3.3.4.7: Size-improved antenna gain pattern at 900 MHz

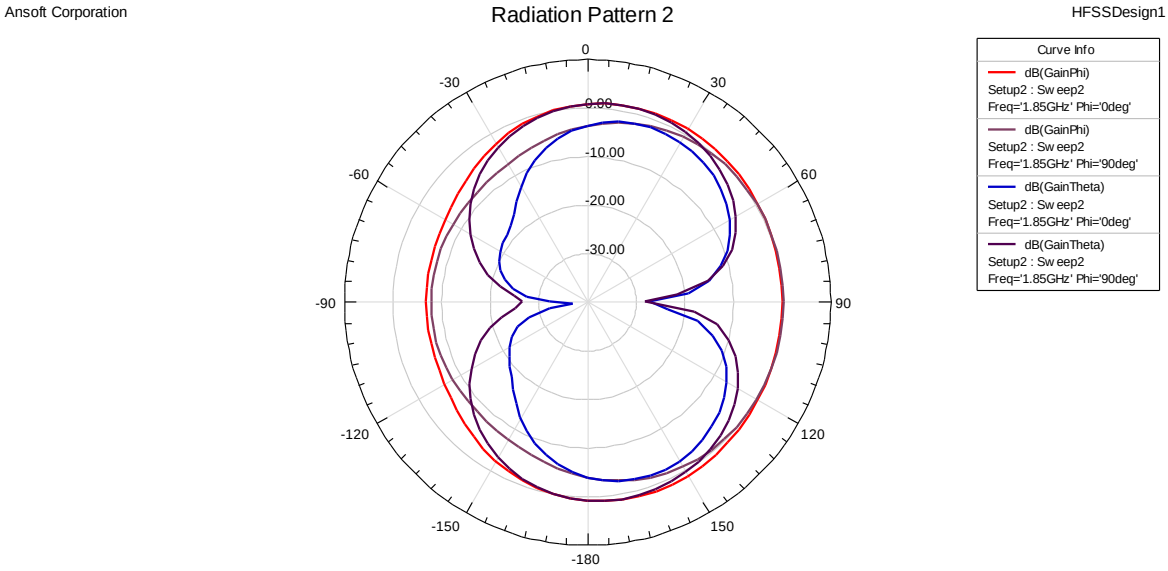

Fig. 3.3.4.8: Size-improved antenna gain pattern at 1.85 GHz

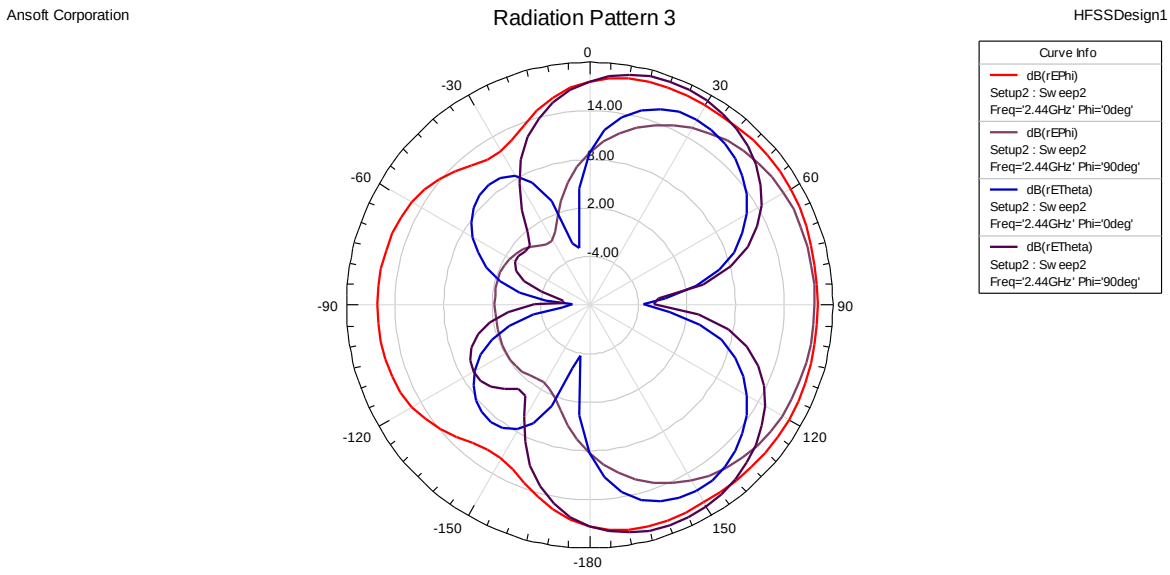

Fig. 3.3.4.9: Size-improved antenna gain pattern at 2.45 GHz

3.4 Antenna Fabrication and measurements

3.4.1 Fabrication

For the manufacture of the antennas, a LPKF Protomat C100 HF Milling machine (Fig. 3.4.1.1) was used. This machine has a set of drills to fit the milling desired size (Fig. 3.4.1.2). First we exported the antenna design file from the HFSS11 software to the software used by the machine. This machine cuts the metal layer of the used substrate (A25N) so that we "draw" the antenna shape (Fig 3.4.4.2). After having the shape of the antenna, we have to turn the substrate to repeat the same procedure to "draw" the ground shape. After it, all the substrate is separated from the entire substrate plate by making a deeper cut. Then, using a hand cutter, we remove the exceeding copper layers (Fig. 3.4.1.4) that are not part of our antenna design. Finally, we have to solder a 3.5mm SMA female connector on the fed line.

Fig 3.4.1.1: Milling machine

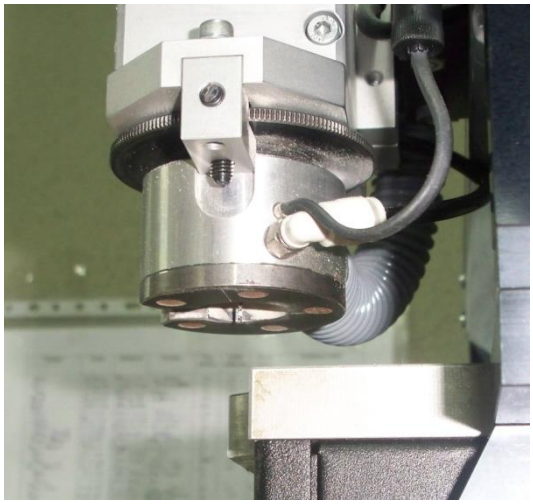

Fig 3.4.1.2: Cutting Drill

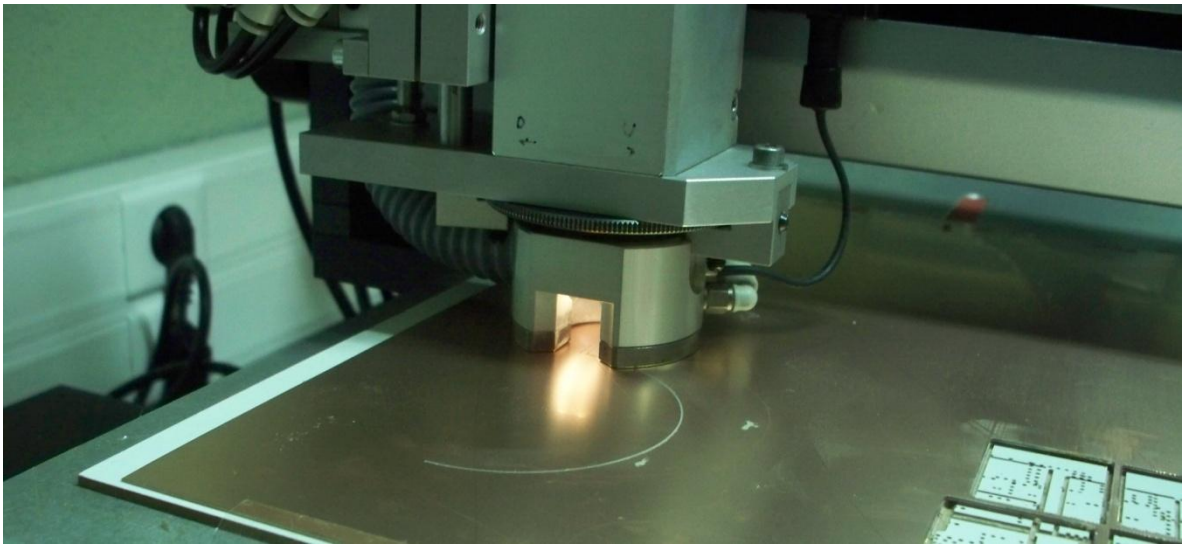

Fig 3.4.1.3: Milling machine shaping our antenna

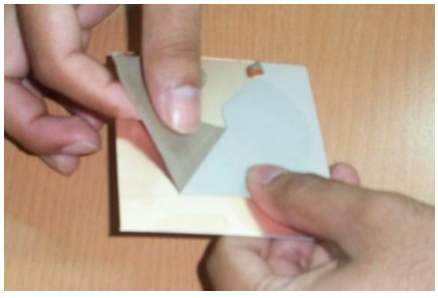

Fig 3.4.1.4: Exceeding Cupper

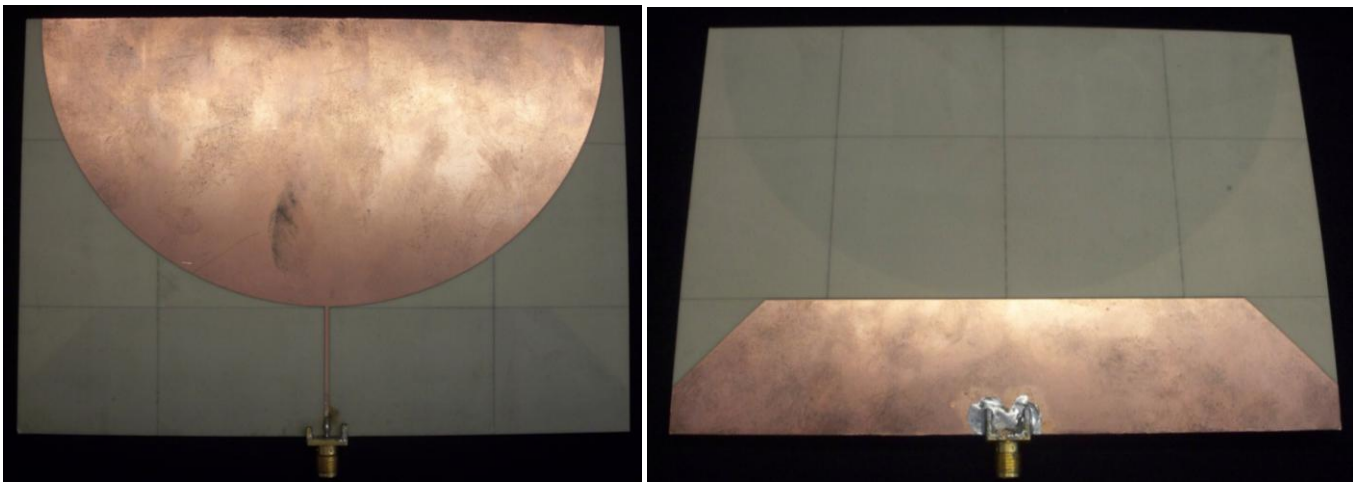

Fig. 3.4.1.5: base-antenna front and back view

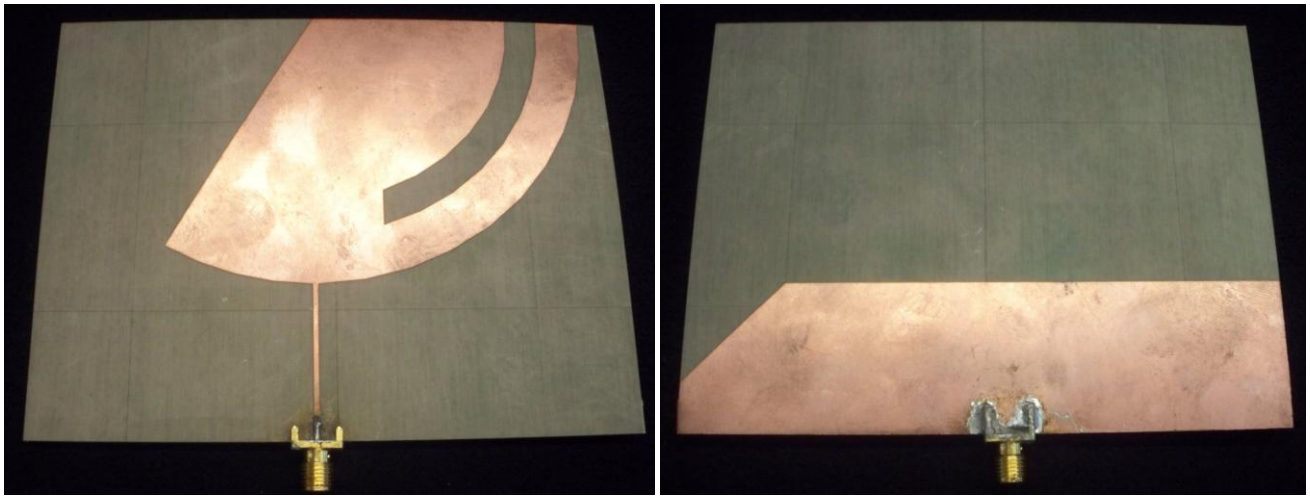

Fig. 3.4.1.5 size-improved antenna front and back view

3.4.2 Measurements

For measurements of the antennas was used a ZVA24 Rohde & Schwarz Vector Network Analyzer (VNA). Since we want to know the energy that our antenna "bounces" and these frequencies, then we have to measure the S11 parameter. A deeper explanation of the parameters S in section 4.3.1 will be done.

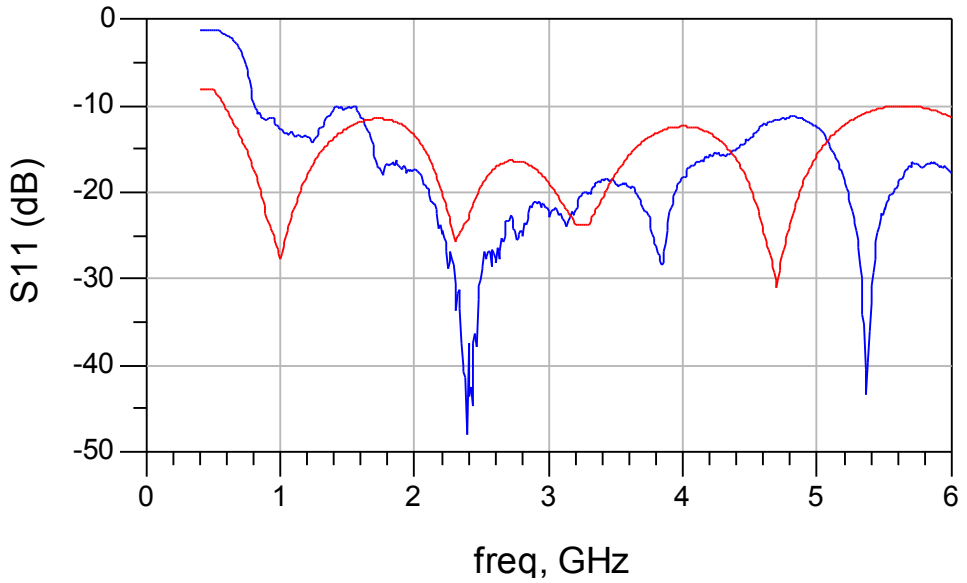

Fig. 3.4.2.1: S11 parameters measured for the base antenna in red compared with the simulated results in blue.

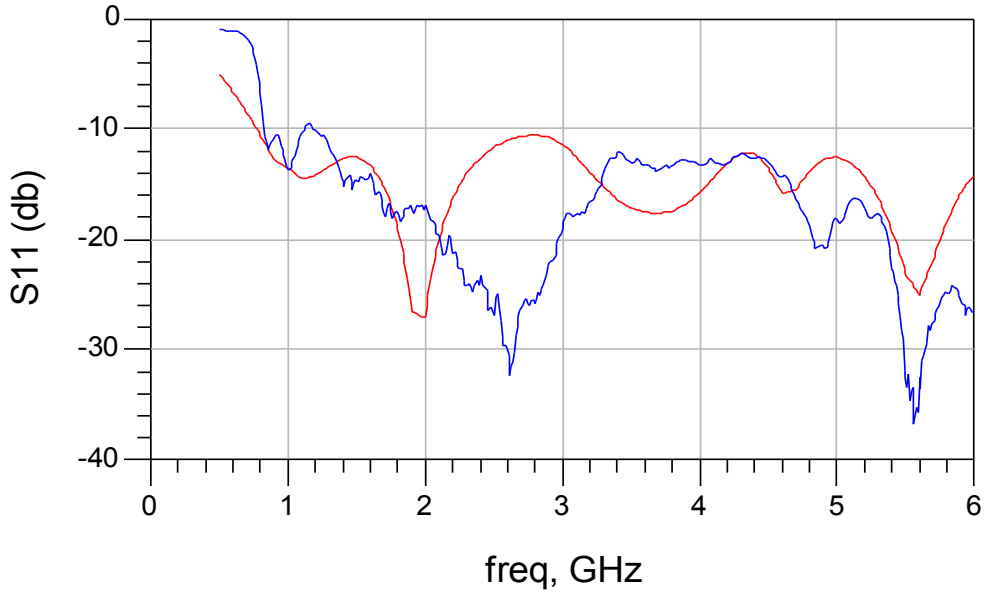

Fig. 3.4.2.2: S11 parameters measured for the size-improved antenna in red compared with the simulated results in blue.

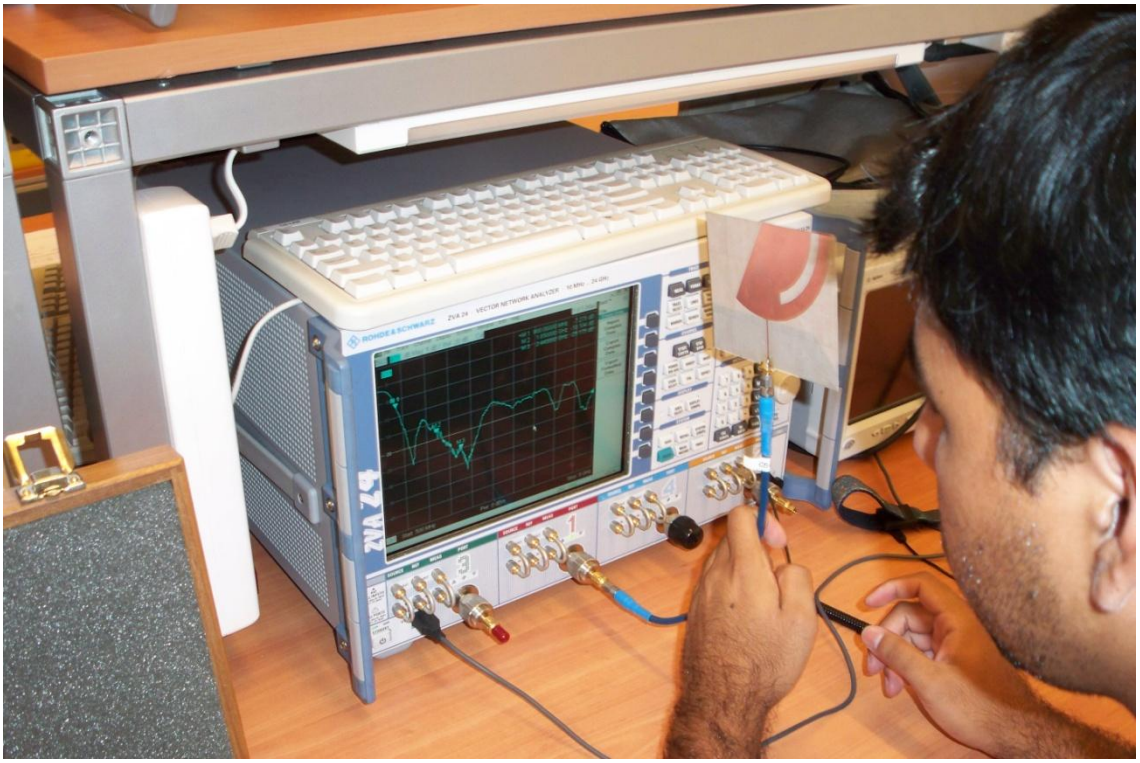

Fig. 3.4.2.3 Vector Network Analyzer, making some measurements.

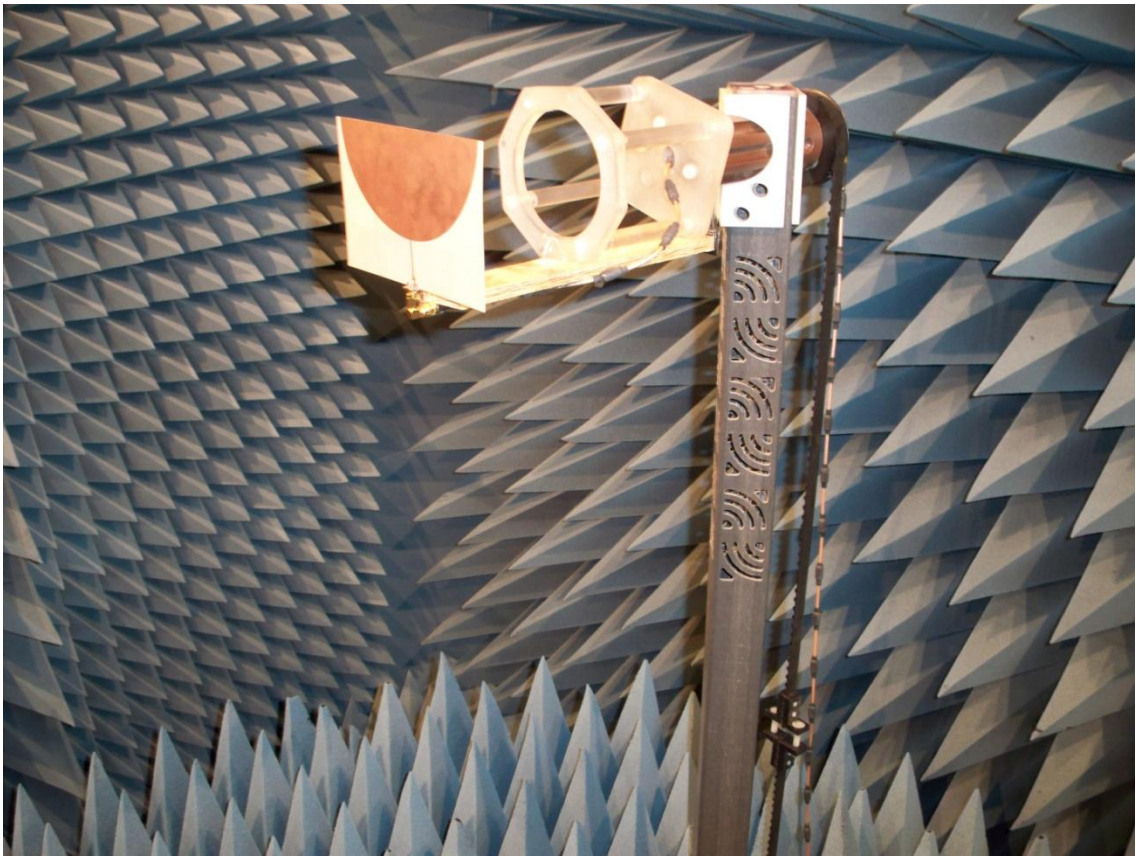
Fig. 3.4.2.4: Anechoic Chamber.

Fig. 3.4.2.1 and Fig. 3.4.2.2 compare the VNA measurements with th software simulations. We can conclude that there is a good correspondence between the measurements and simulations.

Measurements in the anechoic chamber are used for far field antenna characteristics. In Figs. 3.4.2.5 – 3.4.2.8, that show the radiation patterns, rETheta (φ = 0) and rEPhi (φ = 90), are cross-polarization measurements and rETheta (φ = 90) and rEPhi (φ = 0), represent co-polarization measurements. It can be seen that in Figure 3.4.2.5 and 3.4.2.6, which are measurements of the base antenna; there is a marked polarization in the cross-polar direction, and in Fig. 3.4.2.7 and Fig. 3.4.2.8 (Size-improved antenna), theoretically with similar behavior than the first antenna, the measurements show some response in the cross-polar direction.

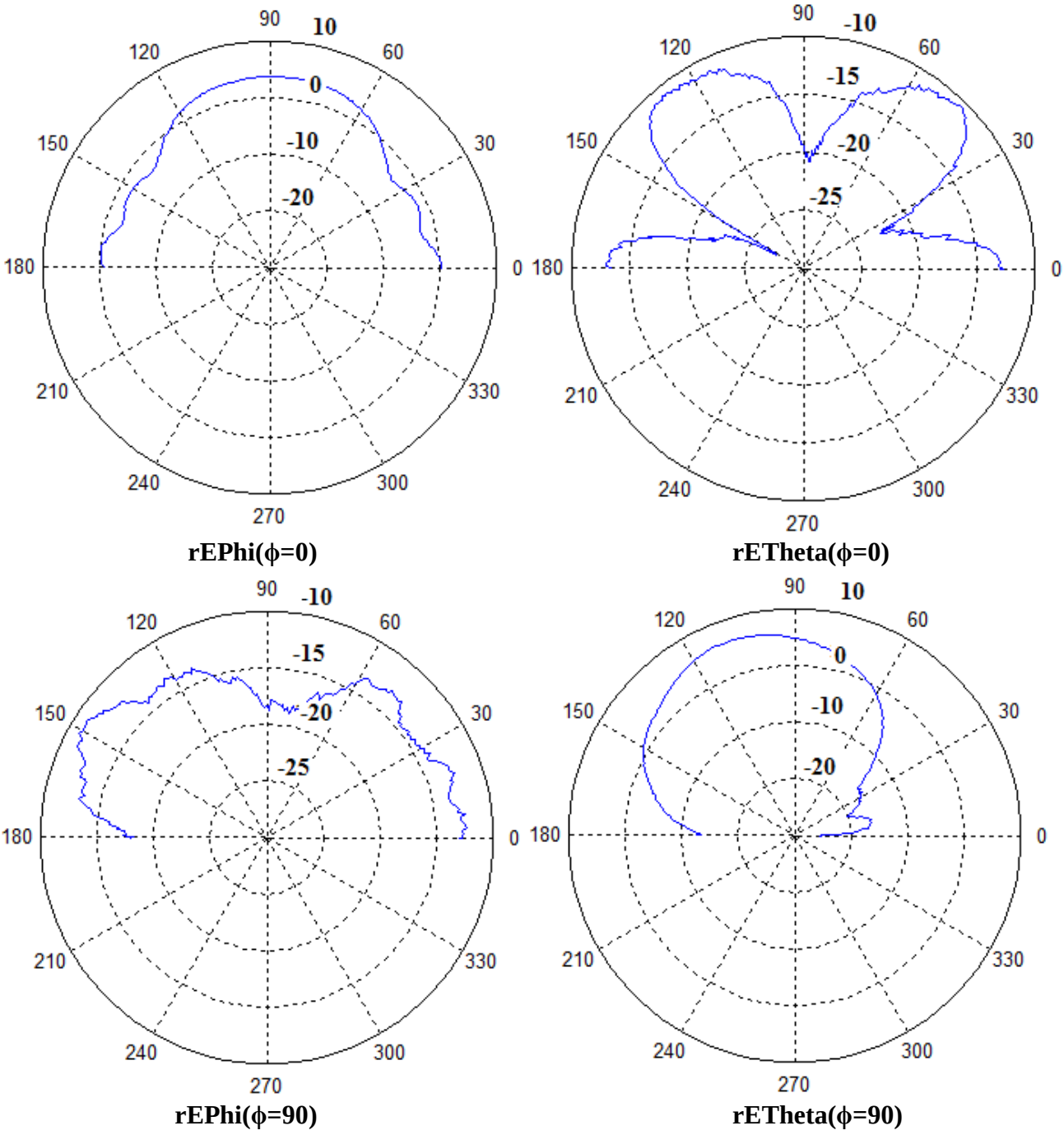

Fig. 3.4.2.5 measured radiations patterns at 1.85 GHz for the base-antenna.

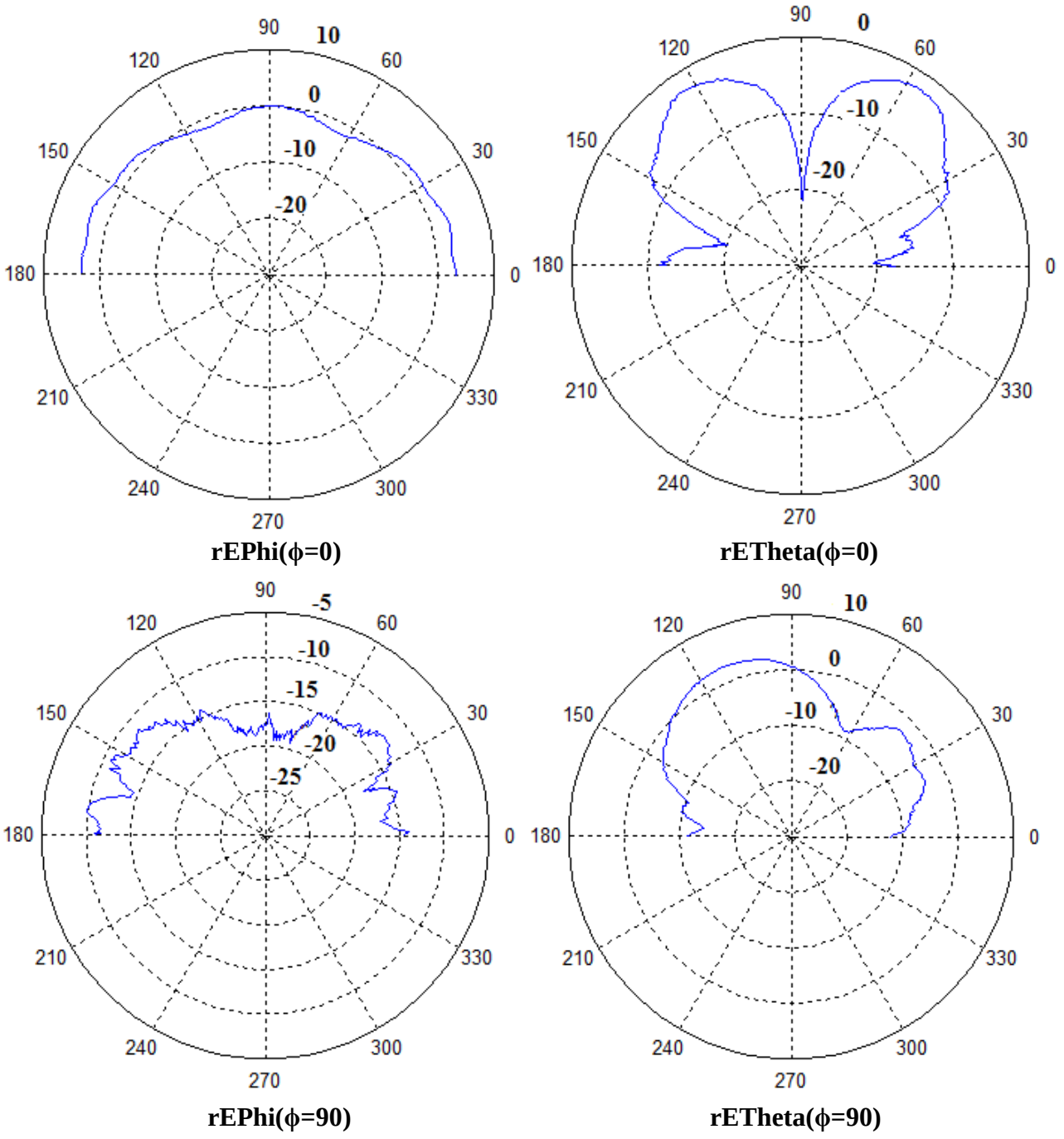

Fig. 3.4.2.6 measured radiations patterns at 2.45 GHz for the base-antenna.

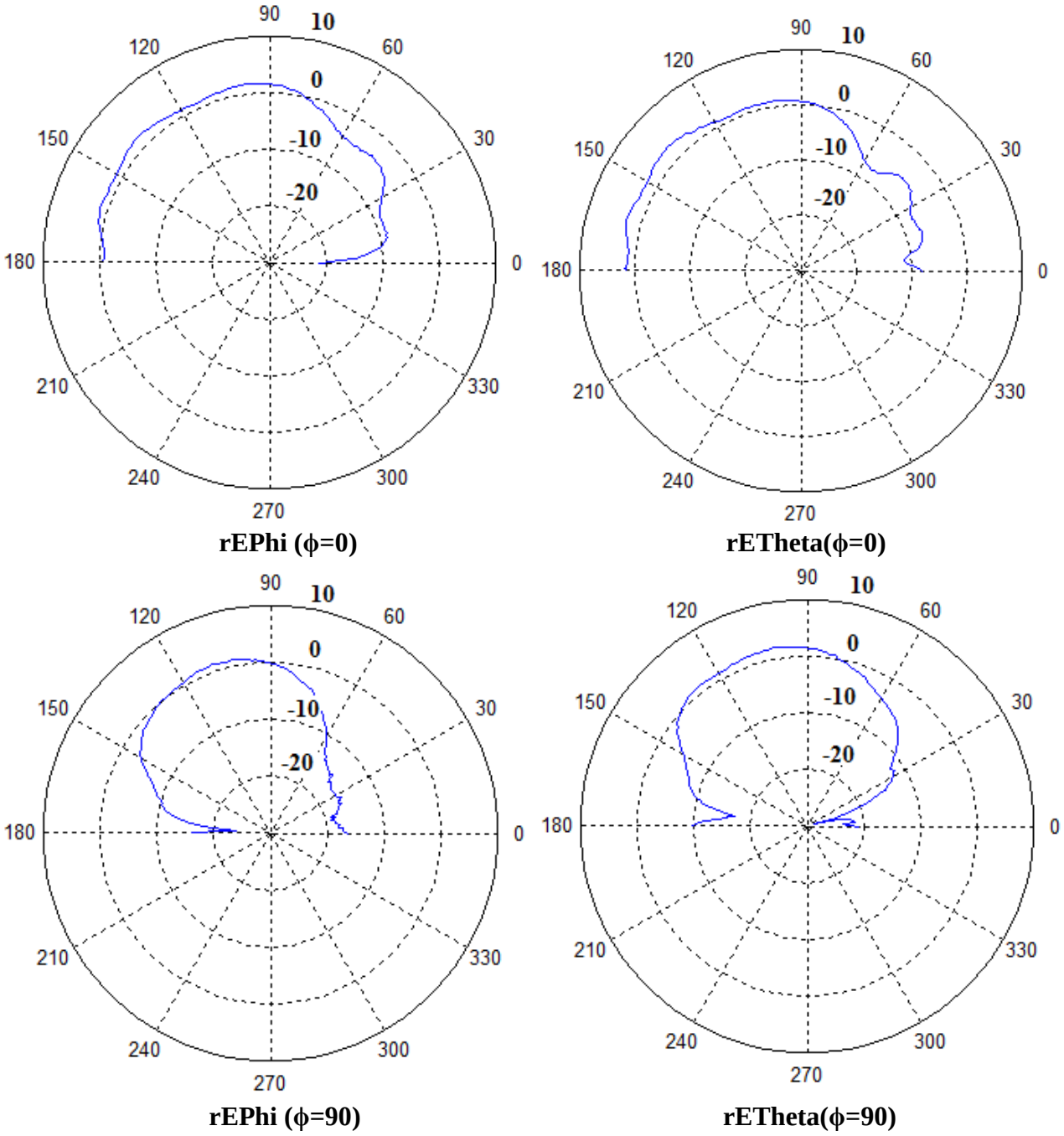

Fig. 3.4.2.2 measured radiations patterns at 1.85 GHz for the size-improved antenna.

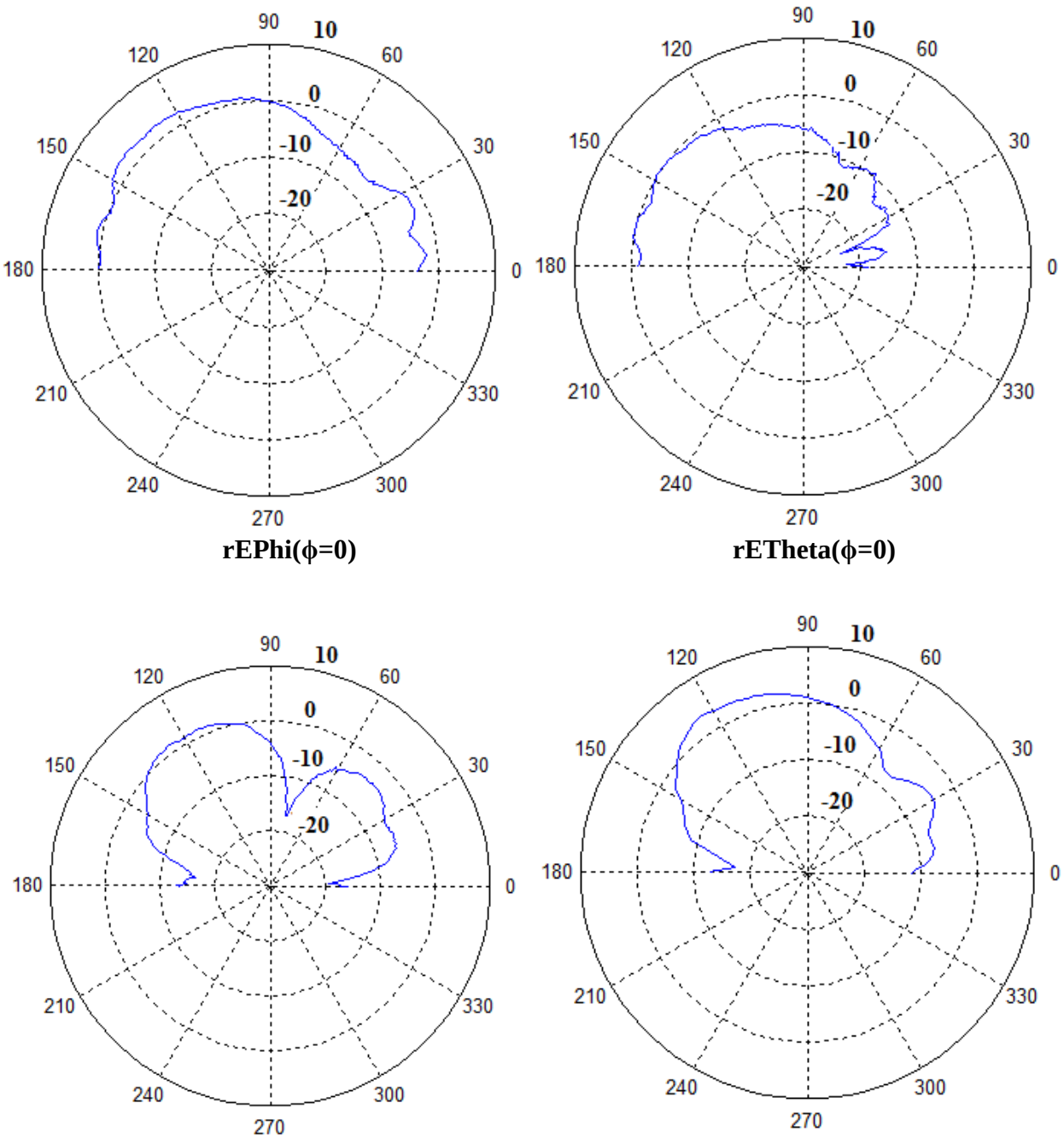

Fig. 3.4.2.8 measured radiations patterns at 2.44 GHz for the size-improved antenna.

Chapter 4

Rectifier Design

4.1 Rectifier

A rectifier is an electrical device that converts alternating current (AC), which periodically reverses direction, to direct current (DC), current that flows in only one direction, in a process known as rectification. Rectifiers have many uses including as components of power supplies and as detectors of radio signals.

There are two types of rectifier, the half wave and full wave. Each type can either be uncontrolled, half-controlled or fully controlled. An uncontrolled rectifier uses diodes, while a full-controlled rectifier uses thyristor or popularly known as Silicon Controlled Rectifier (SCR). A half controlled is a mix of diodes and thyristors. The thyristors need to be turned on using a special triggering circuit. In our application, given the ease of matching because of the fewer number of components, has been used a half-wave rectifier.

4.1.1 Commutating Diode

Mostly, for half or uncontrolled circuit they include also a diode across the load as shown in Fig. 4.1.3.1 This diode is variously described as a freewheeling diode (FWD), flywheel or bypass diode, but is best described as a commutating diode as its function is to commutate or transfer load current away from the rectifier whenever the load current away from the rectifier whenever the load voltage goes into a reverse state.

4.1.2 Schottky diode

The Schottky diode is a semiconductor diode with a low forward voltage drop and a very fast switching action. A Schottky diode is a special kind of diode with a very low forward-voltage drop. When current flows through a diode there is a small voltage drop across the diode terminals. A normal silicon diode has between 0.6–1.7 volt drops, while a Schottky diode voltage drop is between approximately 0.15–0.45 volts. This lower voltage drop can provide higher switching speed and better system efficiency. For our rectifier, we have used a SKYWORKS® Schottky diode (Fig. 4.1.2).

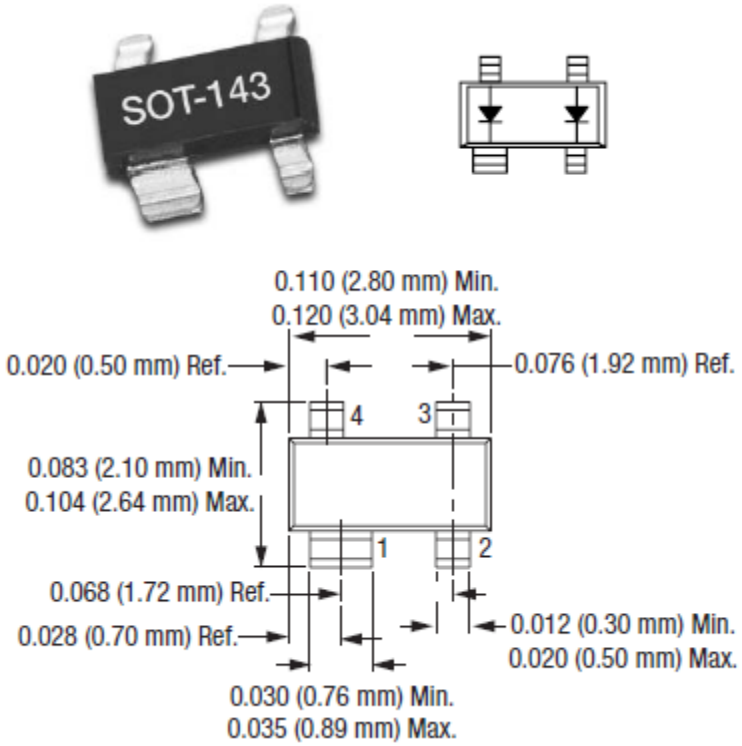

Fig. 4.1.2 SKYWORKS Schottky diode picture, pins and dimensions

4.1.3 Half-Wave Rectifier

In practice, the half-wave rectifier is used most often in low-power applications because the average current in the supply will not be zero. This may cause problems in transformer performance.

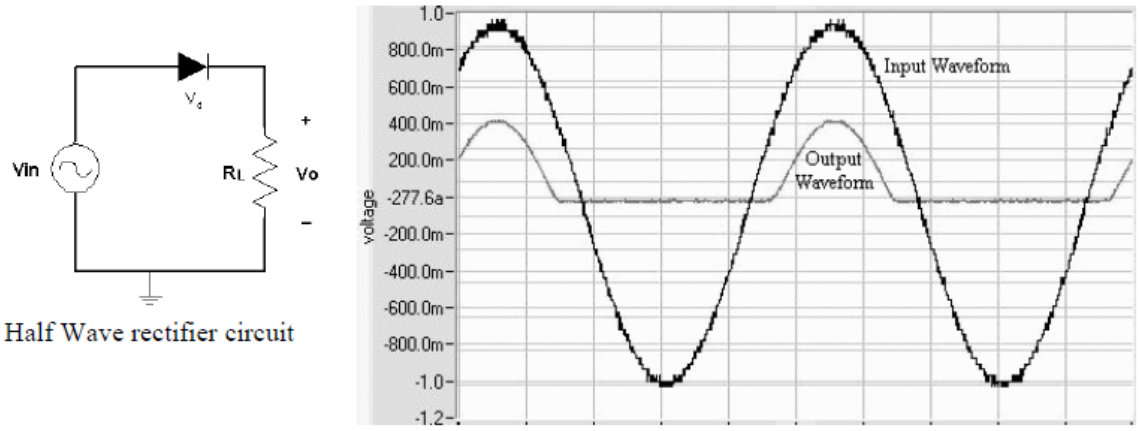

Fig. 4.1.3.1 Half wave rectifier input and output wave example

When a capacitor is connected in parallel with RL, the half wave output becomes a "filtered" DC. As the voltage of the input sine wave increases, the diode will begin to conduct and charge the capacitor. When the input sine wave voltage falls below the capacitor voltage, the diode turns off and the capacitor discharges into the load.

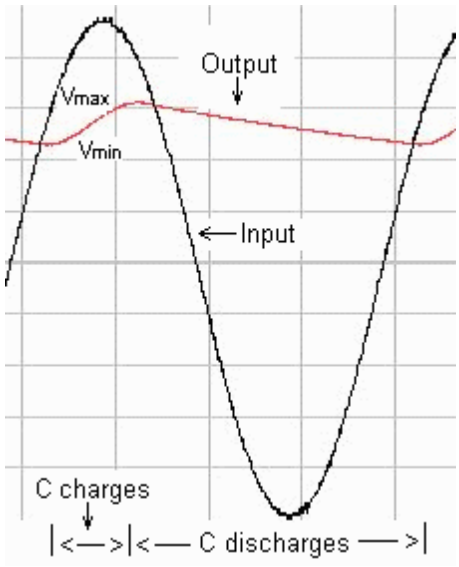

Fig. 4.1.3.2: Operation of the rectifier when placing a capacitor in parallel with RL

The size of the resistor will determine Vmin. As the load resistance is increased: IL decreases, the capacitor discharges less, Vmin increases, Vrms (effective voltage) increases, and Vpp (ripple voltage) decreases. Vmax does not change much because the diode forward voltage drop is relatively constant and Vmax = Vin – Vd.

4.2 RF to DC efficiency

At some applications explained in chapter two and others like the reception of a microwave beam sent to the earth by a geostationary solar power satellite, distributed DC powering of actuator, or DC supplying of RFID passive tags, the RF to DC conversion efficiency is the parameter to improve over the range of incident power or output voltage of interest. Different solutions have been reported, mainly based on combining dipole or patch printed elements with diode detectors. The RF-DC conversion efficiency of the rectenna with a diode depends on the microwave power input intensity and the connected load. We need to get the optimum microwave power input intensity and the optimum load to achieve maximum efficiency. When the power or load is not well matched, the transferred power is not the optimal and the efficiency becomes quite low. The efficiency is also determined by the characteristic of the diode; the diode has its own junction voltage and breakdown voltage. If the input voltage to the diode is lower than the junction voltage or is higher than the breakdown voltage, the diode does not show a rectifying characteristic. As a result, the RF-DC conversion efficiency drops with a lower or higher input than the optimum.

The average RF power over a range of frequencies at any instant in time is given by:

$$\left(\frac{1}{f_h - f_l}\right)\int_{f_l}^{f_h}\int_{0}^{4\pi} S(\theta,\phi,f,t)A_{eff}(d\Omega df)$$

The DC power for a single frequency (fi) input RF power is given by:

$$P_{DC}(f_i) = P_{RF}(f_i,t)\eta[P_{RF}F(f_i,t),\rho,Z_{DC}]$$

where η is the conversion efficiency:

$$\eta[P_{RF}F(f_i,t),\rho,Z_{DC}] = \frac{P_{DC}(f_i)}{P_{RF}(f_i,t)}$$

4.3 Rectifier Simulation Tools

For rectifier simulations and also each of its components, we have used the Agilent ADS2008 software. In this section we describe some of the modules and tools used, and a brief explanation of its operation is also made.

4.3.1 S-parameter analysis.

The objective of microwave circuit analysis is to move from the requirement to solve all the fields and waves of a structure, to an equivalent circuit that is amenable to all the tools of the circuit analysis. However, the tools that are appropriate for lumped circuits must be extended to apply to distributed networks.

A matrix that is of great use in microwave network problems is the "scattering" matrix, so-called by analogy to the scattering or reflection of waves by a free-space reflector. S-parameters have become the preferred description of microwave n-ports for the following reasons:

- Voltage and current are difficult to define and measure in distributed circuits
- Incident and reflected waves are the natural description for microwave structures
- Conversion from S-parameters to other parameter sets is a matter of routine algebra
- S-parameters benefit from the matrix operations.

S-parameter simulation is a type of small-signal AC simulation. It is most commonly used to characterize a passive RF component and establish the small-signal characteristics of a device.

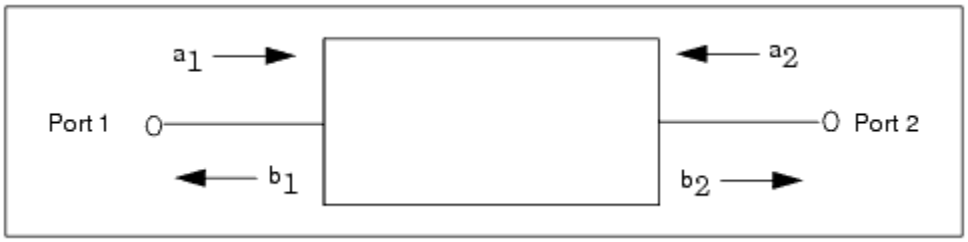

Fig. 4.3.1.1: Representation of a signal wave in a two-port electrical-element.

Fig. 4.3.1.1 shows a representation of a signal wave in a two-port electrical-element where:

- *a1* is the wave into port 1
- *b1* is the wave out of port 1
- *a2* is the wave into port 2
- *b2* is the wave out of port 2

The S-parameters for this conventional element are:

- $b1 = a1.S11 + a2.S12$
- $b2 = a1.S21 + a2.S22$

where:

- S11 is the port-1 reflection coefficient: S11= *b1/a1* when *a2*= 0
- S22 is the port-2 reflection coefficient: S22=*b2/a2* when *a1*= 0
- S21 is the forward transmission coefficient: S21= *b2/a1* when *a2*= 0
- S12 is the reverse transmission coefficient: S12= *b1/a2* when *a1*= 0

These equations can be solved for *b1* and *a1* in terms of *a2* and *b2* to yield the transmission T-parameters as follows:

- *b1*= *a2*.T11+ *b2*.T12
- *a1*= *a2*.T21+ *b2*.T22

Fig. 4.3.1.2 shows the T-Parameters matrix.

$$\begin{bmatrix} t_{11} & t_{12} \\ t_{21} & t_{22} \end{bmatrix} = \begin{bmatrix} s_{12} - s_{11} & s_{22}/s_{21} \\ -s_{22}/s_{21} & 1/s_{21} \end{bmatrix} \quad s_{11}/s_{21}$$

Fig. 4.3.1.2: relationship between the T-parameters and the S-parameters

S-parameters are defined with respect to reference impedance that is typically 50 ohms. For 50-ohm S-parameters-with the 2-port element terminated with 50 ohms at each port, the s21 parameter represents the voltage gain of the element from port 1 to port 2.

4.3.2 Harmonic Balance

Harmonic balance is a method to analyze the distortion in non-linear circuits or systems. This method is usually applied when we need to simulate RF or microwave problems since these are most naturally handled in the frequency domain.

Source voltage and current of a circuit can generate discrete frequencies by generating a discrete frequency spectrum at different points in the system. Linear components of a circuit are modeled in the frequency domain while non-linear components are modeled first in the time domain and then Fourier-transformed in the frequency domain before each solving step.

This method first divides the circuit into two groups, the linear elements, where are also included input impedances of the sources, and the group of non-linear elements. Fig. 4.3.2 shows a schematic of these two groups.

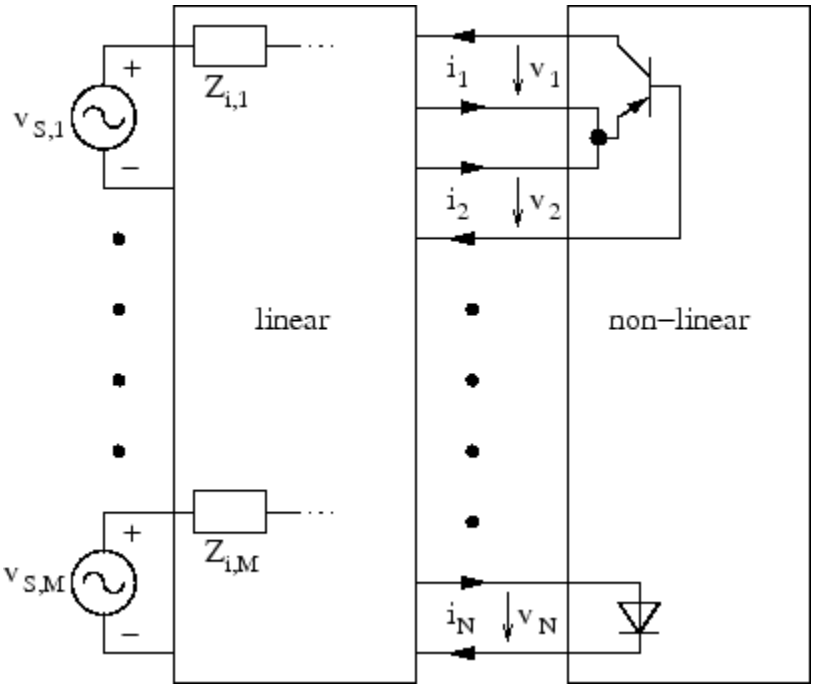

Fig. 4.3.2 Schematic of Harmonic Balance component division [20]

It is considered that a solution has occurred when the current between the groups is the same for the linear elements and for the non-linear. That is why the method is called harmonic balance, because the current between the two groups must be balanced for each harmonic frequency. It is also possible to know all the voltages at each of the interconnections between the two groups, once known these values of balanced voltages and currents, it performs a classic AC analysis and we can know the voltage and current value at any point of the circuit.

In our application we have used this method because the circuit has only one non-linear element that is the diode, moreover, the circuits that we have simulated does not require much computer processing, which makes the simulation faster.

4.3.3 ADS2008 Matching Utility

Since our application consists basically of an antenna and a rectifier circuit, is required an impedance matching to ensure good power transfer and performance. The ADS2008 impedance matching utility is a software tool that allows us to place a component in our scheme and, according to certain parameters manually defined, generate a matching circuit which can then be optimized according to our goals.

Fig. 4.3.3.1 shows an example of how the impedance matching component is placed in the circuit scheme. For our application we chose a band-pass matching circuit, that was

subsequently optimized for best performance in our application bands, because matching a network over a broad band is complex and it will require a larger amount of components.

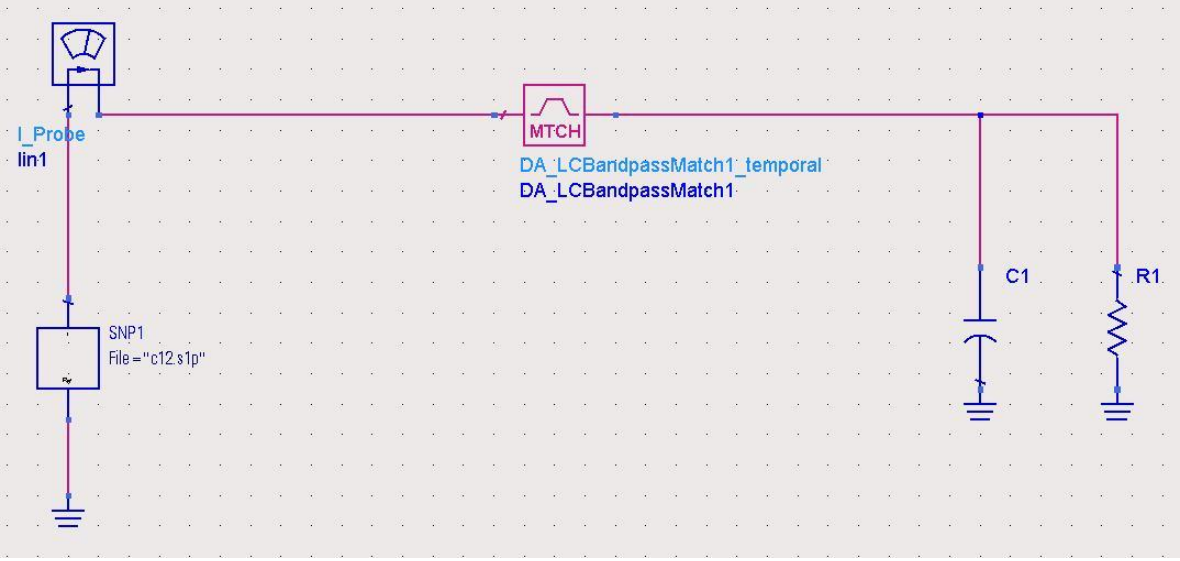

Fig. 4.3.3.1 Example circuit and Band pass matching component.

Although this component is placed in a circuit context, to generate the impedance matching circuit is not necessary that the component terminations are connected to any node, this is just done for further simulations, where the matching component replaces a whole (matching) circuit. When we deploy the menu of impedance matching (Fig. 4.3.3.1), we can enter the necessary parameters that will be implemented internally as well as the creation of the adaptation circuit.

Once we have defined our matching circuit, whose values were optimized according to our application bands, the next step is to optimize the whole set (adaptation circuit and rectifying circuit) to achieve our goals.

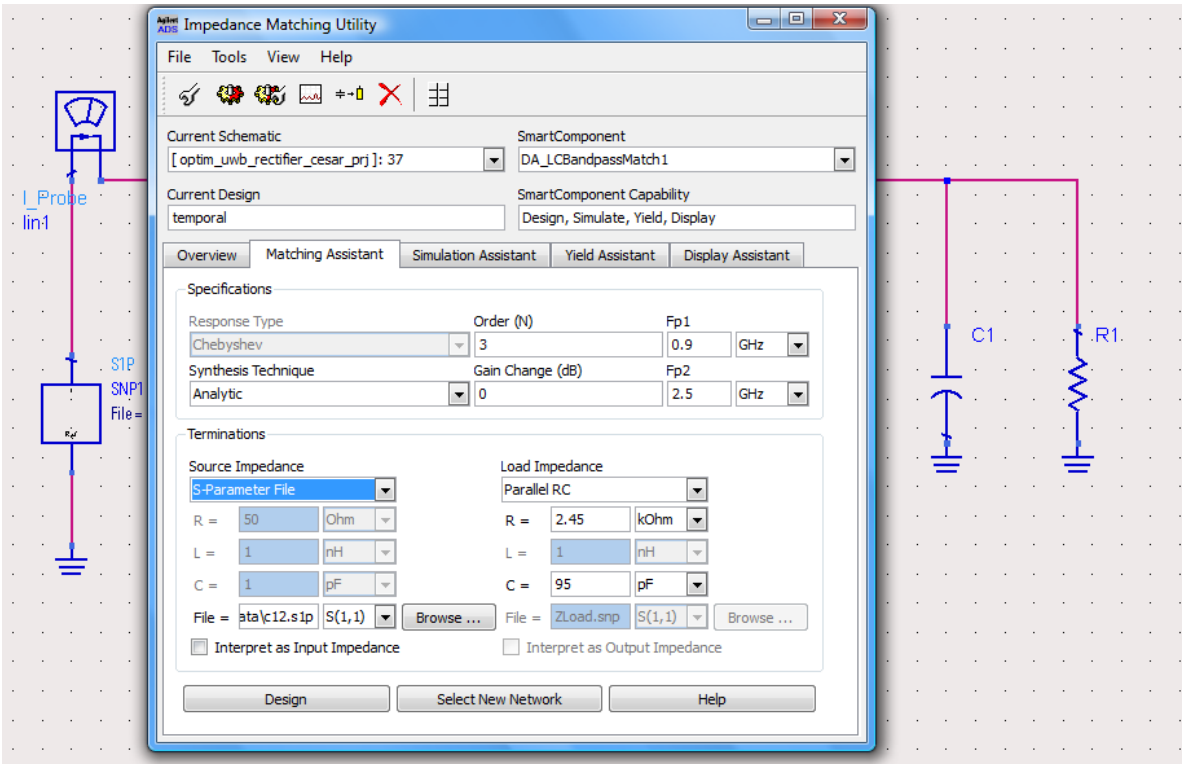

Fig. 4.3.3.2: Impedance matching assistant window. Main parameters to the filled: Lower Frequency (Fp1), Upper Frequency (Fp2). Source / Load Impedance

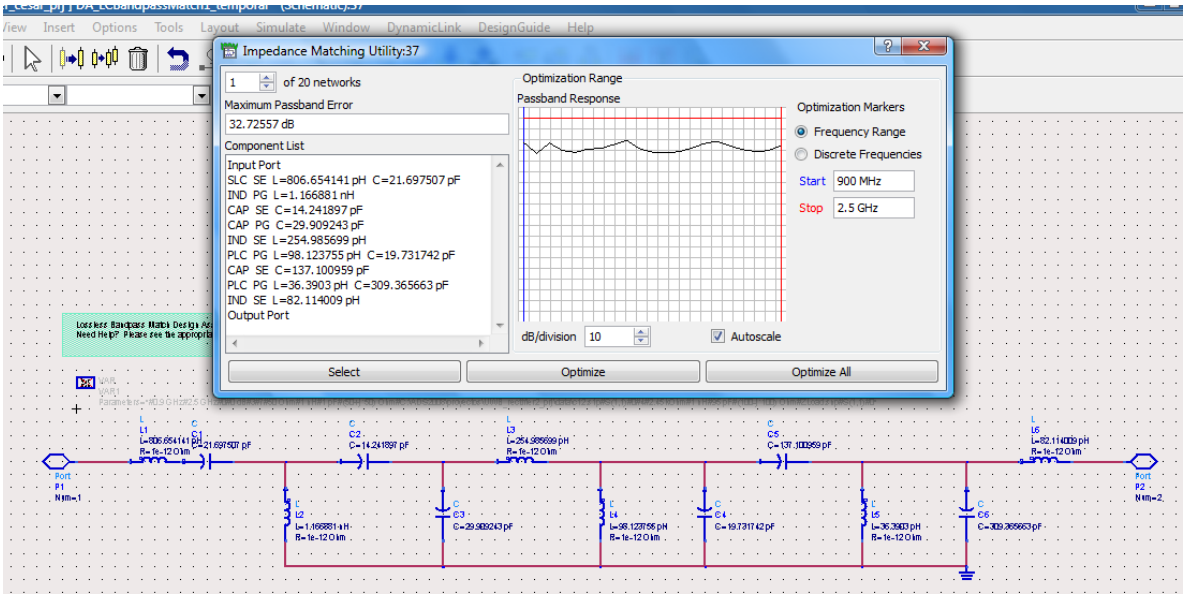

Fig. 4.3.3.3 automatically generated matching circuit. Note that there is more than one generated network.

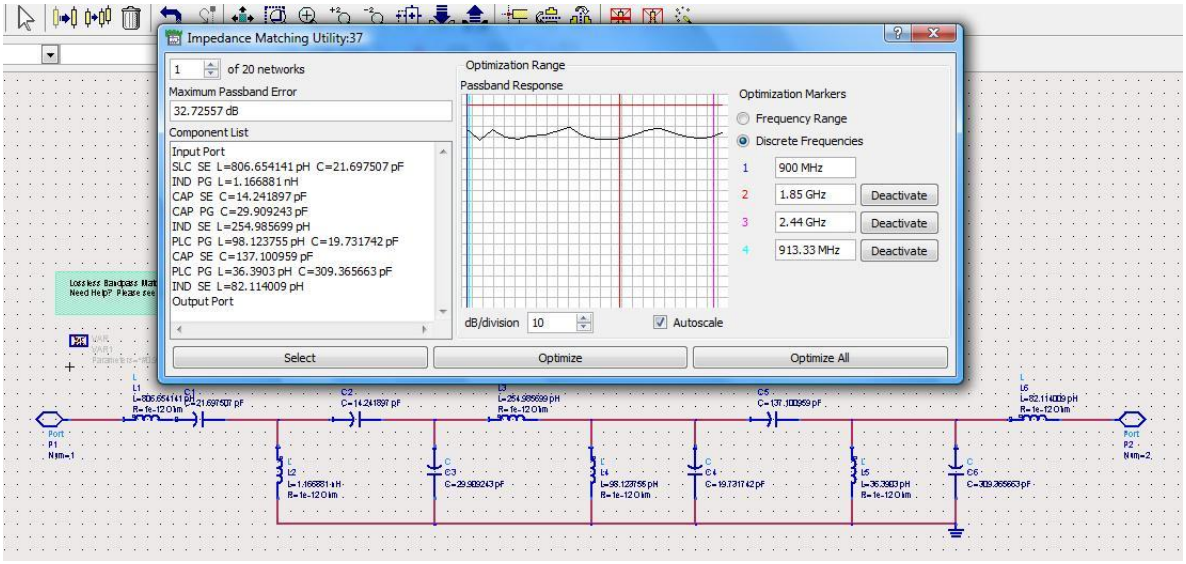

Fig. 4.3.3.4: Post Optimization for best performance in our application bands.

4.3.4 Nominal Optimization

Nominal optimization (also called Performance Optimization) is a technique to design a circuit where, under specific performance goals and a value-search method, the values of each component (or a set) are modified and then simulated, if the result of this simulation does not meet the goals, values are "searched" and simulated again until performance goals are achieved. The value-search method used for this application was the Gradient Search.

4.3.5 Gradient Search Method

The method of gradient search, adjust a set of variables according to an error function and its gradient. The simulator in the first iteration evaluates the error function and its gradient, and then the set of variables will be moved in the direction of the gradient of the error so that the error function is minimized. The simulation stops automatically when the goals are reached, when the iteration limit is reached or when there is a gradient zero. The error function used by the gradient method is the Least-Squares error function.

4.4 Simulations

Once explained the methods used for analysis and simulation of our circuits, we will show the simulations results and analysis for specific rectifier circuits. In this study we have simulated seven rectifiers that can be classified in three groups:

- Series diode rectifiers

- Parallel diode rectifier
- Two diode rectifier.

Moreover, a study of the first two groups has been made showing the differences between different methods of adaptation and different frequency bands of use.

4.4.1 Parasitic

To characterize the diode and capacitor, we took into account the parasitic. Parasitic are mechanical and electrical unwanted characteristics that limit the circuit performance. The notation used in the parasitic components is as follows

- Lp: Is an inductor placed in series with the component and can be explained as the inductance associated with the external terminations of metal that connect the internal component with the (external) circuit.
- Cp: Capacitance that is placed in parallel with the component and is due that all package solid materials have dielectric constants related that behave as capacitors.
- Rp: The metal conductor used to connect the internal component with the (external) circuit is usually a gold or gold plated with an associated very low resistance. This resistance can affect the performance of a microwave circuit.

4.4.2 Series diode rectifier matched with the ADS2008 matching utility and focusing on 900 MHz, 1.85 GHz and 2.45 GHz bands.

After optimizing the values of each component in Fig. (4.4.2.1) to achieve the maximum performance, we have obtained the values shown in Table 4.4.2.1.

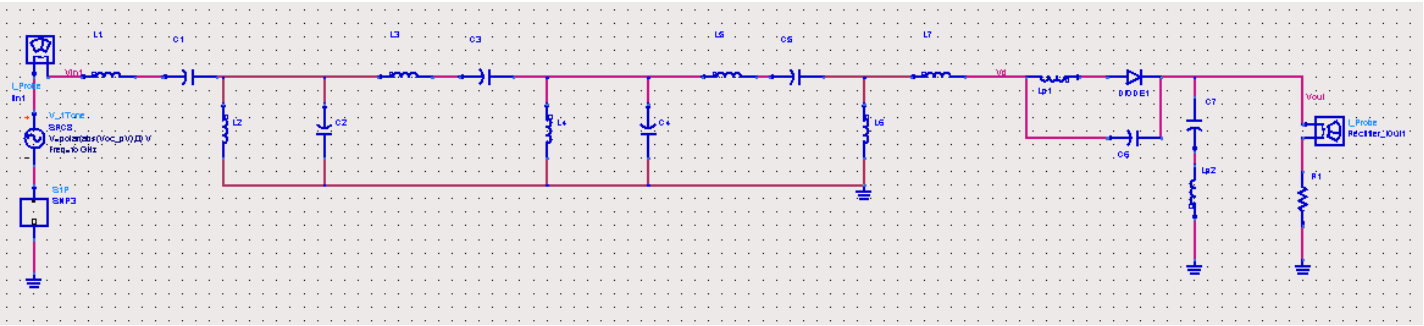

Fig. 4.4.2.1: Complete schematic: antenna S parameters, matching circuit and series diode rectifier.

Fig. 4.4.2.2 shows that the maximum efficiency for the 900 MHz, 1.85 GHz and 2.45 GHz bands is achieved when the received power is -6 dBm, -4 dBm and -6dBm respectively; we can also conclude that the maximum efficiency is 52%, 62% and 59% respectively. If we

observe the efficiency for low input power (-20 dBm), we can note that the values are 25%, 30% and 28% respectively. The main disadvantage of this circuit is the large number of components (18), if we would implement it, the soldering loss of each component would affect the performance significantly.

Table 4.4.2: Simulation values for Fig.4.4.2

Component Name	Value	Component Name	Value
L1	3.3 nH	**C1**	2.2 pF
L2	6.8 nH	**C2**	1.8 pF
L3	16 nH	**C3**	1 pF
L4	12 nH	**C4**	1.2 pF
L5	15 nH	**C5**	0.5 pF
L6	36 nH	**C6**	68 pF
L7	15 nH	**Cp1**	0.25 pF
Lp1	0.6 nH	**R1**	2.2 KOhm
Lp2	0.36 nH		

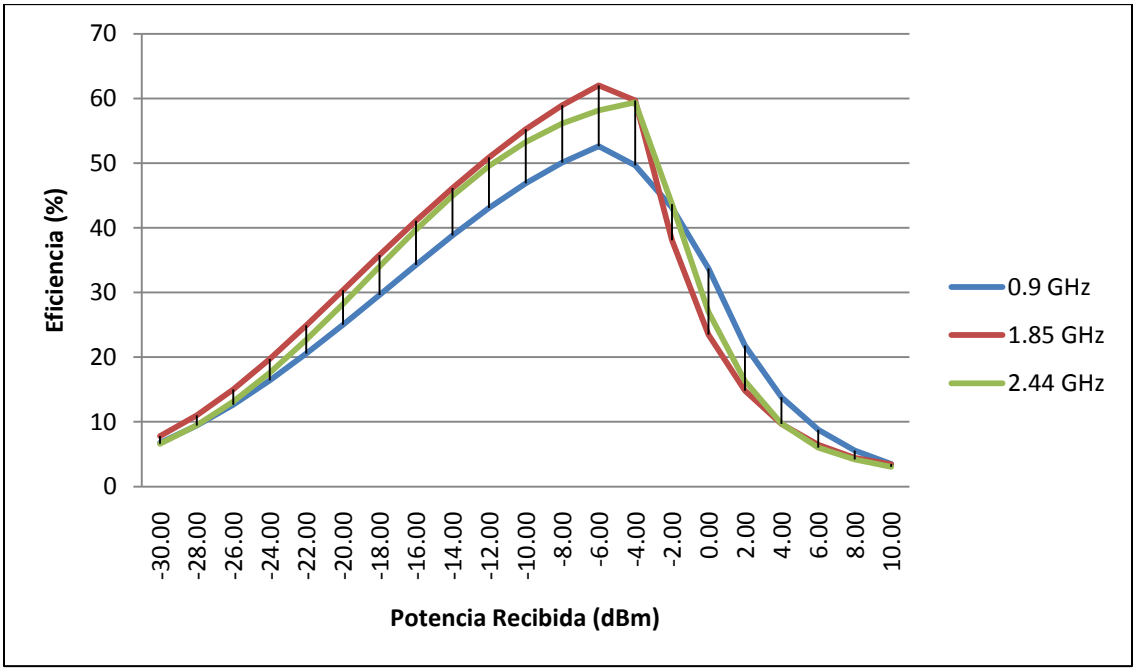

Fig. 4.4.2.2: Rectenna efficiency versus input power showing the behavior for low input power (Agilent ADS).

4.4.3 Series diode rectifier matched with LC circuit over the entire band.

After optimizing all the values of each component in Fig. (4.4.3.1) to achieve the maximum performance, we have obtained the values shown in Table 4.4.3.1.

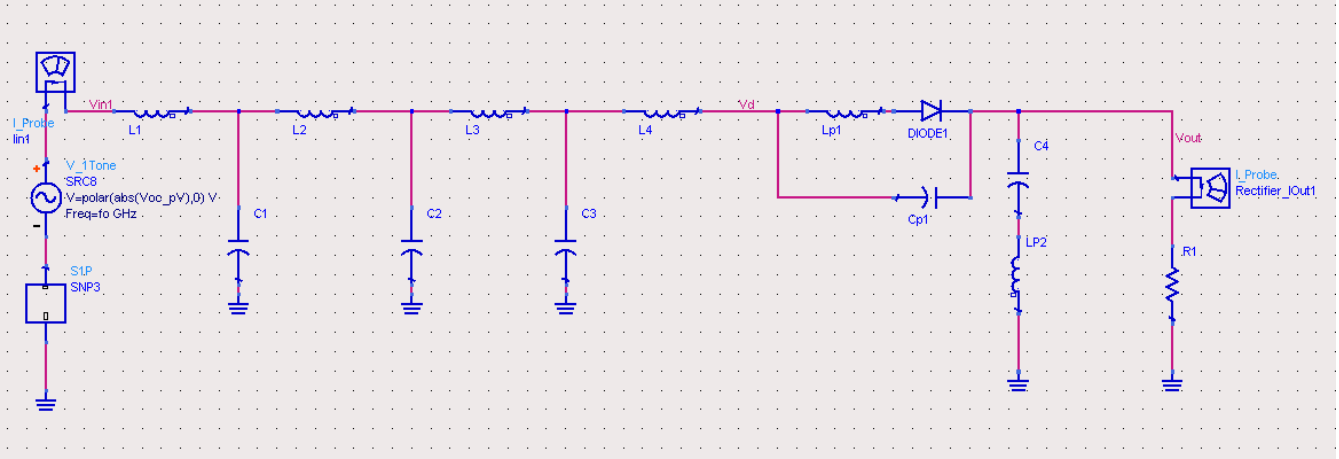

Fig. 4.4.3.1: Complete schematic: antenna S parameters, matching circuit and series diode rectifier.

Fig 4.4.3.2 shows that the maximum efficiency for the 900 MHz, 1.85 GHz and 2.45 GHz bands is achieved when the received power is -2 dBm. We can also conclude that the maximum efficiency is 44%, 41% and 50% respectively. If we observe the efficiency for low input power (-20 dBm), we can note that the values are 15.5%, 8.9% and 11% respectively, well below the Fig. 4.4.2.1 rectifier. The drop in efficiency has been remarkable, and this is because the matching over a broad band is more complicated.

Table 4.4.3: Simulation values for Fig. 4.4.3.1

Component Name	Value	Component Name	Value
L1	4 nH	**C1**	1 pF
L2	1 nH	**C2**	1 pF
L3	14 nH	**C3**	1 pF
L4	30 nH	**C4**	140 pF
Lp1	0.3 nH	**Cp1**	0.25 pF
Lp2	0.36 nH	**R1**	2.2 KOh

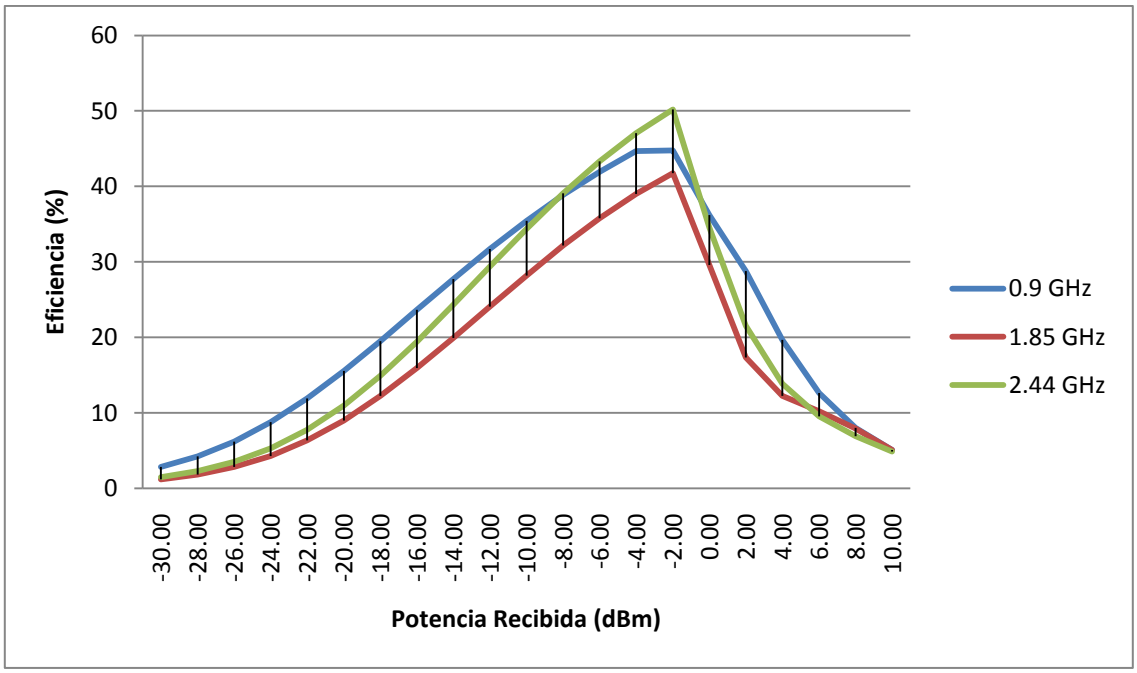

Fig. 4.4.3.2: Rectenna efficiency versus input power for low input power (Agilent ADS) at 900 MHz, 1.85 GHz and 2.45 GHz.

4.4.4 Series diode rectifier matched with LC circuit focusing on the bands of use.

After optimizing the values of each component in Fig. (4.4.4.1) to achieve the maximum performance, we have obtained the values shown in Table 4.4.4.

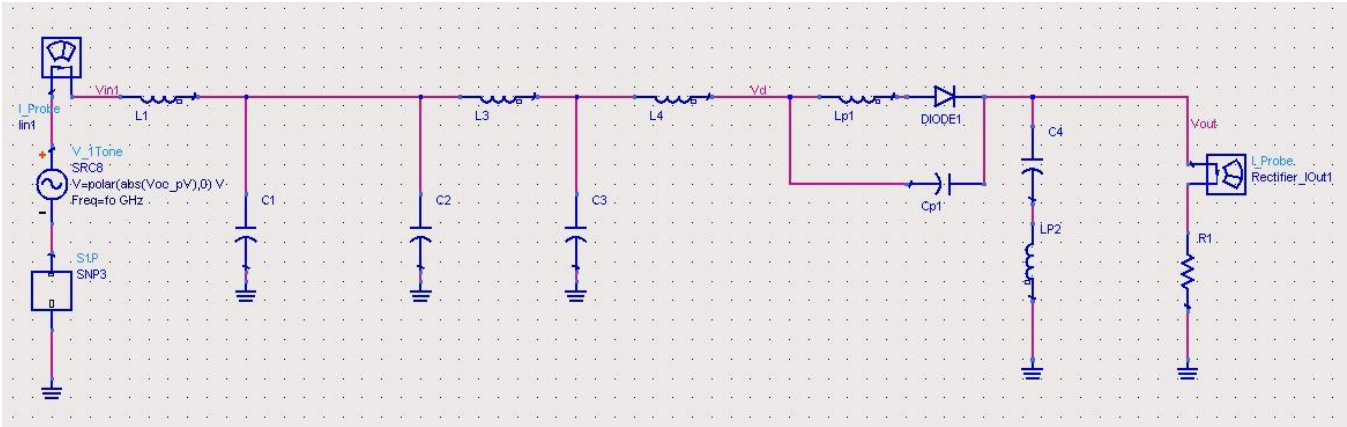

Fig. 4.4.4.1: Complete schematic: antenna S parameters, matching circuit and series diode rectifier.

Fig. 4.4.4.1 shows that the maximum efficiency for the 900 MHz, 1.85 GHz and 2.45 GHz bands is achieved when the received power is -4 dBm, -2dBm, -4dBm respectively. We can also see that the maximum efficiency is 49.2%, 44.9% and 59.8% respectively, higher than the last network. If we observe the efficiency for low input power (-20 dBm), we can note that the values are 18.7%, 13.3% and 20.9% respectively. This circuit would be a good

balance between efficiency and component amount, as the circuit of Fig. 4.4.2.1 has many components but has a very good performance and the circuit of Fig. 4.4.3.1 has few components and low performance as the band is very extensive. However, in this circuit, we have the advantage that it has fewer components than the other two shown above and also you get an acceptable efficiency.

Table 4.4.4: Simulation values for Fig. 4.4.4.1

Component Name	Value	Component Name	Value
L1	8.9 nH	**C1**	1 pF
L3	20 nH	**C2**	1 pF
L4	31.5 nH	**C3**	1 pF
Lp1	0.6 nH	**C4**	60 pF
Lp2	0.36 nH	**Cp1**	0.25 pF
		R1	2.1 KOhm

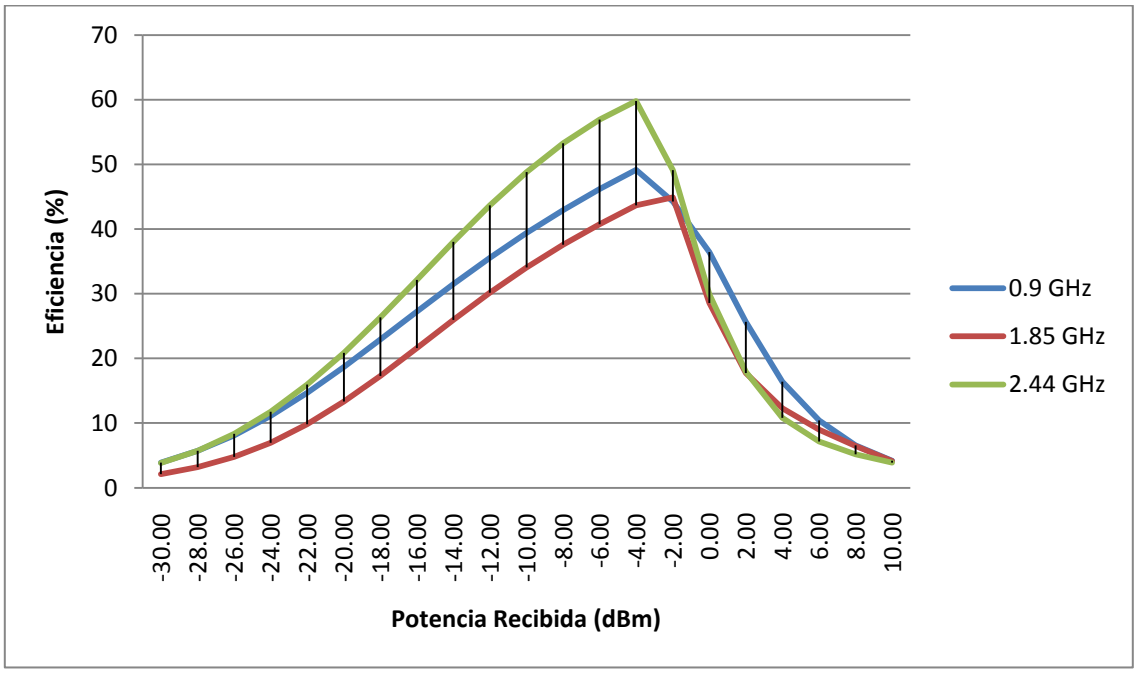

Fig. 4.4.4.2: Rectenna efficiency versus input power for low input power (Agilent ADS) at 900 MHz, 1.85 GHz and 2.45 GHz.

4.4.5 Parallel diode rectifier Matched using the ADS2008 matching utility and focusing on the bands of use.

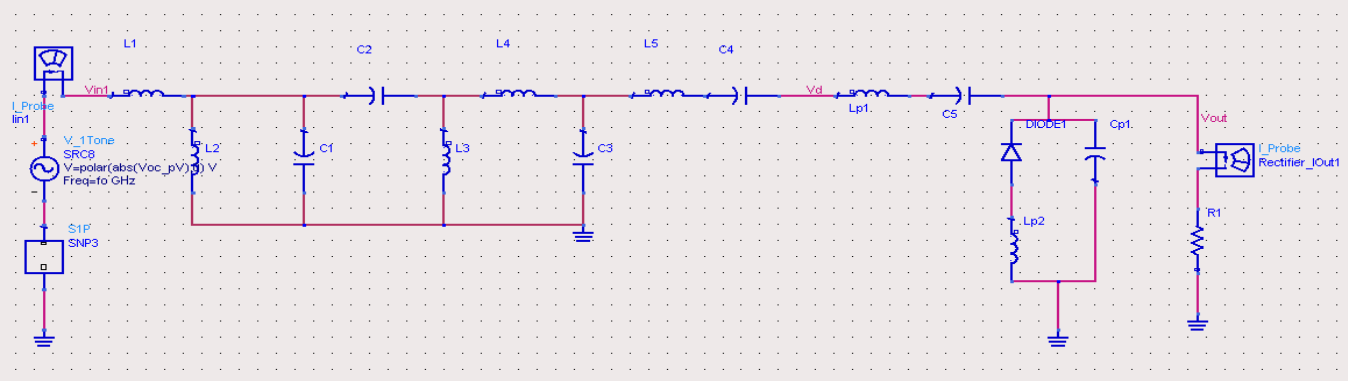

Fig. 4.4.5.1: Complete schematic: antenna S parameters, matching circuit and parallel diode rectifier.

Table 4.4.5 Simulation values for Fig. 4.4.5.1

Component Name	Value	Component Name	Value
L1	1 nH	**C1**	8.2 pF
L2	19 nH	**C2**	2 pF
L3	9 nH	**C3**	1 pF
L4	15 nH	**C4**	300 pF
L5	24 nH	**C5**	112 pF
Lp1	0.6 nH	**Cp1**	0.25 pF
Lp2	0.36 nH	**R1**	5.4KOh

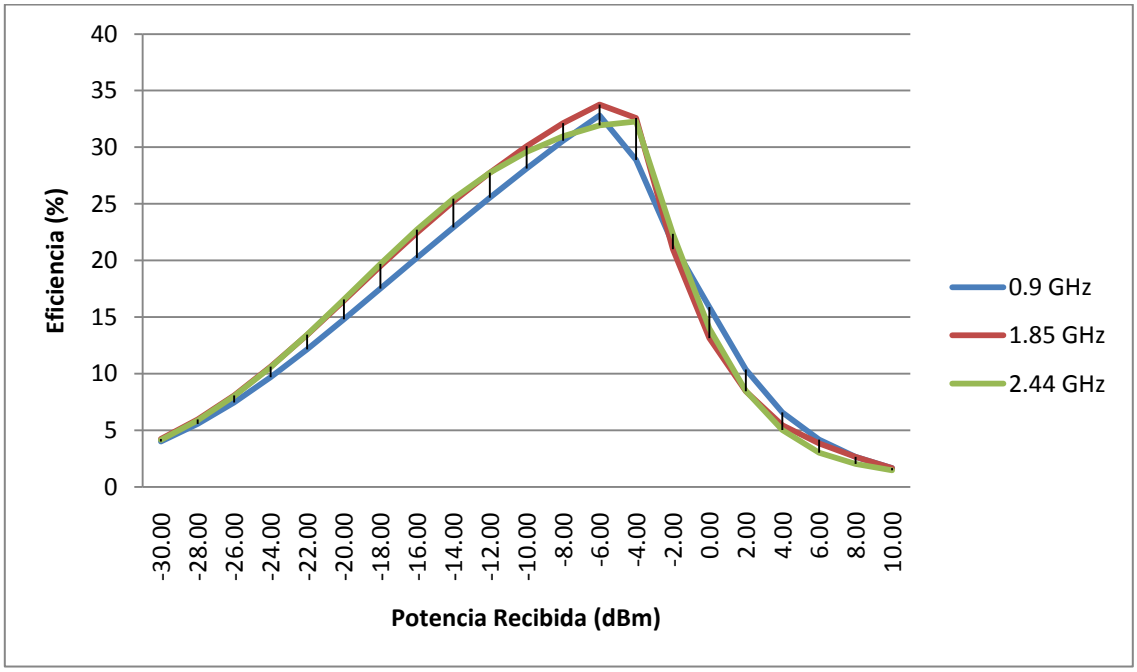

Fig. 4.4.5.2: Rectenna efficiency versus input power for low input power (Agilent ADS) at 900 MHz, 1.85 GHz and 2.45 GHz.

4.4.6 Parallel diode rectifier matched with LC circuit over the entire band.

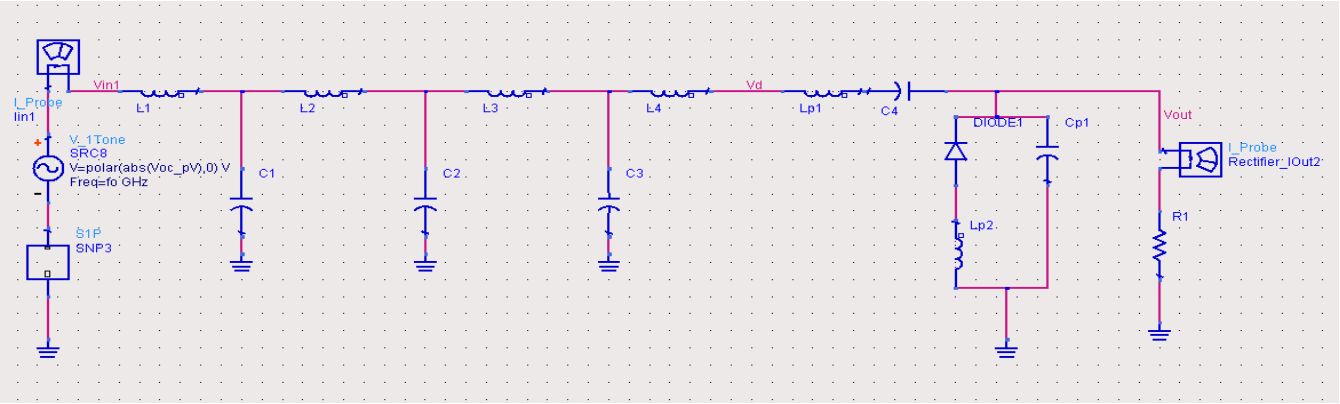

Fig. 4.4.6.1: Complete schematic: antenna S parameters, matching circuit and parallel diode rectifier.

Table 4.4.6: Simulation values for Fig. 4.4.6.1

Component Name	Value	Component Name	Value
L1	4 nH	**C1**	1.5 pF
L2	8.2 nH	**C2**	1 pF
L3	8 nH	**C3**	1 pF
L4	25 nH	**C4**	60 pF
Lp1	0.6 nH	**Cp1**	0.25 pF
Lp2	0.36 nH	**R1**	3.5KOh

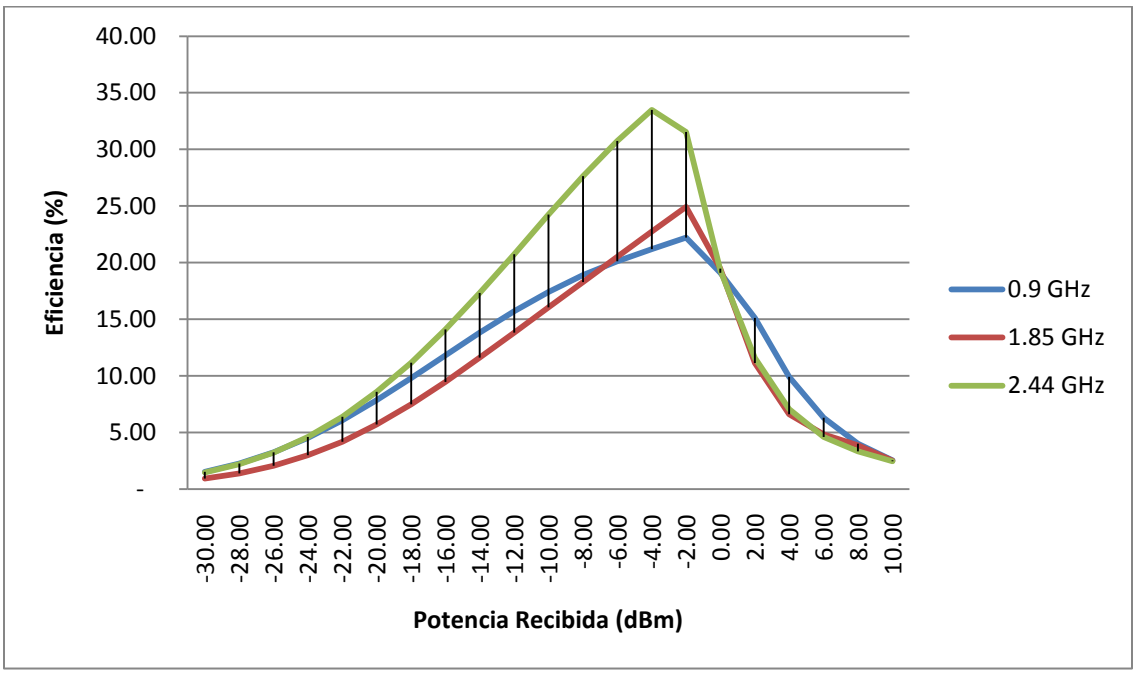

Fig. 4.4.6.2: Rectenna efficiency versus input power for low input power (Agilent ADS) at 900 MHz, 1.85 GHz and 2.45 GHz.

4.4.7 Parallel diode rectifier matched with LC circuit focusing on the bands of use.

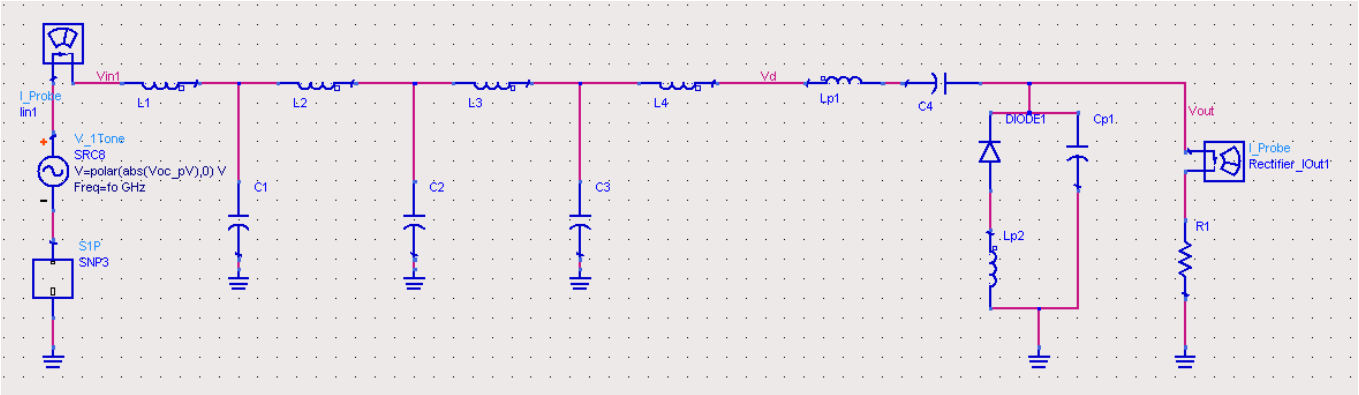

Fig. 4.4.7.1: Complete schematic: antenna S parameters, matching circuit and parallel diode rectifier.

Table 4.4.7: Simulation values for Fig. 4.4.7.1

Component Name	Value	Component Name	Value
L1	2.2 nH	**C1**	2 pF
L2	11.6 nH	**C2**	1 pF
L3	24 nH	**C3**	1 pF
L4	32 nH	**C4**	90 pF
Lp1	0.6 nH	**Cp1**	0.25 pF
Lp2	0.36 nH	**R1**	4.3KOh

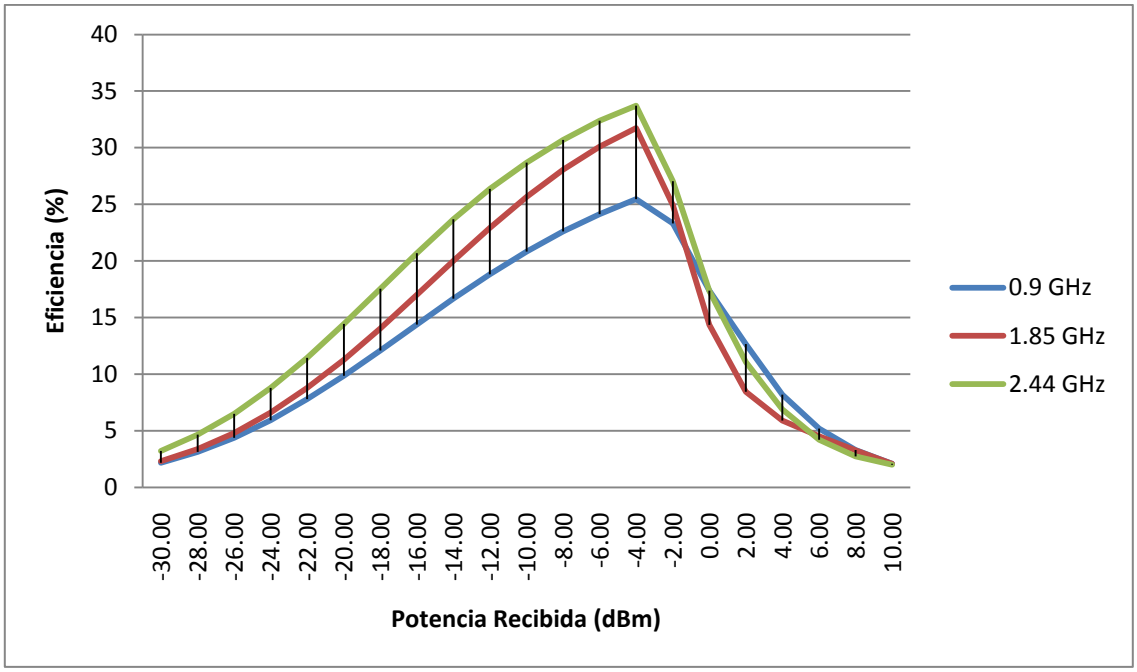

Fig. 4.4.7.2: Rectenna efficiency versus input power for low input power (Agilent ADS) at 900 MHz, 1.85 GHz and 2.45 GHz.

4.4.8 Two diode rectifier matched using the ADS2008 Impedance Matching Utility and focusing on the bands of use.

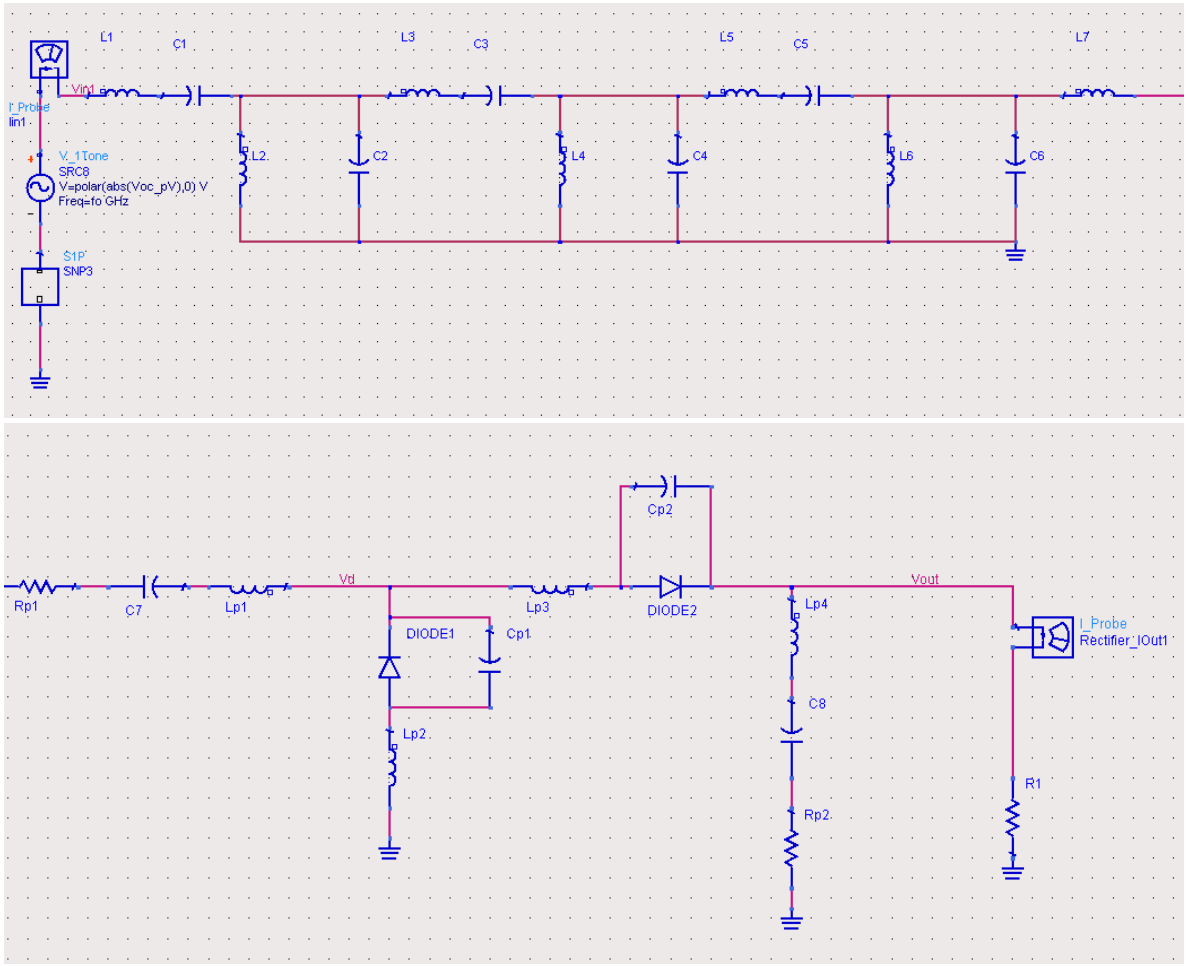

Fig. 4.4.8.1: Complete schematic: antenna S parameters, matching circuit and two diode rectifier.

Table 4.4.8: Simulation values for Fig. 4.4.8.1

Component Name	Value	Component Name	Value
L1	9.1 nH	**C1**	1.5 pF
L2	6.4 nH	**C2**	2.6 pF
L3	6.2 nH	**C3**	2.5 pF
L4	6.5 nH	**C4**	4 pF
L5	13 nH	**C5**	0.7 pF
L6	8.8 nH	**C6**	2.2 pF
L7	9.6 nH	**C7**	63 pF
Lp1	0.6 nH	**Cp1**	0.25 pF
Lp2	0.36 nH	**Cp2**	0.25 pF
Lp3	0.6 nH	**R1**	6.6KOh
Lp4	0.36 nH		

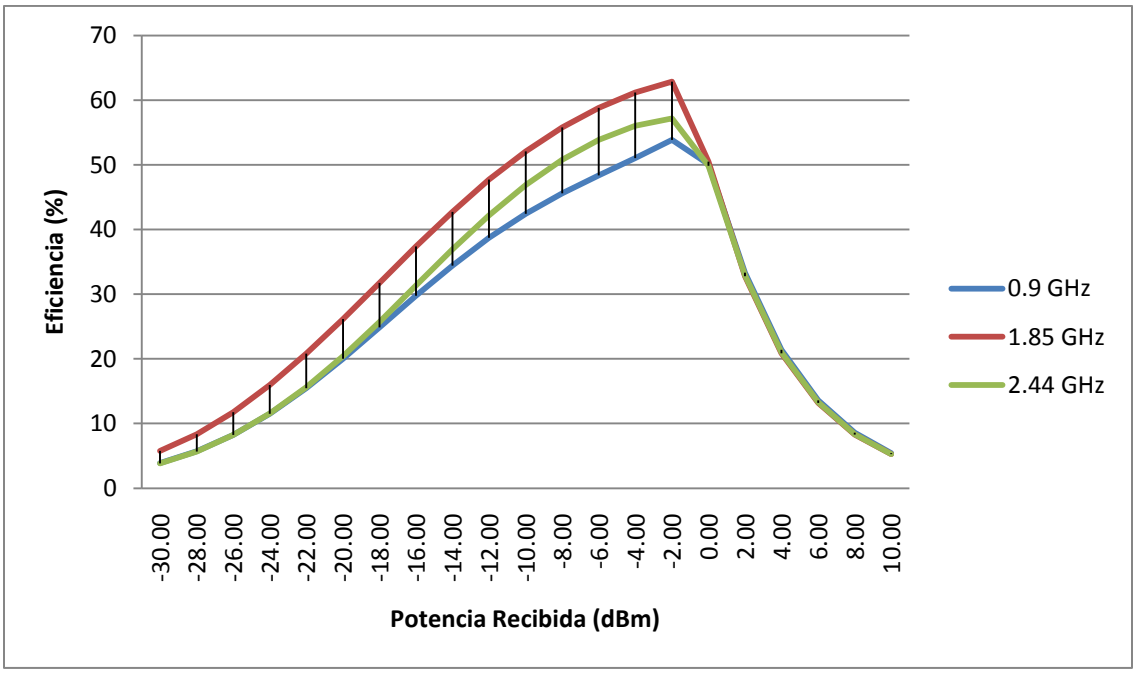

Fig. 4.4.8.2: Rectenna efficiency versus input power for low input power (Agilent ADS) at 900 MHz, 1.85 GHz and 2.45 GHz.

4.5 Efficiency Analysis for Low Input-power.

After analyzing the efficiency of each band in a power range, we will now analyze the efficiency when the received power is -20 dBm (which is a good example of an electromagnetic signal in the environment) and for frequencies ranging from 500 MHz to 3 GHz.

Fig. 4.5.1 (a) shows the efficiency of the rectifiers that have been adapted using the ADS2008 matching utility. A better performance is appreciated in the series rectifier; the parallel diode rectifier, shows an efficiency about 13% less for all bands while the two diode rectifier, in the 900 MHz, 1.85 GHz and 2.45 GHz bands has an efficiency of 8%, 5% and 8% respectively, lower than the series diode rectifier. As explained above, the difficulty with this method of adaptation is the great quantity of components required and the consequent loss of performance when soldering. Fig. 4.5.1 (b) shows the efficiency versus frequency for the rectifiers adapted with LC circuits and for all 700 MHz- 2.5 GHz band, we can observe that the results are similar but less efficient than other methods of adaptation, improved efficiency is achieved with the rectifier diode series that has reached about 5% higher efficiency than the parallel rectifier diode; this low efficiency is the result of adapting a broad band of frequencies with a limited number of components. Fig. 4.5.2 shows the efficiency of the rectifier adapted with LC circuit over the bands of interest, again we see that a higher performance was obtained with the series diode rectifier diode,

this is because it is more feasible to adapt rectifier using the same number of components to smaller frequency bands.

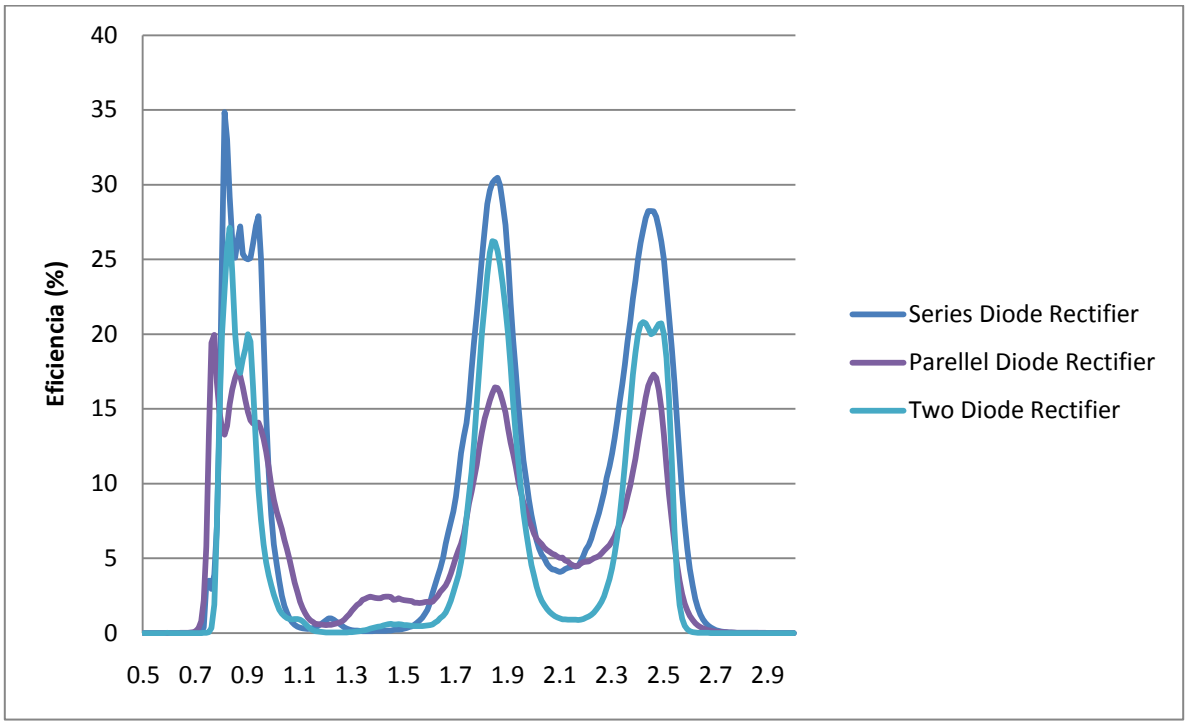

(a)

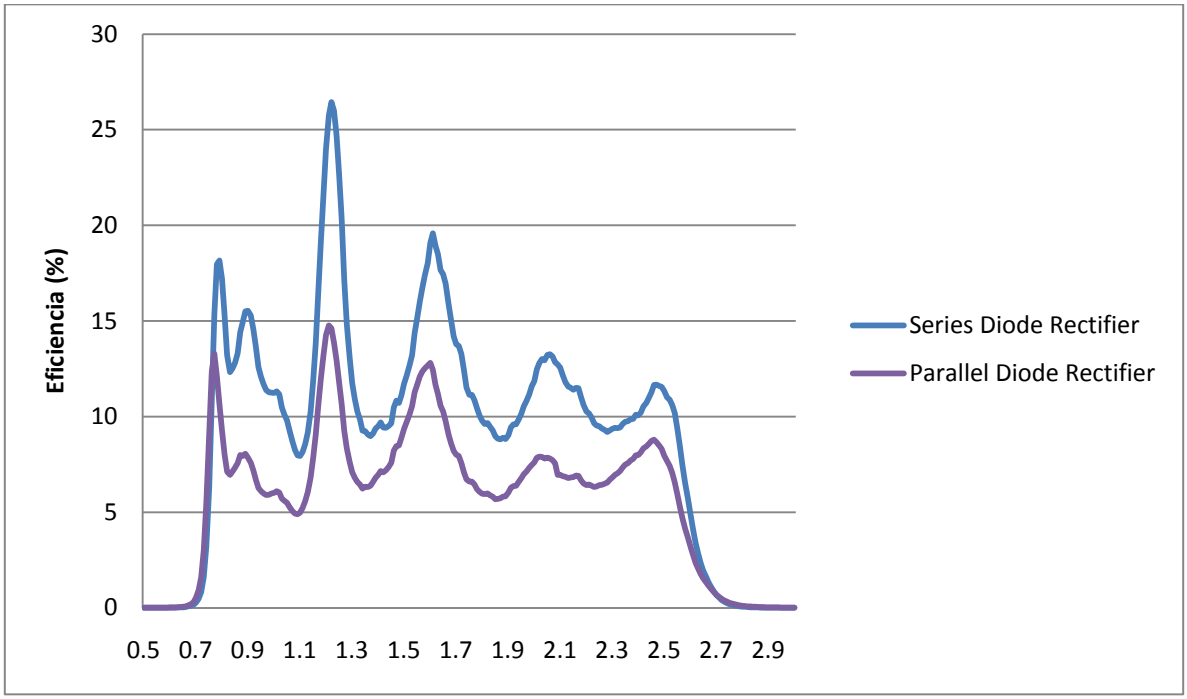

(b)

Fig. 4.5.1: Efficiency versus frequency for -20dBm input power for (a) the rectifiers adapted with the ADS2008 matching utility and with focus over the 900 MHz, 1.85 GHz and 2.45 GHz bands (b) the rectifiers adapted with LC circuits for the entire 700 MHz – 2.5 GHz band.

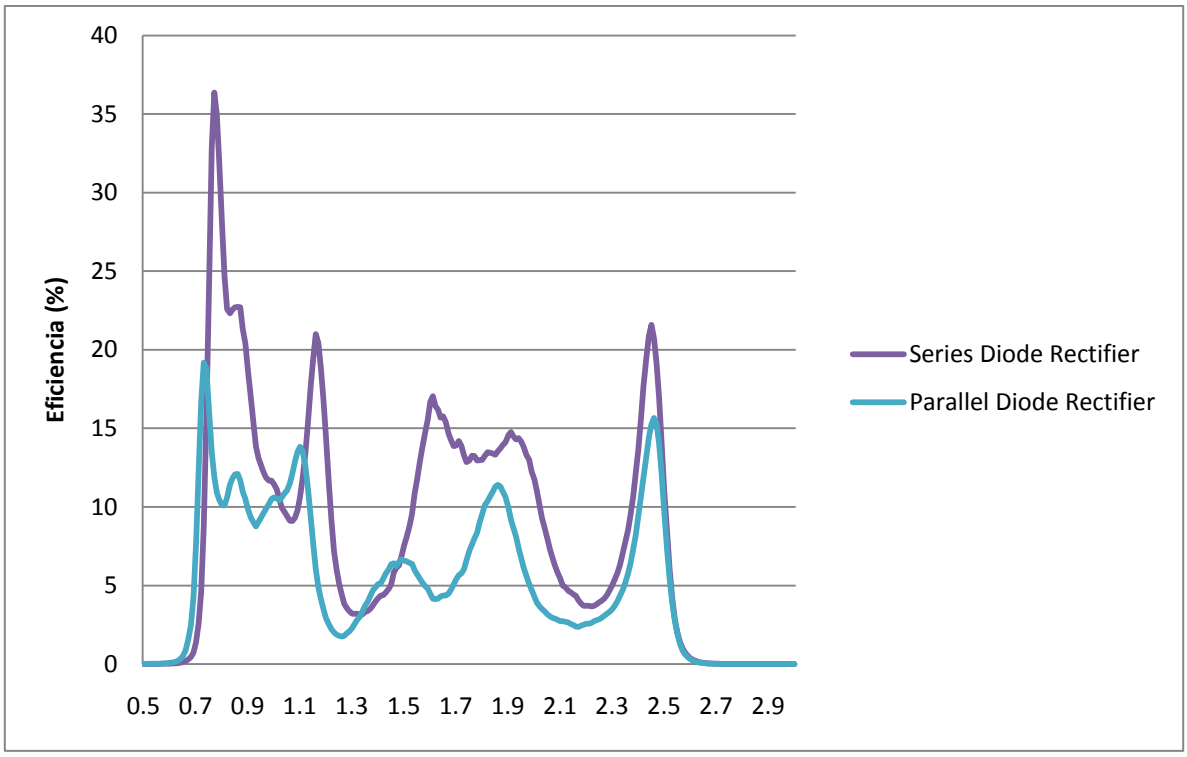

Fig. 4.5.2: Efficiency versus frequency for -20dBm input power for the rectifiers adapted with LC circuit with focus over the 900 MHz, 1.85 GHz and 2.45 GHz bands

4.6 LC to Microstrip-Lines Transformation

According to the simulations shown above, the series diode rectifier was chosen to proceed with the application for showing the best performance in simulations; the problem now would focus on choosing the proper matching method. Given the low efficiency of the rectifier circuit adapted with LC elements, we have decided to improve the rectifier adapted with the ADS2008 matching utility but with a LC-Microstrip line transformation to avoid the effects of soldering and to exploit the characteristics of microstrip lines.

Fig. 4.6.1 shows the equivalence for the transformation from LC elements to microstrip lines; we can see that the series inductor and capacitor have been transformed into a transmission line, the parallel grounded inductor and capacitor have been transformed into a grounded parallel stub and the parallel grounded inductor has been transformed into a not grounded parallel stub. Fig. 4.6.1 shows the complete circuit schematic where the inductors and capacitors have been transformed into transmission lines.

To improve the efficiency of our circuit, the techniques of harmonic balance and nominal optimization were applied again. In this case, the parameters that were optimized were: the lengths and widths of each transmission line, the inductor value, the rectifier capacitor and the load resistance. Table 4.6 shows the final values of optimization. Fig. 4.6.2 shows the

efficiency as a function of the frequency when the input power is -20 dBm, a good example of electromagnetic signal in the environment.

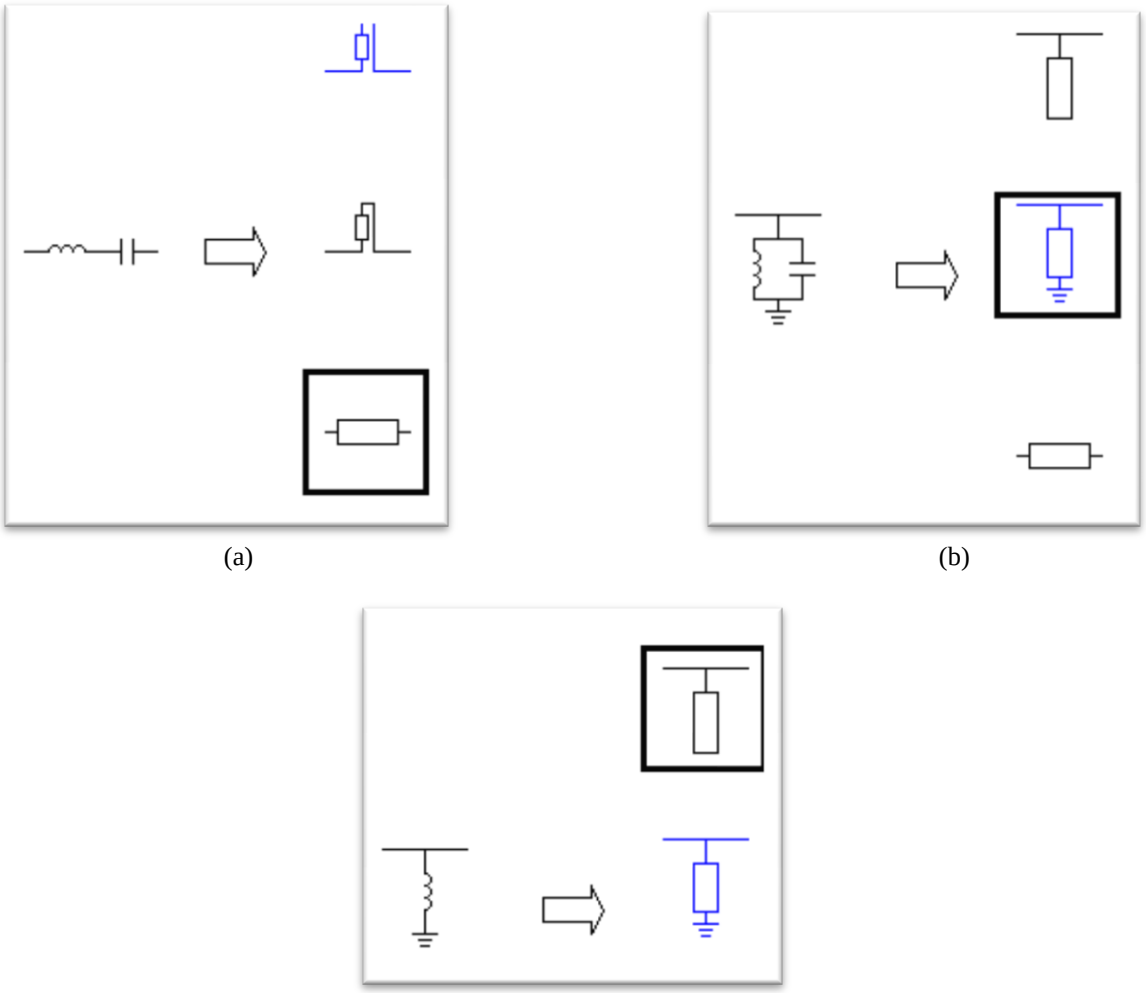

(a) (b) (c)

Fig. 4.6.1: (a) series inductor and capacitor (b) parallel grounded inductor and capacitor (c) parallel grounded inductor possible transformations, components in a box were selected

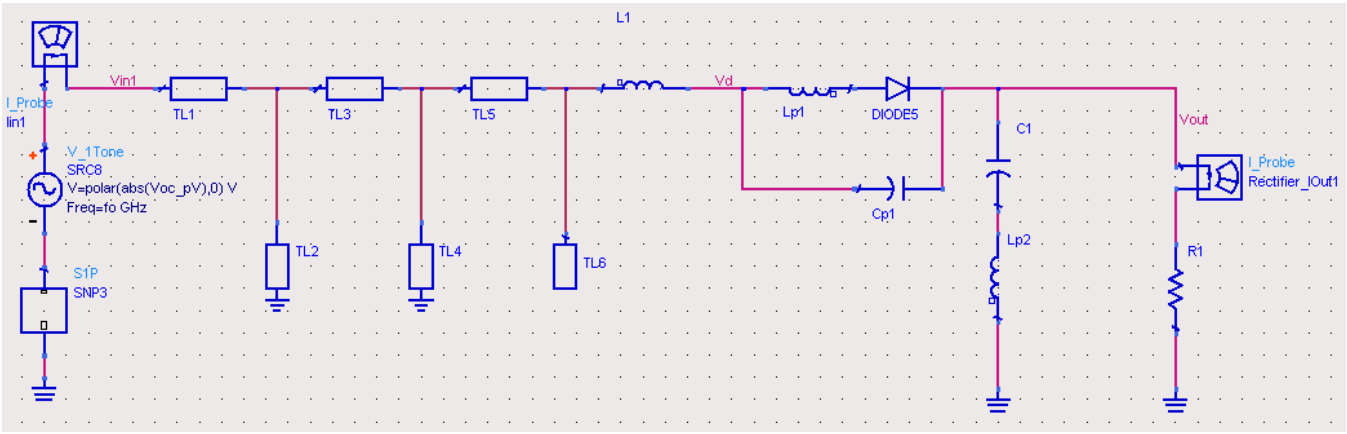

Fig. 4.6.2: Complete schematic: antenna S parameters, matching microstrip lines and the series diode rectifier.

The Fig. 4.6.3 also shows a comparison of efficiency as a function of frequency between the classical LC circuit components and the new transmission lines circuit. We can observe that the efficiency is almost identical with the exception of some small details such as that the implementation of transmission lines has improved by 5% the 900 MHz band performance and the 1.85 GHz band shows efficiency drop of 4%.
In Fig. 4.6.4 a comparison of the efficiency as a function of received power shown, we can observe that the maximum efficiency for 900 MHz, 1.85 GHz and 2.45 GHz is achieved when the received power is -6 dBm, - 6 dBm and -4 dBm respectively and the efficiency at this values are 48.6%, 64.8% and 53.6% respectively.

Table 4.6: Simulation values for Fig. 4.6.1

Component Name	Value	Component	Value
L1	12 nH	**TL5**.L	2.7 cm
TL1.L	3.2 cm	**TL5**.A	0.3 mm
TL1.A	3.5 mm	**TL6**.L	0.25 cm
TL2.L	2.7 cm	**TL6**.A	1.8 mm
TL2.A	0.4 mm	**C1**	100 pF
TL3.L	2.7 cm	**Cp1**	0.25 pF
TL3.A	0.8 mm	**Lp1**	0.36 nH
TL4.L	2.4 cm	**Lp2**	0.6 nH
TL4.A	0.73 mm	**R1**	0.36 nH

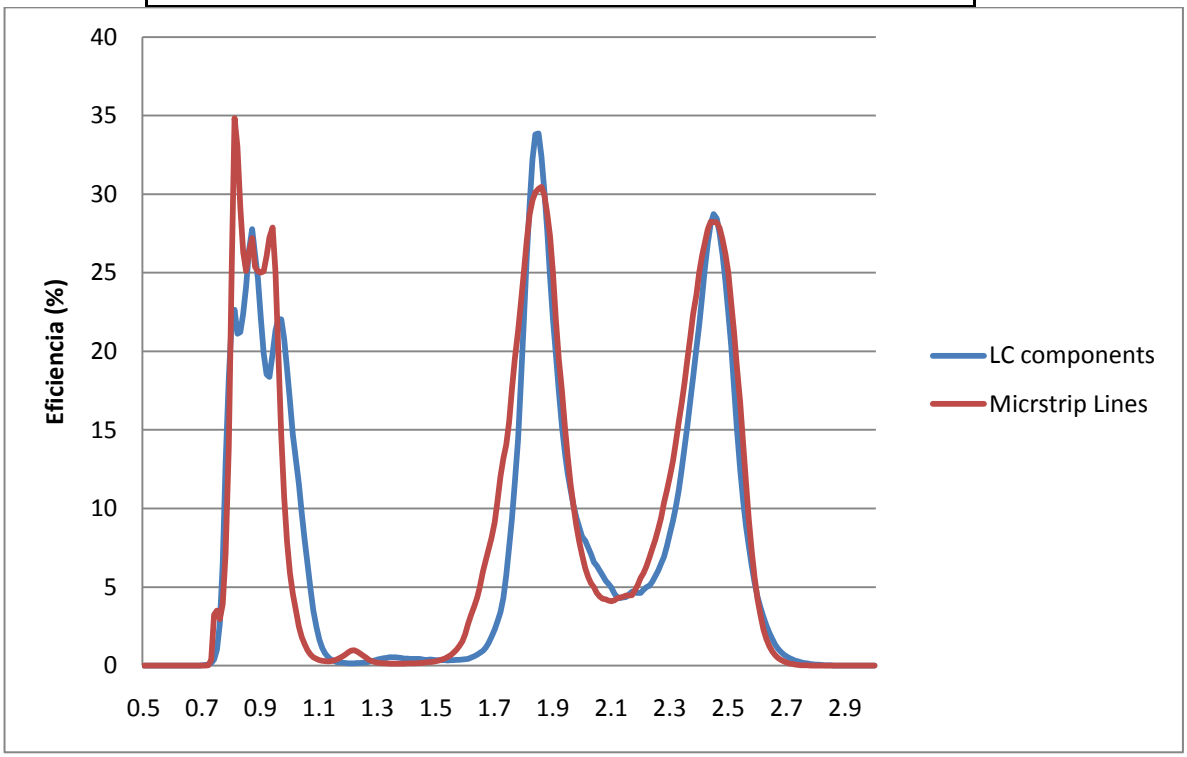

Fig. 4.6.3: Efficiency versus frequency for -20dBm input power for the rectifiers adapted with LC components and Microstrip Lines for the 900 MHz, 1.85 GHz and 2.45 GHz bands

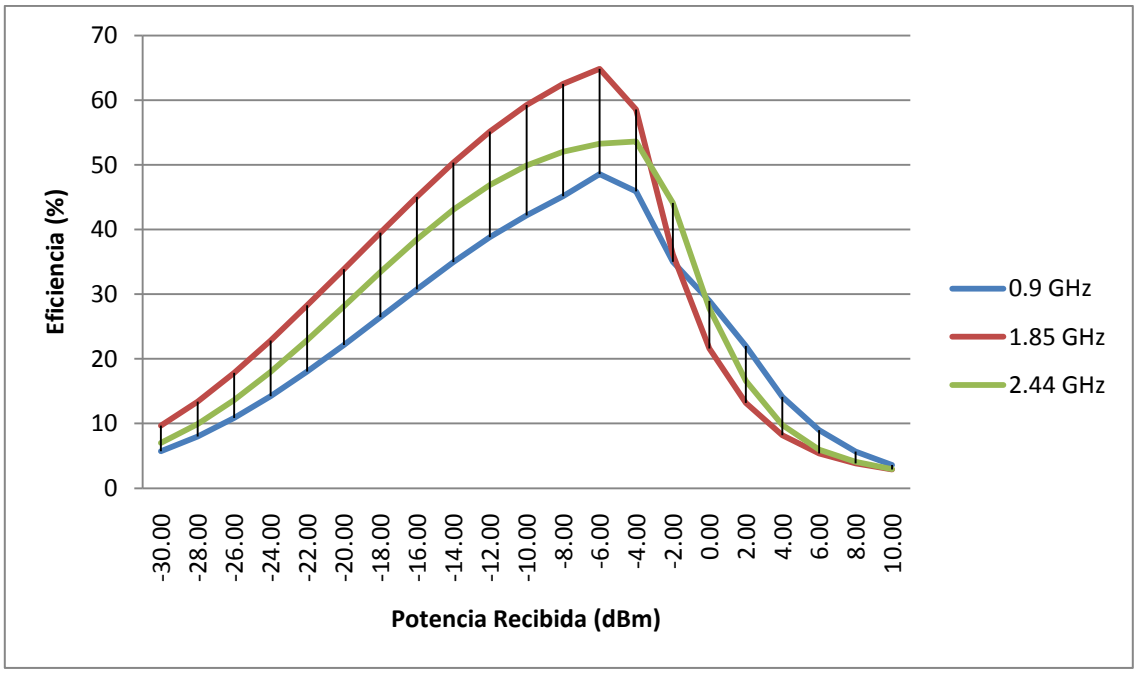

Fig. 4.6.4: Rectenna efficiency versus input power for low input power (Agilent ADS) at 900 MHz, 1.85 GHz and 2.45 GHz.

4.6.1 Momentum

Momentum is an electromagnetic simulator that computes S-parameters for various topologies such as ours that presents vias (holes that connect two layers of the topology). This tool is very useful to predict circuit performance at high frequencies and one of the main advantages of momentum is that, from a schematic, you can create a physical layout to simulate the characteristics of the substrate and also allocate the necessary ports to simulate the different components of our circuit. Momentum is based on the numerical discretization method called method of moments.

In general, the method of moments, fragments transmission lines into smaller segments to find the current distribution in each of these, so at the end of the simulation, we can know the joint behavior of these to characterize the entire system.

4.6.2 Momentum Layout

Once we have the LC component values optimized as well the transmission lines lengths, the next step is to generate the layout of our matching circuit to simulate the transmission lines together with the substrate. In Fig. 4.6.2.1 the auto generated matching circuit layout is shown.

According to the values in Table 4.6, the lengths of transmission lines L1, L3 and L5, are 3.2cm, 2.7cm and 2.7cm respectively, giving a total of 8.6cm.

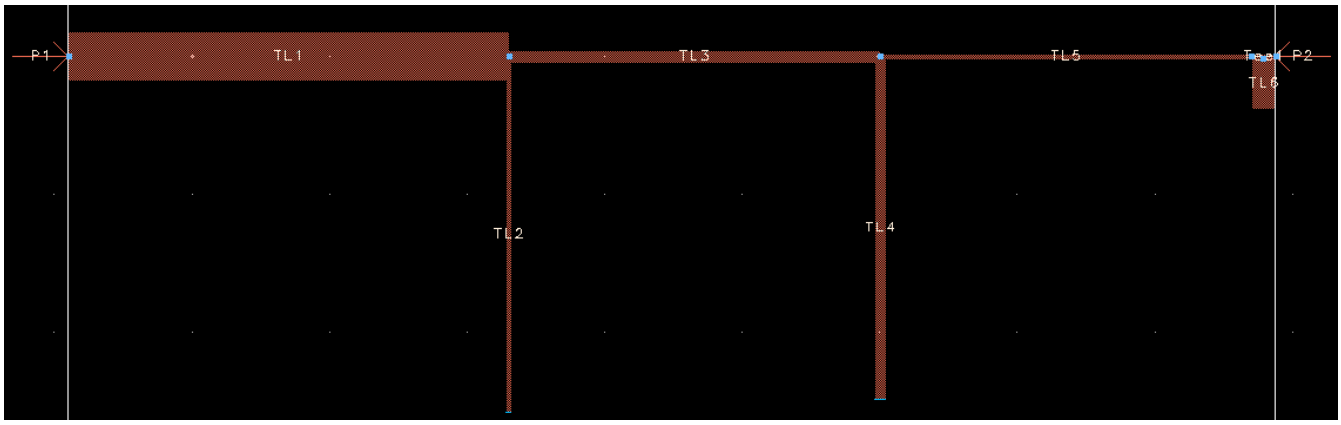

Fig. 4.6.2.1: auto generated matching circuit layout by ADS2008 Momentum

To improve the circuit size and make it more compact, a technique has been applied; we have kept the lengths of the transmission lines but instead of straight lines we have used curved transmission lines. The measures of the complete layout with straight lines were: 8.75cm x 2.75cm, while the measurements of the size-improved layout are: 2,97cm x 2.31cm, 66% and 16% shorter.

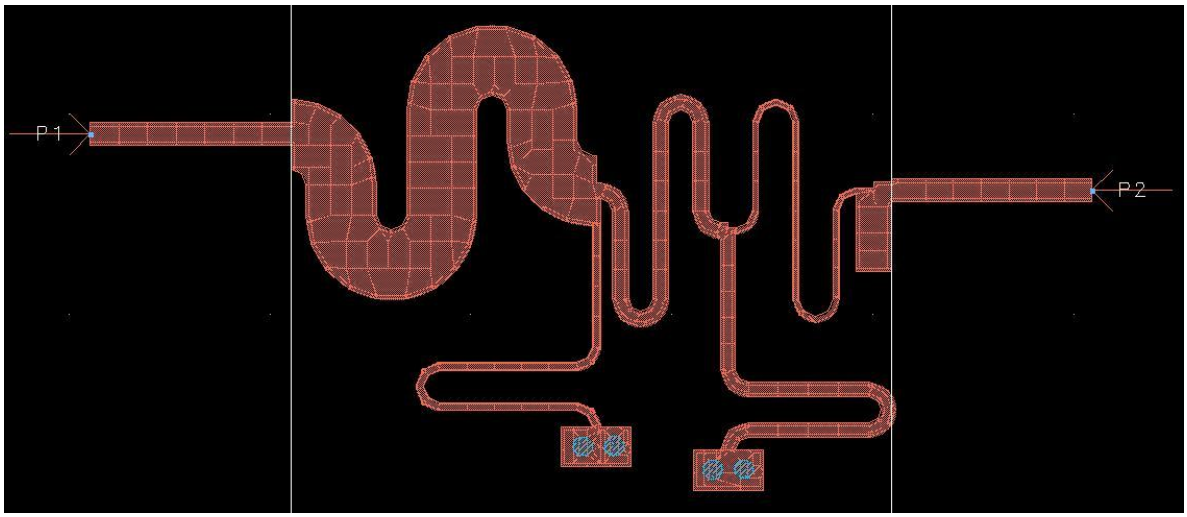

Fig. 4.6.2.2: size-improved matching circuit and momentum meshing.

In Fig. 4.6.2.1 and 4.6.2.2, we can observe that the ground lines are different, this is because the ADS2008 generates an ideal model of ground connection, which is not desirable when simulating since the simulations should adjust to real parameter, what is we really want, that's why in Fig. 4.6.2.2 the ideal ground has been replaced by a transmission line with two vias that connects the top layer with the ground plane through the

substrate. This hole will be subsequently filled with a conductor paste; this will be discussed in detail in Section 4.7.

Since the results after simulating with Momentum could be different and therefore not reach the goals, some adjustments in the transmission lines should be made; we have seen empirically that by adjusting the length of the third stub, the 2.45 GHz band moves to the right or the left if ,respectively, the length decreases or increases. A similar behavior has been observed in the other stubs, so that the efficiency for the frequency bands has been adjusted successfully. Fig. 4.6.2.3 shows the efficiency as a function of frequency for the rectifier with the data that Momentum has generated. To implement momentum data in the simulation of the entire circuit, the implementation of a data module is necessary. Fig. 4.6.2.4 shows the module has been implemented.

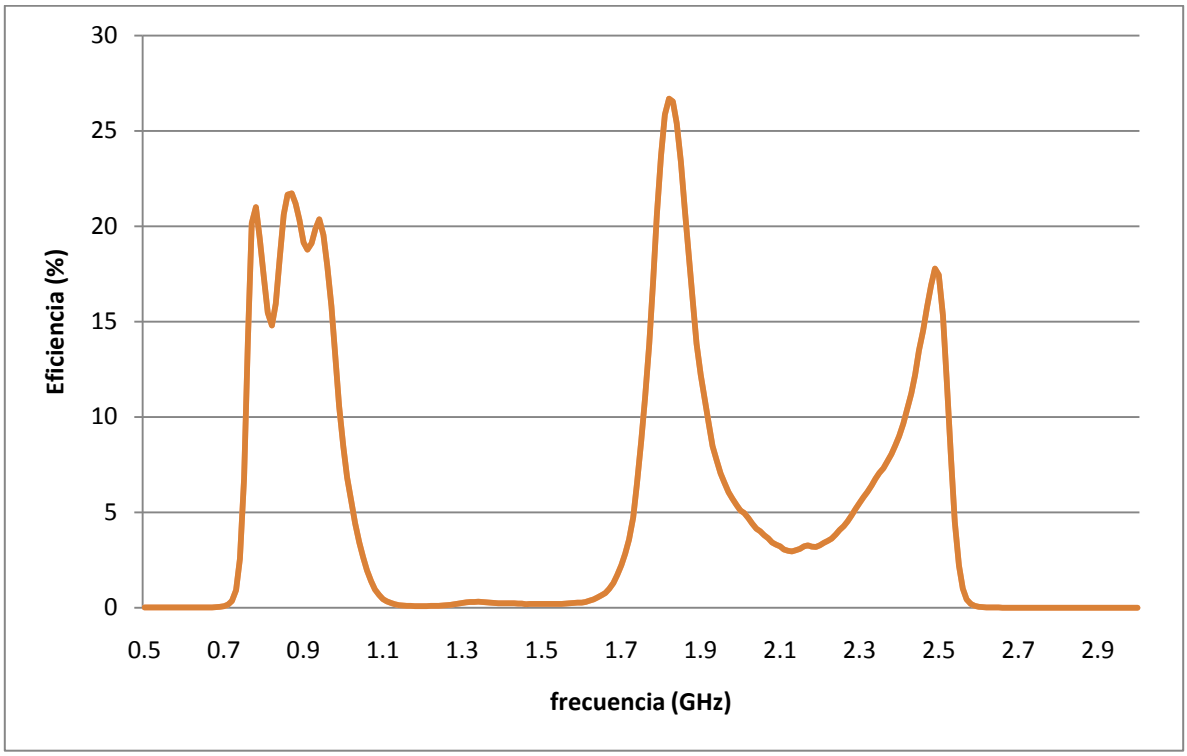

Fig. 4.6.2.3: Efficiency versus frequency showing the behavior for -20dBm input power with the matching circuit Momentum data implemented.

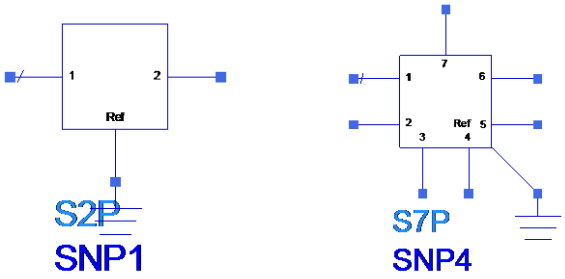

Fig. 4.6.2.4: 2 and 7-port S-Parameter module, the data generated by Momentum is loaded into these items and then simulated with the other circuit components.

The rectifier layout was designed based on the measurements of the components to be attached. Fig. 4.6.2.5 shows the layout of the rectifier that, for the schematic simulation, components such as diodes, inductors, capacitors and resistors are replaced by ports; each of these ports corresponds to one pin of the module data (Fig. 4.6.2.4) in the schema.

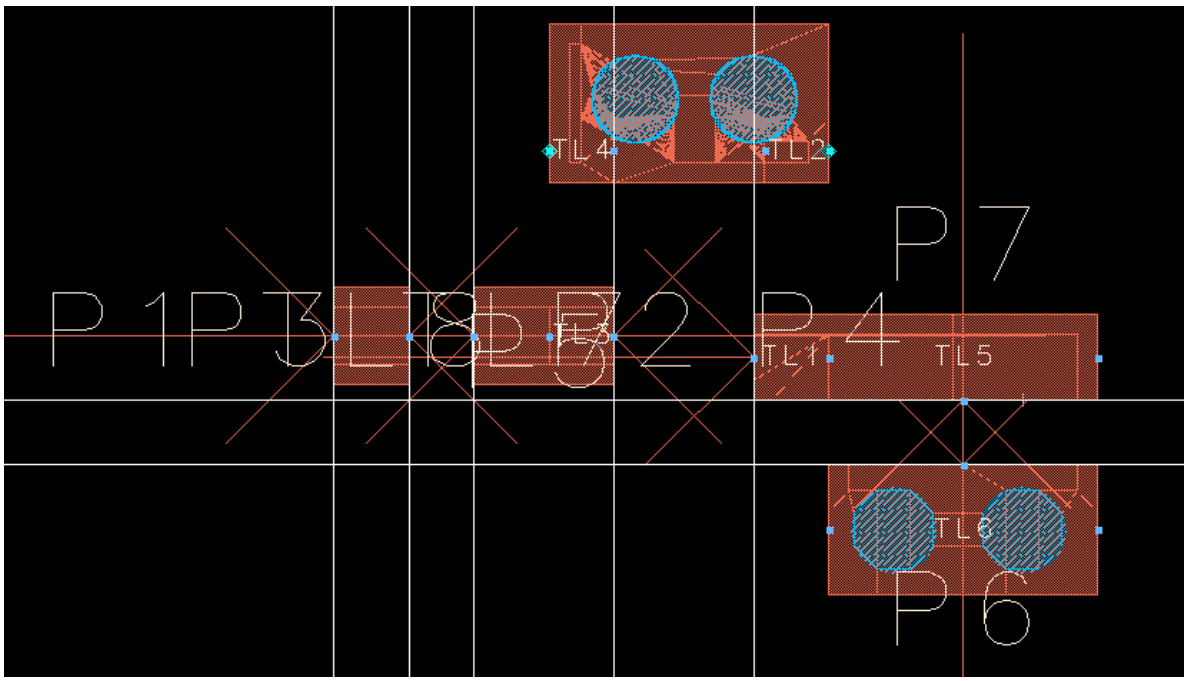

Fig. 4.6.2.5: Rectifier layout, the dimensions are 7.1 x 5.3mm

Fig. 4.6.2.6 shows the complete schematic with the integrated data modules. The first module, has the matching circuit momentum simulation data, the second module, has the momentum simulation data of the transmission lines of the rectifier, so that the ports that had been placed before in the layout now are in the respective pins on the module to simulate with the components.

Fig. 4.6.2.7 shows the efficiency versus frequency, we can observe that the maximum efficiency for the 900 MHz, 1.85 GHz and 2.45 GHz bands is about 20%. Fig. 4.6.2.8 shows the efficiency for the power received, we can see that for the bands mentioned above, the maximum efficiency is 48.6%, 64.8% and 53.6% respectively and are achieved when the received power is of -6 dBm,-4dBm and -6dBm respectively.

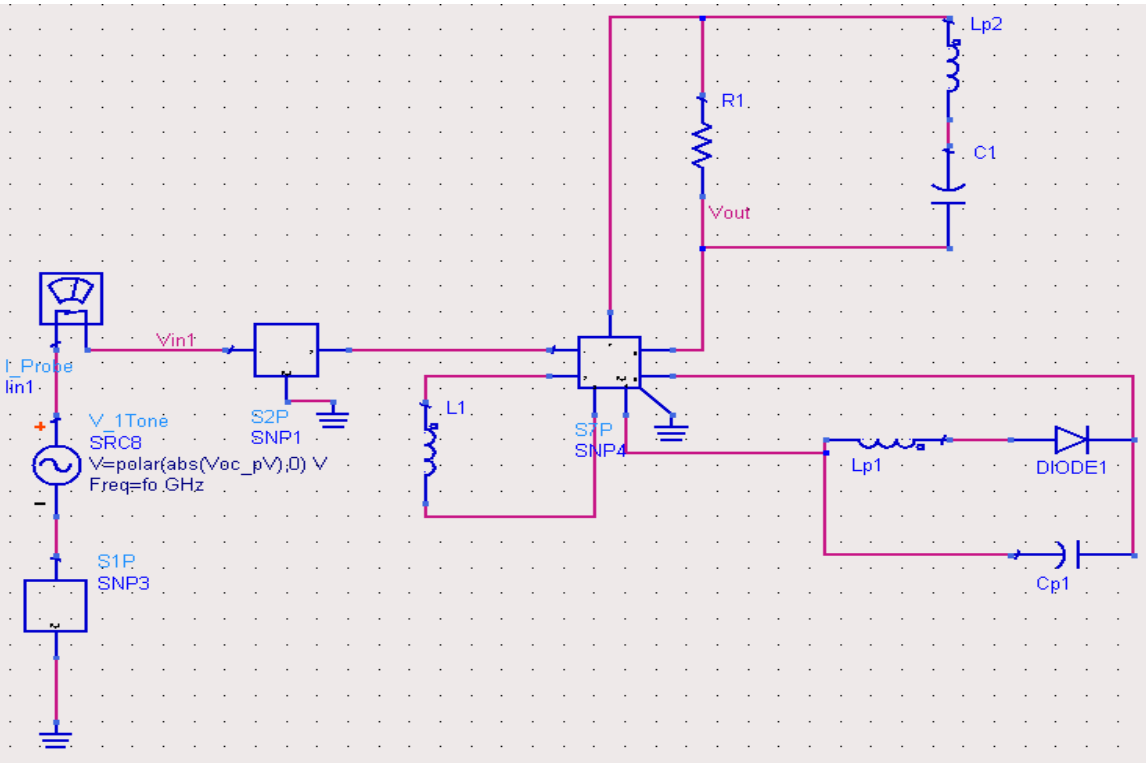

Fig. 4.6.2.6: Complete final schematic including matching lines and rectifier transmission lines momentum data

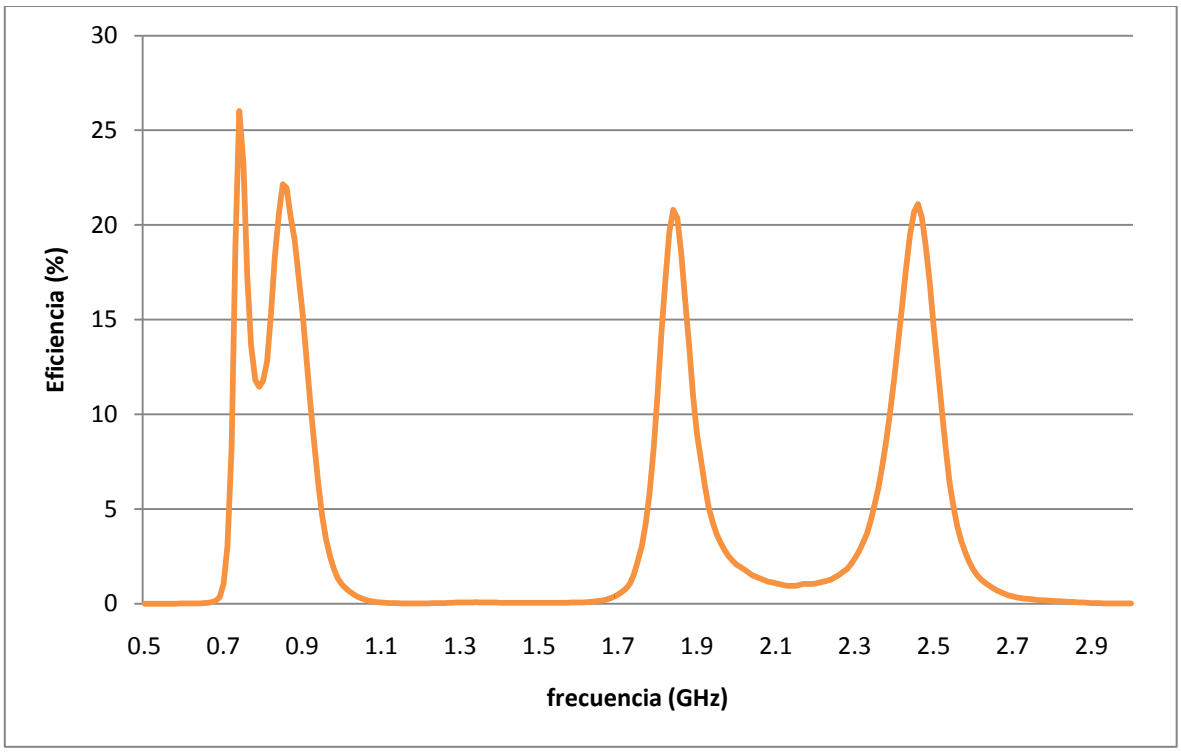

Fig. 4.6.2.7: Efficiency versus frequency showing the behavior for -20dBm input power with the matching and rectifier lines Momentum data implemented.

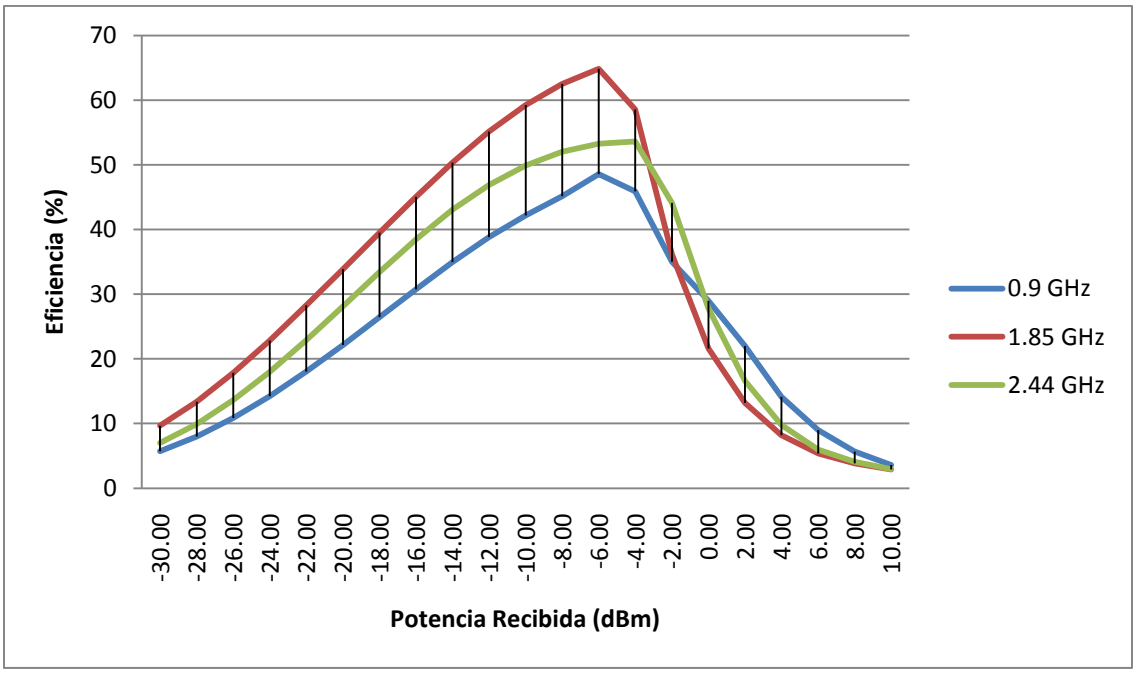

Fig. 4.6.2.8: Rectenna efficiency versus input power for low input power (Agilent ADS) at 900 MHz, 1.85 GHz and 2.45 GHz.

4.7 Rectifier Fabrication and Measurements

The manufacturing process of the rectifier circuit, as it is made from the same substrate as the antenna, is almost the same. The only difference is that to make the VIA holes, we need to follow a procedure called metallization of circuit boards [21]. The first step of this procedure is to protect the circuit with a plastic protective film before drilling the holes. The second step is the application of the LPKF Pro Conduct ® paste that, with the help of a vacuum table to suck it, will coat the walls of the hole. Finally, after removing the plastic protective film, the circuit is introduced in a hot air oven at 160 º C for 30 minutes.

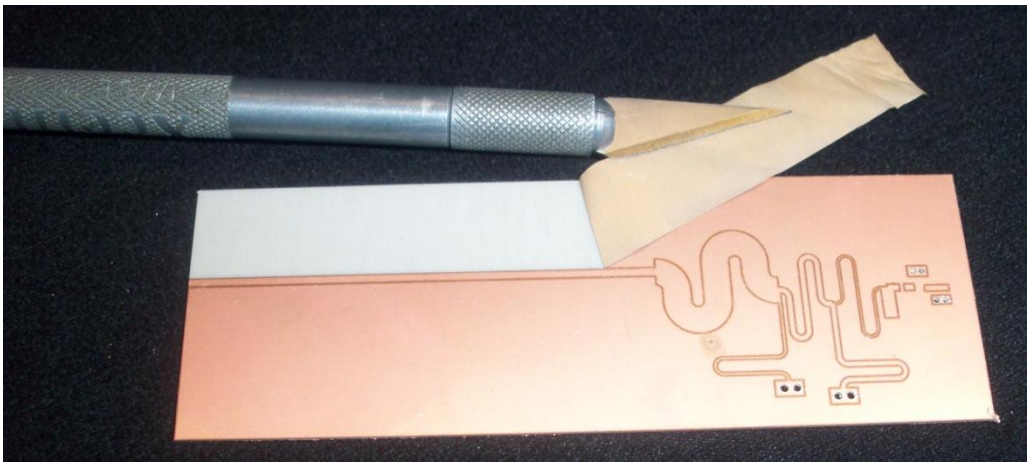

Fig. 4.7.1: Recent fabricated matching-rectifier circuit with copper excess.

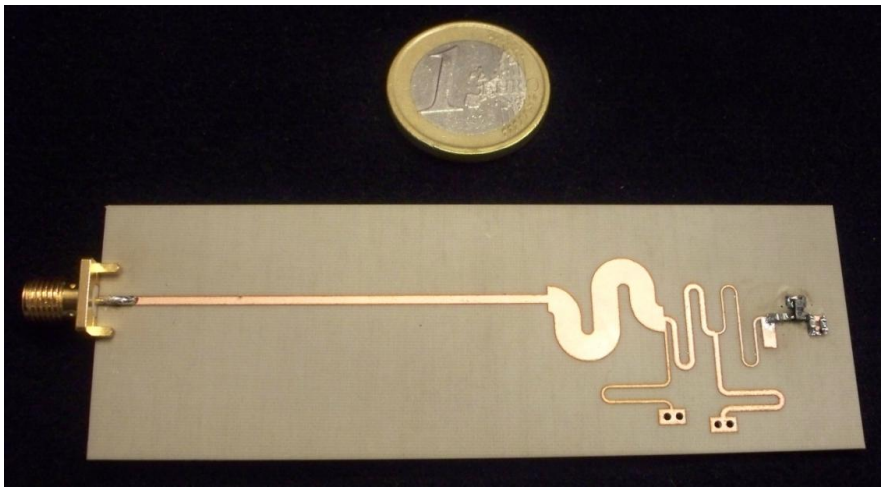

(a)

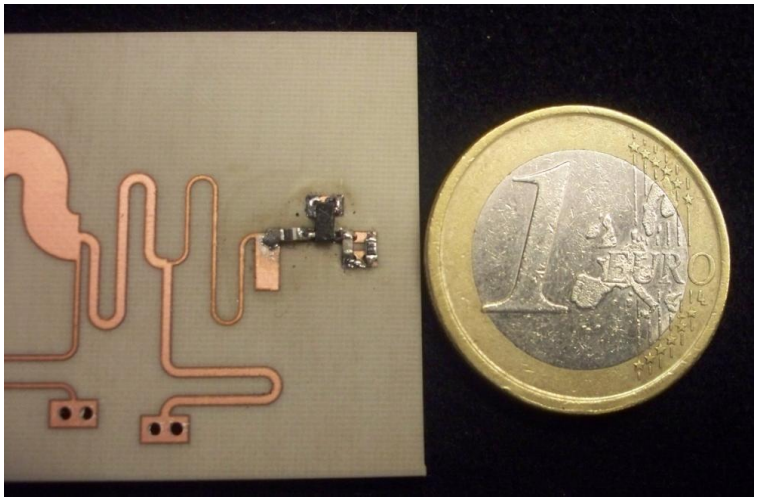

(b)

Fig. 4.7.2: shows the matching circuit (a), the rectifier circuit (b) and a zoom to the soldered components(c)

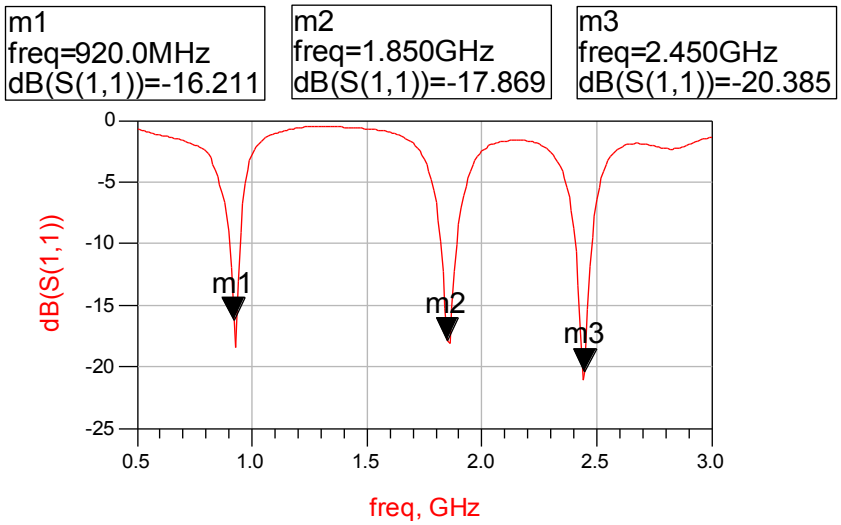

Fig. 4.7.3: shows the S11 parameters of the rectifier.

Fig. 4.7.1 shows, similarly to the antenna fabrication, the way to remove the copper excess that covers the top layer of the substrate with a cutter; and Fig. 4.7.2, as a form of demonstration, shows the dimensions of the newly manufactured circuit compared with a euro coin to the side. Note that the exact measurements have been detailed in section 4.2.6.
The parameters measured and compare with the simulations were the S-parameters (section 4.3.1). To carry out these measurements a Rohde & Schwarz ZVA24 Vector Network Analyzer (VNA) has been used.

Fig. 4.7.4: Rectenna measurement: analog signal generator and multimeter

The measurements for the full rectification circuit were made, therefore, with the matching circuit attached to it. To make these measurements, we used the Agilent E8257D analog signal generator, an Agilent E4407B spectrum analyzer and a Promax MC-859 digital multimeter. The first thing we did was to "calibrate" the cable which would connect the rectifier circuit to the analog signal generator, this is done because minimal DC power is lost in the cable; for this "calibration" the same cable to be used later was connected from the analog signal generator to the spectrum analyzer in order to obtain more accurately delivered power measures from the signal generator. After this, we connect the rectifier to the signal generator, and with the help of a multimeter, the output DC voltage was measured.

Once we have the measurement system ready, we can proceed to take some measures. The measurements were taken as follows:

- An input power sweep, ranging from -25 dBm to 5 dBm for each frequency (900 MHz, 1.85 GHz and 2.44 GHz).
- A frequency sweep, ranging from 800 MHz to 2.5 GHz for an input power of -10 dBm.
- A frequency sweep, ranging from 800 MHz to 2.5 GHz for an input power of -20 dBm.

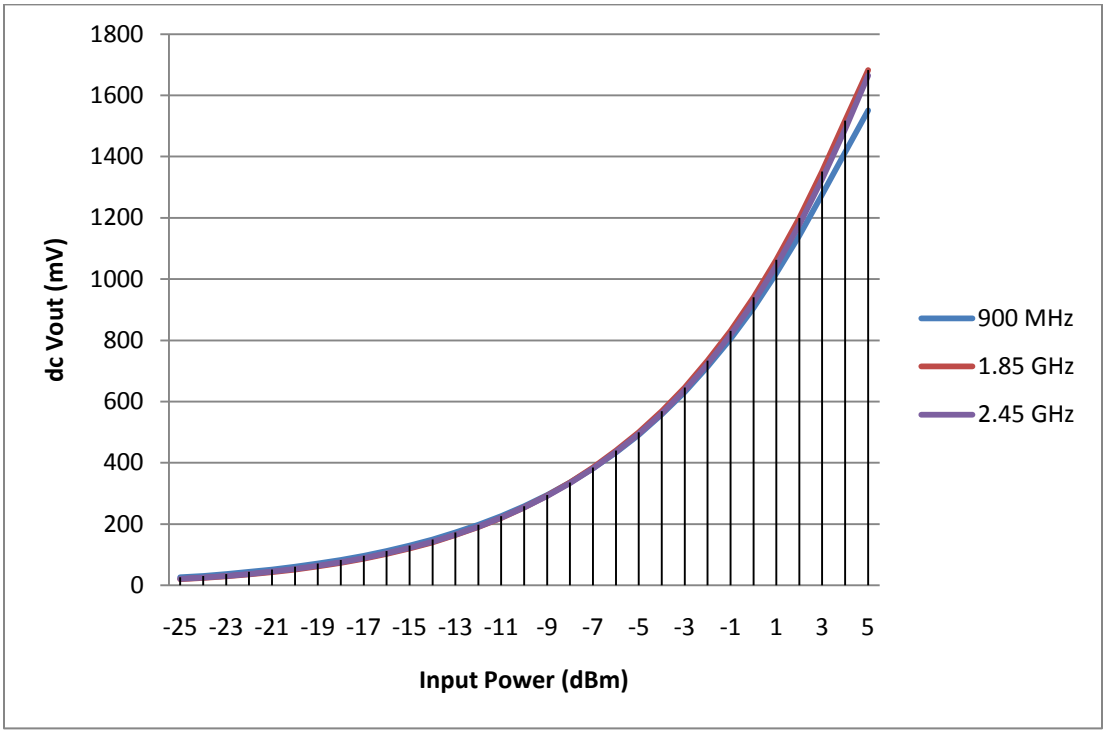

Fig. 4.7.5: Output voltage vs. input power for 900MHz, 1.85 GHz and 2.45GH

Fig. 4.7.4 shows that as we increase the input-power, the DC voltage increases proportionally, but this does not necessarily indicate that the overall efficiency shows the same behavior. This can be justified by observing the Fig. 4.7.5, where the efficiency vs. input-power plot, denotes that for high values of input power, efficiency begins to fall. For efficiency values: First, we calculated the output power by squaring DC voltage measured with the multimeter (which we have previously converted from mV to V) and was then divided by our radiation resistance. Second, we calculated the RF power by transforming the input power from dBm to Watts and finally, we divided the value of the output power by the RF power value.

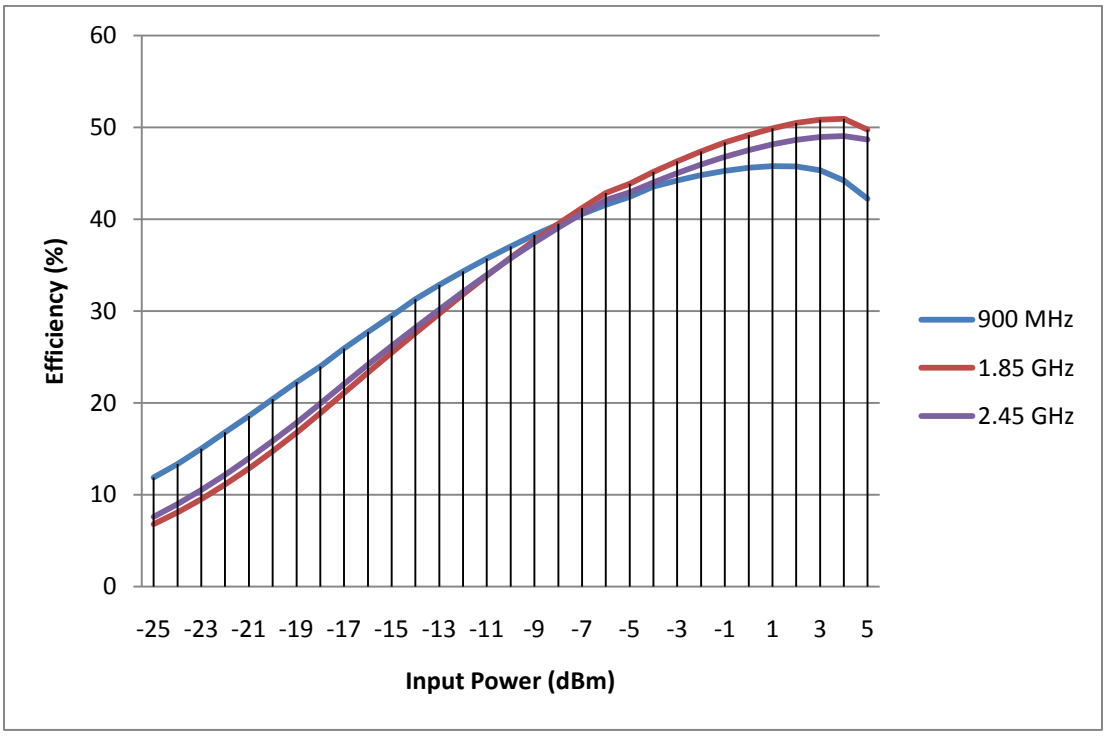

Fig. 4.7.6: Efficiency vs. input power for 900MHz, 1.85 GHz and 2.45GH

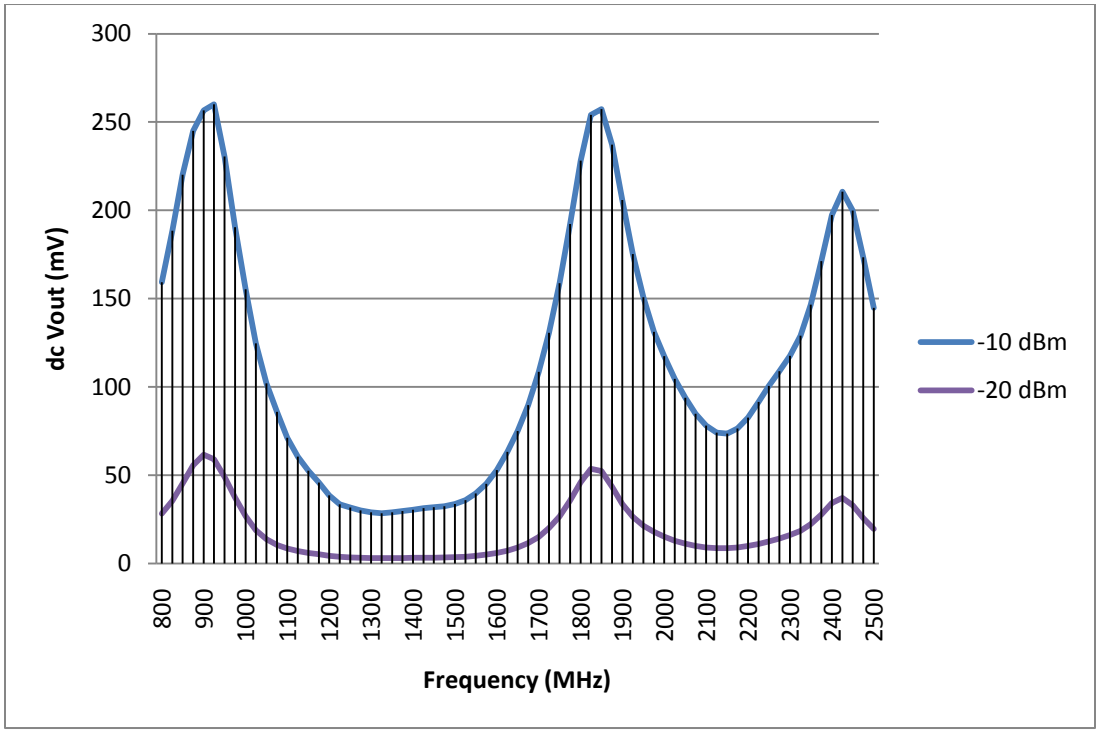

Fig. 4.7.7: Output voltage vs. frequency for -10 and -20 dBm input power

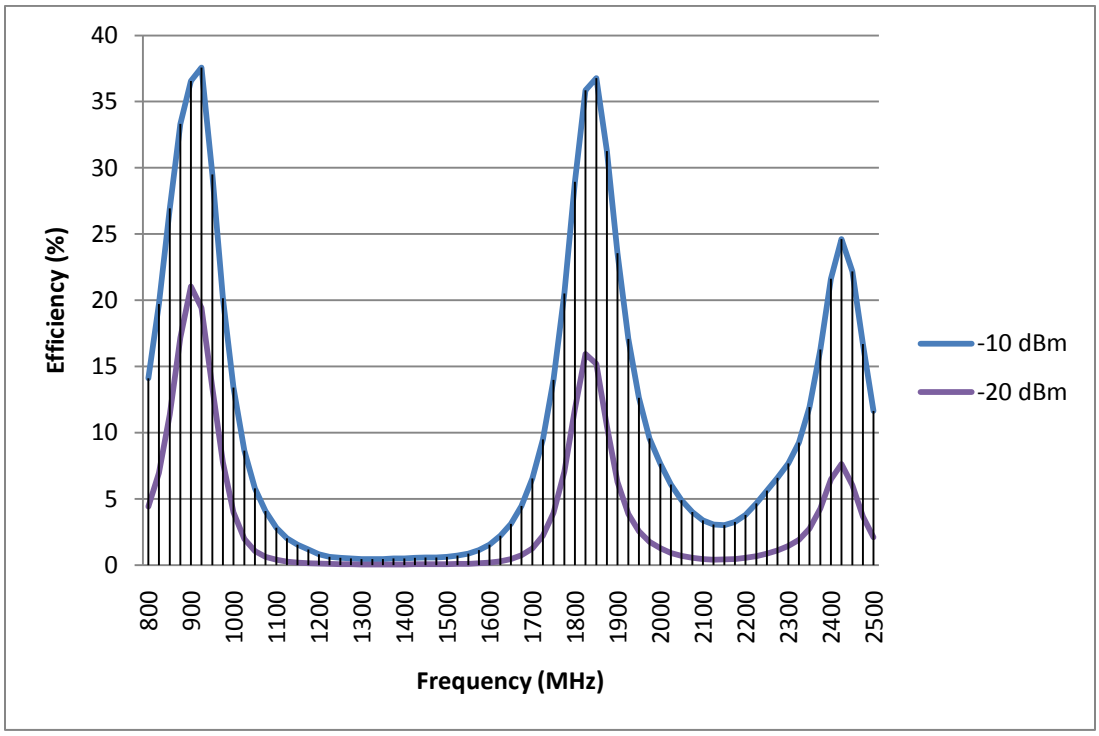

Fig. 4.7.8: Efficiency vs. frequency for -10 and -20 dBm input power

Fig. 4.7.6 shows measurements of the output voltage for a known input power, but now, making a frequency sweep ranging from 800 MHz to 2.5 GHz. The results show a better performance in the frequency bands that are involved in our application for both -10 dBm and -20 dBm input power values. We can conclude it that proper rectifier circuit design and fabrication has been done. A similar behavior is shown in Fig.4.7.7where the efficiency shows a similar pattern to the output voltage. Can be seen that for 900 MHz, 1.85 GHz and 2.45 GHz bands, the efficiency values with -10 dBm input power are around 37%, 36% and 24 % and for -20 dBm input power, the efficiency values are around 21%, 16% and 7% respectively.

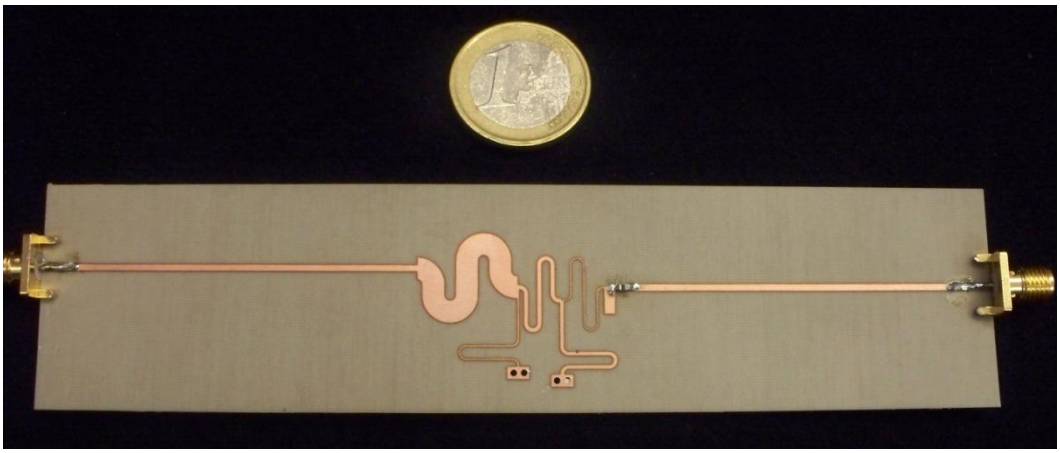

Fig. 4.7.9: matching network

If we compare the measurements results with those of the simulations, we can see that there is a considerable loss of efficiency (especially at the 2.45 GHz band). In order to try to explain this loss, we decided to fabricate and test the matching circuit and check if there is any considerable loss.

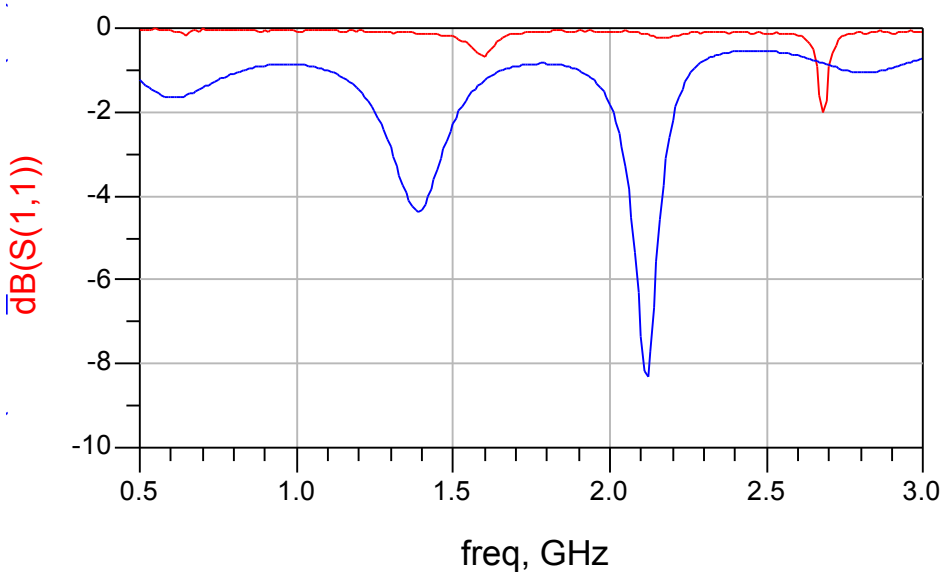

Fig. 4.7.10: S11 comparison: red line = measurement, blue line = simulation

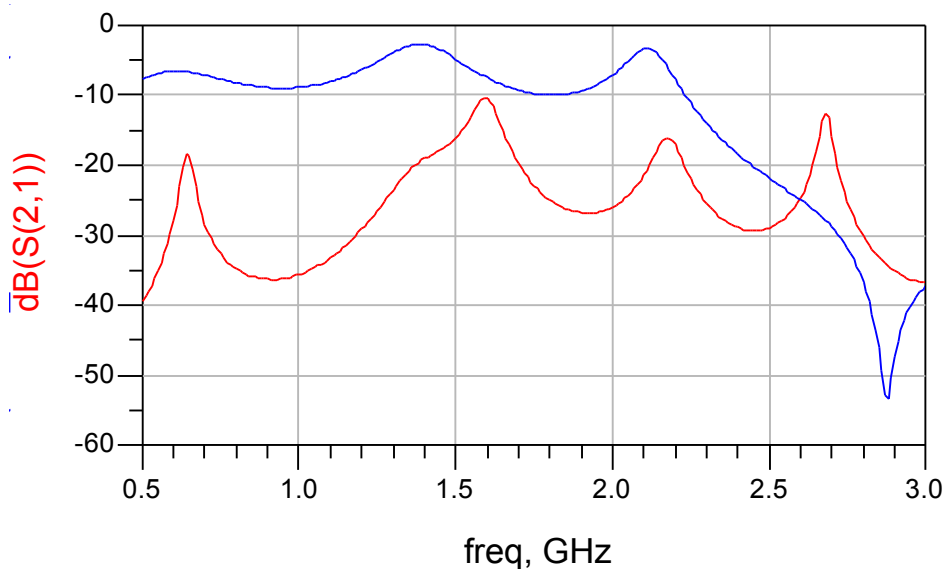

Fig. 4.7.11: S21 comparison: red line = measurement, blue line = simulation

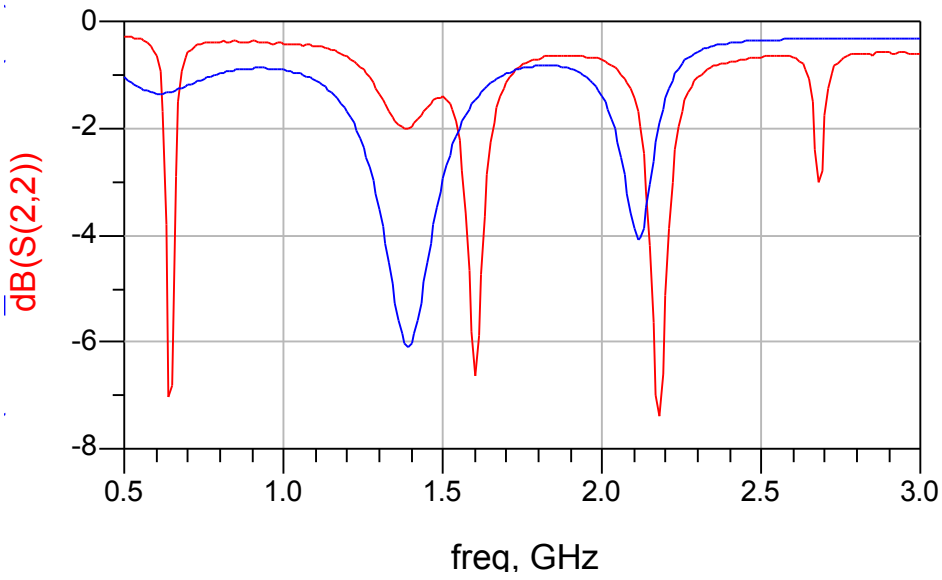

Fig. 4.7.12: S22 comparison: red line = measurement, blue line = simulation

To carry out this measurements a Rohde & Schwarz ZVA24 Vector Network Analyzer (VNA) that, after a SOLT (Short / Open / Load / Thru) calibration for a 500MHz – 3 GHz swept, was used to measure the S-parameters of the circuit. Fig. 4.7.10 – 4.7.11 – 4.7.12, show the results of the measurements.

As we expected, from Figs 4.7.10 and Fig. 4.7.11we can conclude that there is a notable difference that denotes gain loss and high refection coefficients. The reason of this behavior will be an issue of future work that will not be included in this project.

Chapter 5

Future Work and Conclusions

5.1 Future Work

Future work in the energy harvesting field is based on applying these concepts to everyday environments of a person or critical situations, where wireless powering is the only, safe, solution. In this way, it will be feasible to continuously storage energy and perform actions that, until now, conventional methods don not allow making them possible. Some possible new technologies that can be applied to this concept will be briefly described.

5.1.1 Textile Material for Antennas

Textile UWB antennas for WBAN applications have small physical size and can be easily integrated into clothing [22]. Results confirmed the good transient performance over UWB frequencies. As a conductor, high conductive metalized Nylon fabric is commonly used. Its metalized layers provide high conductivity and protection against corrosion, as well as flexibility. As dielectric substrate, acrylic fabric is often used.

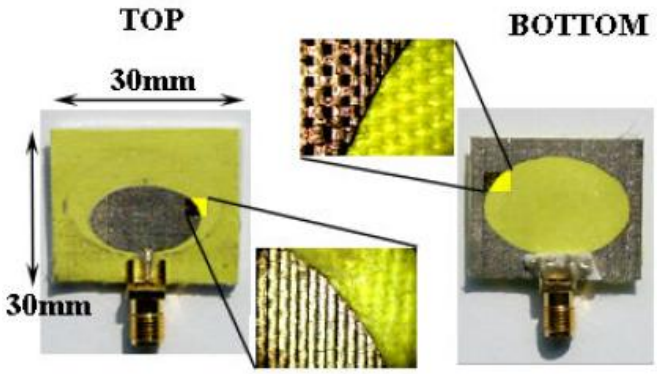

Fig. 5.1.1: textile UWB antenna [22]

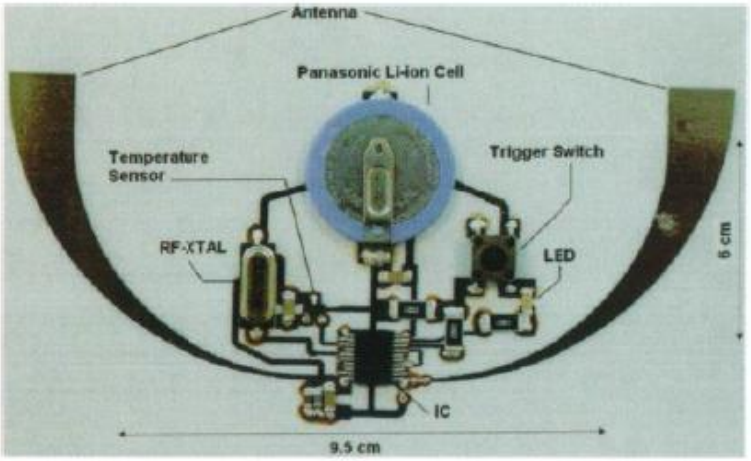

Fig. 5.1.2: wireless-sensor transmitter, on a paper substrate, using silver inkjet-printing technology [23]

5.1.2 Inkjet-Printed Antennas on Flexible Low-Cost Paper-Based Substrates

Paper, which holds one of the biggest market shares in the world, can potentially evolve the electronics market. It could eventually take the first step in creating an environmentally friendly first generation of truly "green" RF electronics and modules.

In addition, paper is one of the lowest-cost materials produced. Inkjet-printing technology (Fig. 5.1.2), which is a much faster and cleaner method than conventional wet-etching techniques that use several chemicals, can serve as a low-cost technology for fabricating RFID tags, produced in large processes on paper

5.1.3 Flexible Antenna on Polyethylene Terephthalate (PET) Substrate

These prototype antennas use low cost, wet deposition techniques to deposit silver and copper onto the substrates.

Fig. 5.1.3: Flexible folded dipole made from electro-less silver deposited on a PET substrate [24]

5.2 Conclusions

Concluded this project, we can affirm that the low power energy harvesting (in the environment) is a widespread trend that is becoming more accepted. For this new kind of "alternative energy" with the use of a rectenna, we conclude that there are still some limitations due mainly to delivered power of a mobile base station or a wireless router, is still low; this power levels can be improved using antennas arrays, or new high efficiency rectifiers. On the other hand, this energy can be stored, having as analogous application the solar energy, where sometimes photo voltaic modules are used to charge batteries that, subsequently, will supply power to other devices. We can also conclude that the use of this technology, for everyday applications, is being investigated, as well as cheaper and more flexibility material are being increasingly used at the time of the design of these applications.

Is also concluded that incident power densities, for both GSM-1900 and GSM-1800, are practically in the same order of magnitude, and that the incident power density of the ISM 2.4 GHz band, although the wireless router is closer than a mobile base station, is one order of magnitude below. We also conclude that for both, GSM and WLAN networks, the incident power density depends on the traffic at the time of measurement.

Respect to the antenna, it is concluded that the dimensions can be reduced by analyzing the current distribution on the surface of the conductors, moreover, that non-symmetrical cuts, can modify the radiation pattern of the antenna.

With respect to the rectifier, it is concluded that the use of microstrip lines for the matching circuit design, contributed to a lower soldering loss than if components, such as inductors and capacitors, were used.

References

[1] W. C. Brown, "The history of power transmission by radio waves," *IEEE Trans. Microwave Theory Tech.*, vol. MTT-32, pp. 1230–1242, Sept.1984

[2] http://www.elciudadano.cl/2010/05/07/el-desafio-de-la-transmision-de-energia-desde-el-espacio/

[3] A.S. Weddell, N. R. Harris, and N. M. White, Alternative Energy Sources for Sensor Nodes: Rationalized Design for Long-Term Deployment. In: International Instrumentation and Measurement Technology Conference, Victoria, British Columbia, Canada, May 2008.

[4] Kurt Roth and James Brodrick, "Energy Harvesting For Wireless Sensors", ASHRAE *Journal, May 2008.*

[5] Bergqvist, U. et al., *'Mobile Telecommunication Base Stations - Exposure to Electromagnetic Fields, Report of a Short Term Mission within COST-244bis'*, COST-244bis Short Term Mission on Base Station Exposure, 2000.

[6] Moghe, R., Yi Yang, Lambert, F. Divan, D. , "A scoping study of electric and magnetic field energy harvesting for wireless sensor networks in power system applications."

[7] *T.* Starner, 'Human powered wearable computing', *IBM systems journal*, vol. 35, no. 3-4, 1996

[8] H. J. Visser, A.C.F. Reniers, J.A.C. Theeuwes, *Ambient RF Energy Scavenging: GSM and WLAN Power Density Measurements*, European Microwave Conference 2008, Amsterdam, Netherlands.

[9] S.M. Mann, T.G. Cooper, S.G. Allen, R.P. Blackwell and A.J. Lowe, "*Exposure to Radio Waves near Mobile Phone Base Stations*", Report NRPB-R321, June 2000.

[10] S.I. Henderson and M.J. Bangay, "Survey of RF Exposure Levels from Mobile Telephone Base Stations in Australia", *Bioelectromagnetics*, Vol. 27, No. 1, pp. 73-76, January 2006

[11] N. Shinohara and H. Matsumoto, "Experimental study of large rectenna array for microwave energy transmission," *IEEE Trans. Microwave Theory Tech.*, vol. 46, pp. 261–267, Mar. 1998

[12] L. W. Epp, A. R. Khan, H. K. Smith, and R. P. Smith, "A compact dual-polarized 8.51-GHz rectenna for high-voltage (50 V) Actuator applications," *IEEE Trans. Microwave Theory Tech.*, vol. 48, pp. 111–120, Jan. 2000.

[13] Y. Fujino, T. Ito, M. Fujita, N. Kaya, H. Matsumoto, K. Kawabata, H. Sawada, and T. Onodera, "A driving test of a small DC motor with a rectenna array," *IEICE Trans. Commun.*, vol. E77-B, no. 4, pp. 526–528, Apr 1994

[14] C. Gómez, José A. García, A. Mediavilla, and A. Tazón, "A High Efficiency Rectenna Element using E-pHEMT Technology", *12th GAAS Symposium – Amsterdam*, pp. 315 – 318, 2004.

[15] H. Schantz, *The Art and Science of Ultrawideband Antennas*, Artech House, Boston, Mass, USA, 2005.

[16] C. A. Balanis, Antenna Theory, Analisys and Design, John Wiley & Sons, USA, 1997

[18] Taeyoung Yang, Seong-Youp Suh, Randall Nealy, William A. Davis, and Warren L. Stutzman, "COMPACT ANTENNAS FOR UWB APPLICATIONS", Virginia Tech, Blacksburg, VA, USA.

[19] Zhi Ning Chen, Terence S. P. See and Xianming Qing, "Small Printed UWB antenna with reduced Ground Plane Effect", *IEEE Trans. Microwave Theory Tech.*, vol. 48, pp. 111–120, Jan. 2000.

[20]S. Maas, *Nonlinear Microwave and RF Circuits*, second edition ed. www.artechhouse.com, 2003.

[21]http://www.lpkf.es/productos/creacion-rapida-prototipos-pcb/metalizacion-agujeros/chemiefrei/index.htm

[22] Maciej Klemm, Gerhard Tröster, "Textile UWB antenna for on-body communications", *Proc. 'EuCAP 2006',* Nice, France 6–10 November 2006

[23] Amin Rida, Li Yang, Rushi Vyas, and Manos M. Tentzeris, "Conductive Inkjet-Printed Antennas on Flexible Low-Cost Paper-Based Substrates for RFID and WSN Applications*", IEEEAntennasand Propagation Magazine*, Vol. 51, No.3, June 2009

[24] Griffin, Joshua David, "A Radio Assay for the Study of Radio Frequency Tag Antenna Performance", *School of Electrical and Computer Engineering Georgia Institute of Technology*, August 2005